Educational Material

Colombia
Doctoral Excursion, Earth Sciences Department ETH Zurich, August 21-September 5, 2018

Author(s):
Auderset, Alexandra; Cafagna, Fabio; Echeverria Pazos, Leonardo; Elison, Patrick; Erlanger, Erica; Fomin, Ilya; Guitián, José; Hawemann, Friedrich; Kueter, Nico; Mandl, Maximilian; Mejía, Luz María; Moretti, Simone; Oestreicher, Nicolas Kyochi; Ott, Richard; Paneva, Nadezhda; Petschnig, Paul; Preuss, Simon; Reitano, Riccardo; Renz, Tobias; Revels, Brandi N.; Wang, Yanyan; Winterberg, Sascha; Zhang, Hongrui

Publication Date:
2018-08

Permanent Link:

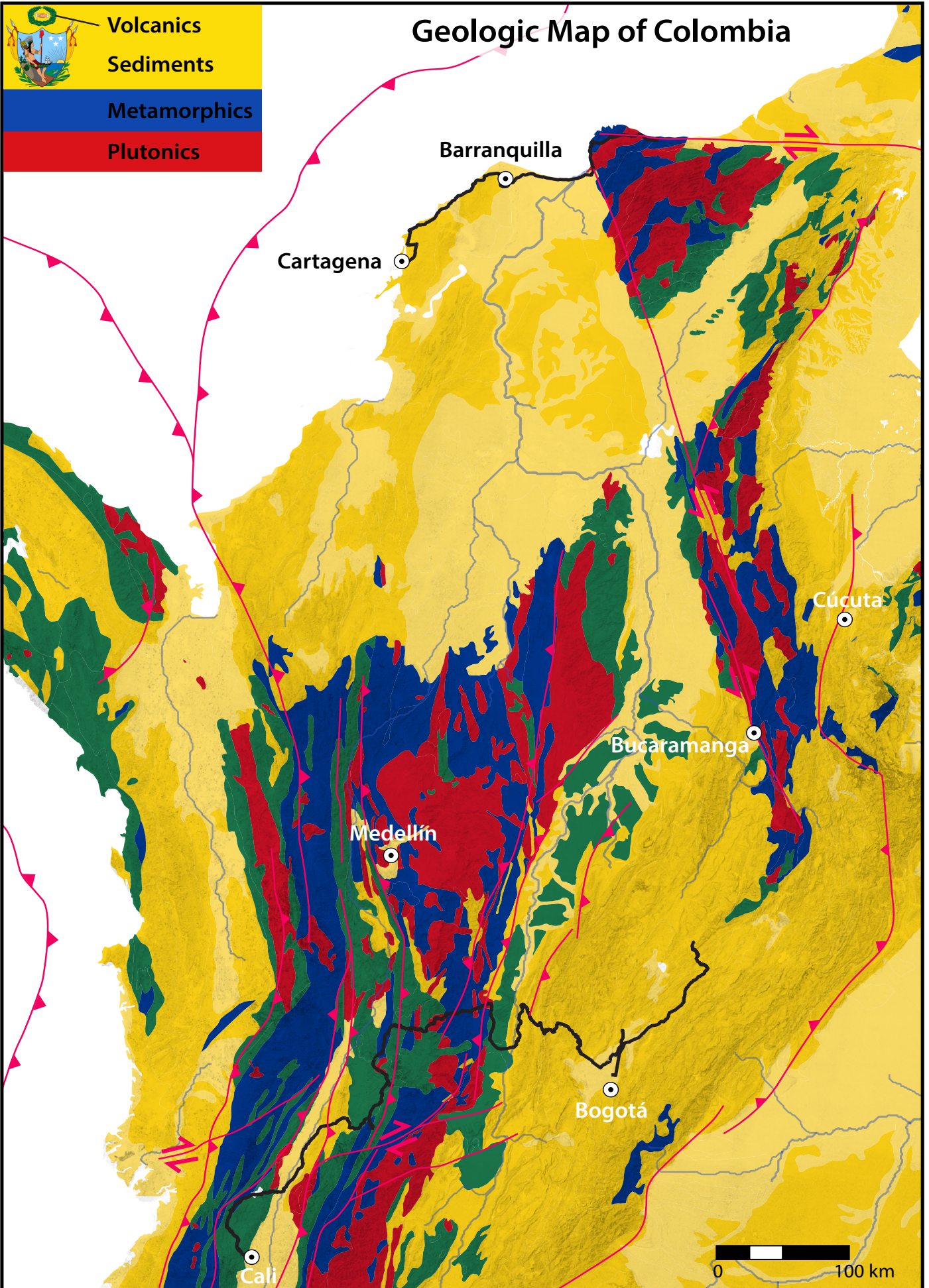https://doi.org/10.3929/ethz-b-000327761 →

Rights / License:

ETH Library

COLOMBIA

**Doctoral Excursion
Earth Sciences Department
ETH Zürich**

21 August - 5 September, 2018

Geologic Map of Colombia

Volcanics

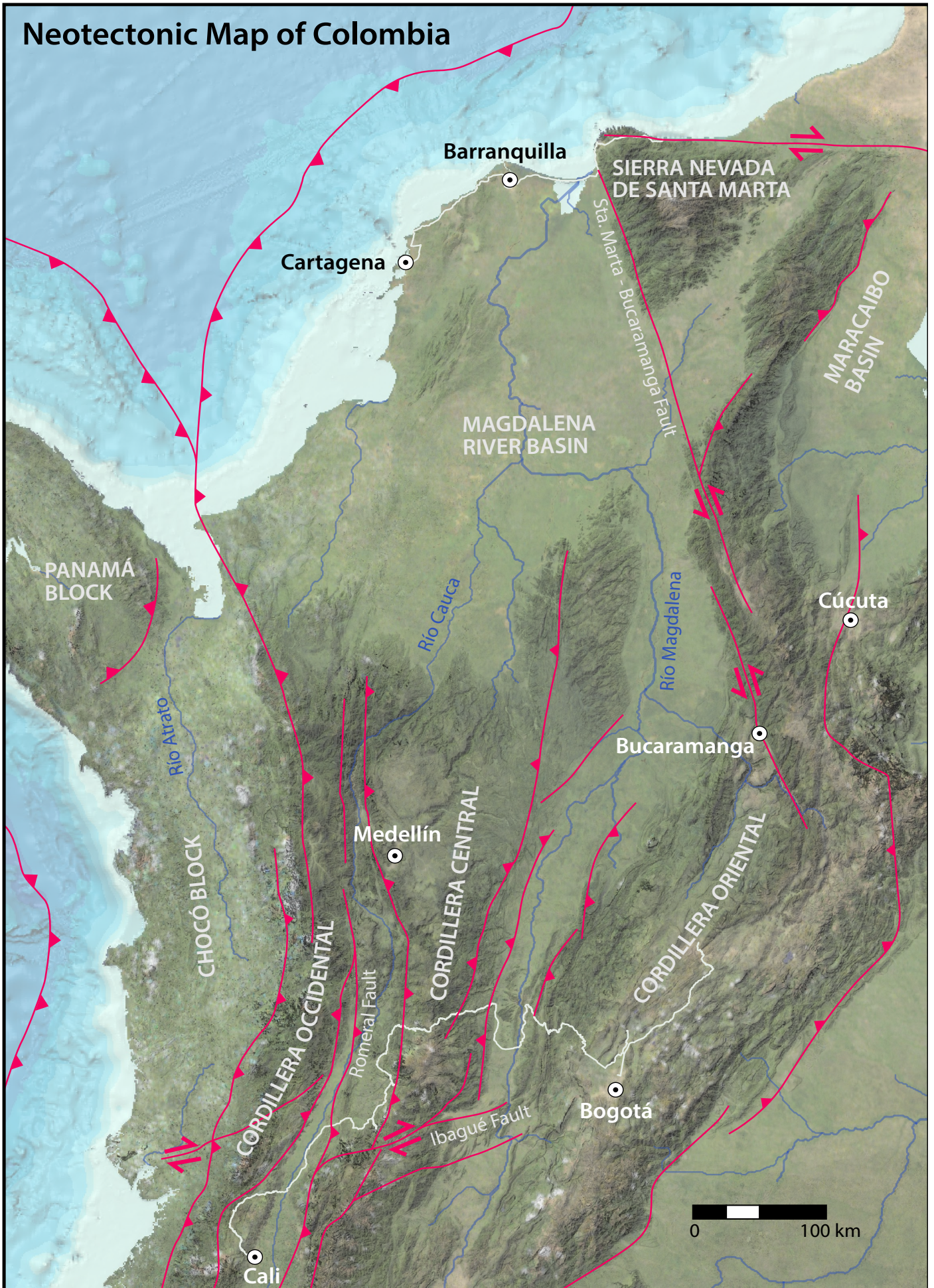**Sediments**

Metamorphics

Plutonics

Barranquilla

Cartagena

Cúcuta

Bucaramanga

Medellín

Bogotá

Cali

0   100 km

Neotectonic Map of Colombia

Barranquilla

Cartagena

SIERRA NEVADA
DE SANTA MARTA

MARACAIBO
BASIN

PANAMÁ
BLOCK

MAGDALENA
RIVER BASIN

Sta. Marta - Bucaramanga Fault

Río Cauca

Río Atrato

Río Magdalena

Cúcuta

CHOCÓ BLOCK

CORDILLERA OCCIDENTAL

Romeral Fault

CORDILLERA CENTRAL

Medellín

Bucaramanga

CORDILLERA ORIENTAL

Ibagué Fault

Bogotá

0   100 km

Cali

Table of Contents

Part I: Logistics

Part II: Chapters

Organisation

Committee

Leonardo Echeverria, Erica Erlanger, Luz Maria Mejía, Richard Ott

Fieldguide Editing

Erica Erlanger, Richard Ott

Program

Day 1 - 21.8.2018 Tuesday
Zürich – Madrid – Bogota *(time zone: MEZ-7 hours; local time zone: COT)*
    Air Europa UX 1676 from Zürich to Madrid   10:50 - 13:10
    Air Europa UX 193 from Madrid to Bogotá   15:15 - 18:15

Accommodation in Bogotá at Hotel Santa Barbara Real

Day 2 - 22.8.2018 Wednesday
Bogota - Villa de Leyva
    Salt Cathedral of Zipaquira
    Salt tectonics and deposition in back-arc basin
    Hike along a large syncline with folded sediments of the Eastern Cordillera

Accommodation in Villa de Leyva at Posada Saquenzipa

Day 3 - 23.8.2018 Thursday
Villa de Leyva - Villeta
    Paleotonological Museum of Villa de Leyva
    Outcrops of sediments near Villa de Leyva

Accomodation in Villeta at Finca Villa Taty

Day 4 - 24.8.2018 Friday
Villeta - Manizales
    Honda fault
    River terraces along Rio Magdalena
    Armero town and lahar

Accommodation at Cafe Hostal la Toscana

Day 5 - 25.8.2018 Saturday
Manizales to Salento
    Nevado del Ruiz
    Overview of the Cauca Valley

Accomodation in Salento at Hostal Estrella de Agua

Day 6 - 26.8.2018 Sunday
Salento
    Hike along Valle del Cocora through metamorphic basement of Central Cordillera

Accomodation in Salento at Hostal Estrella de Agua

Day 7 - 27.8.2018 Monday
Salento - Lake Kajima
    Hike La Maizena Creek section of oceanic crust

Accommodation in Calima

Day 8 - 28.8.2017 Tuesday
Lake Kajima - Cali
    Cisneros Formation, Western Cordillera

Accommodation in Cali at Blue Fox Hostel

Day 9 - 29.8.2018 Wednesday
Cali – Medellín – Cartagena *(time zone: MEZ-7 hours; local time zone: COT)*
    Avancia Airlines AV 9760 from Cali to Medellín   07:33 - 08:25
    Avancia Airlines AV 9760 from Medellín to Cartagena   08:55 - 10:02

Visit of old town Cartagena
El Totumo mud volcano

Accommodation in Hostal Puerta de Oro

Day 10 - 30.8.2018 Thursday
Barranquilla - Taganga
Magdalena River delta
Canoe tour through the Mangroves of the Cienaga Grande de Santa Marta
Overview of the Sierra Nevada de Santa Marta

Accommodation in Taganga at La Tortuga Hostel

Day 11 - 31.8.2018 Friday
Taganga
Diving and Snorkeling
Marine terraces
Metamorphic rocks of the Sierra Nevada de Santa Marta

Accommodation in Taganga at La Tortuga Hostel

Day 12 - 1.8.2018 Saturday
Taganaga - Minca
Hike to Cuchilla San Lorenzo
Metamorphic basement of the Sierra Nevada

Accommodation in Marymonte

Day 13 - 2.8.2018 Sunday
Minca -Palomino
Precambrian basement and sediments

Accommodation in Kanta Sana

Day 14 - 3.8.2018 Monday
Palomino - Arrecifes
Intrusive rocks
Coral reefs

Accommodation in Tayrona National Nature Park

Day 15 - 4.8.2018 Tuesday
Arrecifes - Santa Marta
Metamorphic basement
Marine terraces and Nenguane

Accommodation in Edifico Sandra

Day 16-17 - 5.8-6.8.2018 Wednesday-Thursday
Santa Marta–Bogotá-Madrid-Zurich
Avancia Airlines AV 8485 G from Santa Marta to Bogotá   09:39 - 11:09
Air Europa UX 194 from Bogotá to Madrid   20:15 - 12:50 (+ 1 day)
Air Europa UX 1671 from Madrid to Zürich   14:50 - 17:10

Participants

First Name	Last Name	Country	Institute	Research Group
Alexandra	Auderset	Switzerland	GI	Biogeoscience
Fabio	Cafagna	Italy	IGP	Experimental Petrology
Leonardo	Echeverria Pazos	Peru	Geophysics	Earth and Planetary Magnetism
Patrick	Elison	Germany	Geophysics	Explorational & Environmental Geophysics
Erica	Erlanger	France	GI	Earth Surface Dynamics
Ilya	Fomin	Russia	Geophysics	Geophysical Fluid Dynamics
José	Guitian Bermejo	Spain	GI	Climate Geology
Friedrich	Hawemann	Germany	GI	Structural Geology
Nico	Küter	Germany	IGP	Experimental Petrology
Maximilian	Mandl	Austria	IGP	Planetary Geochemistry
Luz Maria	Mejía	Spain	GI	Climate Geology
Simone	Moretti	Italy	GI	Biogeoscience
Nicolas Kyochi	Oestreicher	Switzerland	GI	Engineering Geology
Richard	Ott	Germany	IGP	Earth Surface Dynamics
Nadezhda	Paneva	Bulgaria	IGP	High Pressue Geology
Paul	Petschnig	Austria	IGP	Experimental Petrology
Simon	Preuss	Germany	Geophysics	Geophysical Fluid Dynamics
Riccardo	Reitano	Italy	GI	Earth Surface Dynamics
Tobias	Renz	Germany	GI	Engineering Geology
Brandi	Revels	USA	IGP	Earth Surface Geochemistry
Yanyan	Wang	China	GI	Earth Surface Dynamics
Sascha	Winterberg	Switzerland	GI	Earth Surface Dynamics
Hongrui	Zhang	China	GI	Climate Geology

Institute Abbreviations: Geological Institute (GI) and Institute for Geochemistry and Petrology (IGP)

Guests

First Name	Last Name	Country	Organization
Dr. Alejandro	Piraquive Bermudez	Colombia	Colombian Geological Survey
Dr. Alejandro	Beltrán Triviño	Colombia	EAFIT University
Dr. Adolfo	Sanjuan Muñoz	Colombia	Universidad Jorge Tadeo Lozano
Dr. Aminta	Jáuregui Romero	Colombia	Universidad Jorge Tadeo Lozano
Dr. Alvaro	Nivia	Colombia	Colombian Geological Survey

Accommodation

Day 1: Tuesday 21.8.2018
Hotel Santa Barbara Real
Calle 127 No. 7-89, Usaquíen, 110010 Bogotá, +57 1 6290944

Day 2: Wednesday 22.8.2018
Posada Saquenzipa
Calle 12 No 11A16, 154001 Villa de Leyva +57 313 2549225

Day 3: Thursday 23.8.2018
Alquiller Finca Villa Taty
Via Principal Villeta, Villeta +57 310 283 6260

Day 4: Friday 24.8.2018
Cafe Hostal La Toscana
Calle 64a 17 36, 170003 Manizales +57 301 5140805

Days 5-6: Saturday-Sunday 25-26.8.2018
Hostal Estrella de Agua
Carrera 5 #6-24, 631020 Salento +57 310 5053160

Day 7 Monday 27.8.2018
Calima

Day 8 Tuesday 28.8.2018
Blue Fox Hostel
Carrera 10 #3-63, 760044 Cali +57 316 4416803

Day 9: Wednesday 29.8.2018
Hostal Puerta de oro
Carerra 69 80 79, 080001 Barranquilla +57 310 3571188

Days 10-11: Thursday-Friday 30-31.8.2018
La Tortuga Hostel
Calle 9 #3-116, Taganga +57 5 421 9048

Day 12: Saturday 1.9.2018
Marymonte
Minca Sector Lomalinda Subida Al Mirador, 470008 Minca +57 310 8118503

Day 13: Sunday 2.9.2018
Kanta Sana
Carrera 10 3-40 segunda entrada al mar, 446009 Palomino +57 301 3260301

Day 14: Monday 3.9.2018
Tayrona National Nature Park
Magdalena +57 1 3532400

Day 15: Tuesday 4.9.2018
Edificio Sandra
Calle 19 No 1b-96 Rodadero Sur, 470006 Sant Marta +57 300 5901078

Emergency Numbers

TSM (ETH Travel Insurance Company	+41 22 819 44 06
National Emergency Number	123
Tourist Police	(1) 3374413
Civil Defense (Bogotá)	7006465
Civil Defense (rest of country)	144
Metropolitain Police	112
Medical Emergency	125
Red Cross (24 Hour Ambulance)	132
GAULA (Kidnapping and Extortion Squad)	165
Fire	119

Hospitals

Armenia
Hospital San Juan de Dios
Avenir Bolivar Calle 17 Norte

+57 6 7493500

Barranquilla
Clínica Portoazul
KM2 Via Puerto Colombia

+57 5 3673600 ext. 7126

Bogotá
Fundación Santa Fe de Bogota
Carrera 7 No. 117-15

+57 1 6030303

Cali
Fundación Valle del Lili
Carrera 98 # 18-49

+57 2 3319090

Cartagena
Clinica Medihelp Services
Carrera 6 # 5-101

+57 5 6475290

Santa Marta
Clínica el Prado
Cr5 26-35 P-3 C.C. Quinta Avenida

+57 5 4329200

Chapter 1
Introduction to Colombia
Leonardo Echeverria

Official Name: Republic of Colombia
Form of Government: Republic
Capital: Bogotá
Population: 44,379,598
Official Language: Spanish
Money: Colombian Peso
Area: 439,619 sq mi (1,138,910 sq km)
Major Mountain Ranges: Andes, Sierra Nevada de Santa Marta
Major Rivers: Magdalena, Cauca, Atrato, Sinú

History

The Spanish set foot on Colombian soil in 1499, and a period of conquest and colonisation took place in the first half of the 16th century; ultimately the New Kingdom of Granada was created. Colombia became independent in 1819, but by 1830 the "Gran Colombia" Federation was dissolved. The name of Colombia is derived from the last name of Christopher Columbus (Restrepo, 1992). Since 1960, the country has suffered from an armed conflict, which escalated in 1990, but it has decreased from 2005 onward (NCHM, 2013).

Geography

Colombia has six main natural regions: the Andes mountain range, the Pacific coastal region, the Caribbean coastal region, the llanos (plains), the Amazon rainforest, and the insular area in the Atlantic and Pacific oceans. Colombia shares borders to the northwest with Panama, to the east with Venezuela and Brazil, and to the south with Ecuador and Peru. It lies between latitudes 12° N and 4°S, and longitudes 67° and 79° W.

Biodiversity

Colombia is the most biodiverse country per square kilometer and one of the megadiverse countries. Colombia is the second most biodiverse country in the world, and it ranks first in bird species. The country has between 40,000 and 45,000 plant species. Colombia has the highest rate of species by area unit worldwide, and it has the largest number of endemic species of any country (inecc.gob.mx, 2014).

Climate

As a consequence of its geographical location near the equator, Colombia's climate is mostly tropical, but the climate presents variations within six natural regions (altitude, temperature, humidity, wind, and rainfalls). Below 1,000 meters is the warm altitudinal zone, where temperatures are above 24° C. About 82.5% of the country's total area lies in the warm altitudinal zone. Between 1,001 and 2,000 meters is the temperate climate altitudinal zone with average temperature between 17 and 24 °C. The cold climate is found between 2,001 and 3,000 meters with temperatures between 12 and 17 °C. Above this zone are the alpine conditions and finally the treeless grasslands of the páramos. Above 4,000 meters, the climate is glacial.

Language

99.2 % of Colombians speak Spanish; 65 Amerindian languages, two Creole languages, the Romani language and Colombian Sign Language are also spoken. English has official status in the archipielago of San Andrés.

Religion

Colombia remains a mostly Roman Catholic country, but the 1991 constitution guarantees freedom of religion and all religious faiths are equally free by law. About 90% of the population is Christian. The majority of them are Roman Catholic (70.0% - 79%) and a minority is Protestant (16.7%). Some are Atheist or Agnostic (4,7%), and 1% belong to other religions like Islam, Judaism, Buddhism, Mormonism, Hinduism, Indigenous religions, Hare krishna, Rastafari, and Orthodox catholic church (Beltrán, 2012).

References

Carlos Restrepo Piedrahita (February 1992). "El nombre "Colombia", El único país que lleva el nombre del Descubrimiento". Revista Credencial (in Spanish). Retrieved 29 February 2008.

Historical Memory Group (2013). ""Enough Already!" Colombia: Memories of War and Dignity". The National Center for Historical Memory's (NCHM).

"Thermal floors" . banrepcultural.org. Archived from the original on 16 October 2014. Retrieved 25 February 2014.

Bushnell, David and Rex A. Hudson. "Geology". In Colombia: A Country Study(Rex A. Hudson, ed.), pp. 70-71. Library of Congress Federal Research Division (2010).

Delegatarios de países megadiversos. "Declaración de Cancún de países megadiversos afínes". inecc.gob.mx. 9 March 2014.

"Languages of Colombia" (in Spanish). banrepcultural.org. Retrieved 9 October 2013.

Beltrán Cely; William Mauricio. "Descripción cuantitativa de la pluralizaciónreligiosa en Colombia" (PDF). Universitas humanística 73 (2012): 201–238. –bdigital.unal.edu.co. Archived from the original (PDF) on 29 March 2014.

Survival Spanish Phrases

English	Spanish
Hello (General greeting)	Hola
Goodbye	Adios/Chao
Thank you	Gracias
Please	Por favor
Excuse me	Disculpe/Perdoname
My name is __	Soy __/Me llamo __
How are you?	¿Cómo estás?
Do you understand?	Comprende?/Entiendo?
Where is ___?	En donde está __?
Do you speak English?	Habla Inglés?
I don't speak Spanish	No hablo Espagñol
Can you please take me to ___?	Me lleva por favor hasta __
Can you repeat more slowly?	¿Puede repetirlo más despacio?
I don't have any money	No tengo dinero
I don't know	No se
The toilet	el baño
Help me!	Ayudame!
Water	Agua
Bus stop	Paradero de bus
How much does it cost?	¿Cuanto cuesta?
One	Uno
Two	Dos
Three	Trés
Four	Cuatro
Five	Cinco
Six	Seis
Seven	Siete
Eight	Ocho
Nine	Nueve
Ten	Diez
One Hundred	Cien
One Thousand	Mil

Chapter 2
Plate Tectonic Evolution and Subduction Dynamics

*Sascha Winterberg, Ilya Fomin, and Friedrich Hawemann*

1. Plate Tectonic Setting

Colombia is situated at the northern tip of the South American Continent. This region south of the North American and Yucatan Plate is dominated by small plates and multiple subduction and extension zones as well as strike-slip faults (Fig. 1). Central America has a highly dynamic plate tectonic history in the late Cenozoic, mainly driven by the Caribbean Plate. Until today, the region remains tectonically active, as seen from an extensive earthquake record, with the Mw 7.0 Haiti earthquake in 2010 as a recent example.

Colombia extends towards the east into the Amazon Basin, which represents part of the South American plate. Colombia is bordered to the south-east by the Guiana Shield, a cratonic shield formed in the Archean. In the west, the Nazca Plate subducts below the continent and is separated in the north by a spreading zone from the Cocos Plate that subducts to the north-east below Panama. The Caribbean Sea north of continental Colombia is made up

by the Colombia Basin. The Colombia and Venezuela Basin, together with smaller fragments, compose the Caribbean Plate. It is therefore, strictly speaking, not a rigid plate, but for the sake of simplicity, the term is commonly used.

The Colombian continental territory spreads over basically four tectonic domains summarized as the Northern Andean Block. In the west above the Nazca subduction the Choco Block defines a low-relief plain. Further east, the Western Cordillera and the Central Cordillera form two mountain chains separated by the Cauca River that widens to a large valley in the area of Cali. Separated by the Magdalena River Valley, the Eastern Cordillera defines a 1200 km long mountain chain. Isolated at its northern tip, a triangular massif, the Sierra Nevada de Santa Marta, reaches altitudes of up to 5700 m. This does not only mark the highest peak of Colombia, but with a distance of only 42 km from the sea, it is one of the world's highest topographic gradients. The Sierra Nevada de Santa Marta form a tectonic domain together with the Maracaibo Basin at the north-eastern border of Colombia. This Maracaibo
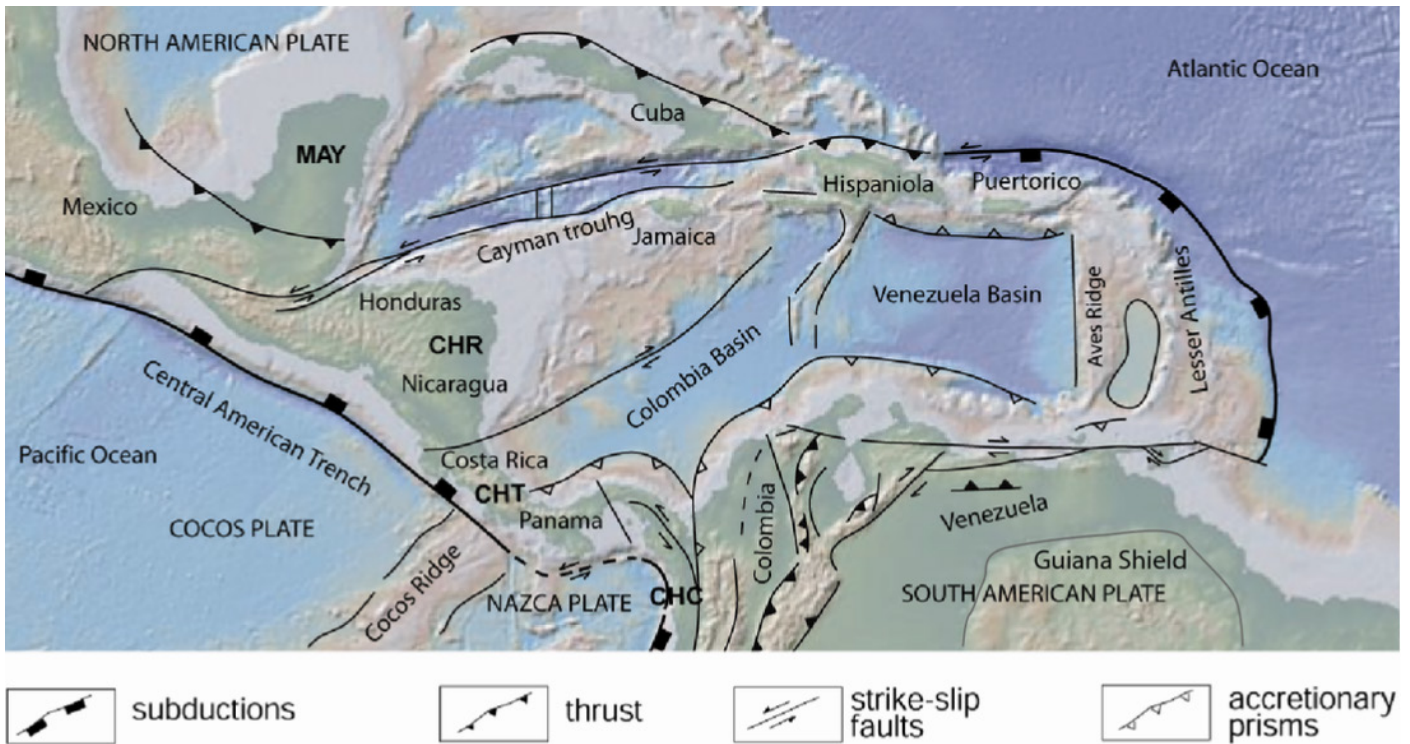
Fig. 1. Overview of the Caribbean tectonic setting (Giunta and Orioli, 2011).

Subplate Realm is separated by the Cordillera de Mérida from the South American Plate.

2. Main Features of Subduction at Plate Boundaries

The western margin of the South America plate is formed by the Nazca plate. Underneath Peru, Ecuador and Southern Colombia, the plate subducts almost sub-horizontally for the first 200-300 km (Schepers et al., 2017). Young and hot oceanic crust underneath continental crust has delayed the basalt-eclogite transition, which supports its thermal buoyancy. Geological data coupled with numerical simulations, allow to put further constraints on the global plate motion rate, resulting in 2 cm/year average velocity in past 50 Ma. Modern-day convergence rate associated with flat slab subduction is up to 6 cm/year (e.g. (Nocquet et al., 2014). Acceleration of the convergence rate results in topographic uplift: The Colombian Eastern Cordillera were only about 20% of their modern height 14 Ma ago, and grew to 50% of their modern height from 6 to 2 Ma (Gregory-Wodzicki, 2000). These data inferred from paleo botanical surveys are important to understand the history of the climate for this particular region.

The northern margin of Colombia is bounded by the Caribbean subduction system, which is fundamentally different from the Nazca subduction zone as its convergence is slow (15 mm/a) and oblique.

3. Seismology and Active Tectonics

The tectonic frame work in Colombia depends on complex mechanisms of different fault zones. Seismic data collected for the Nazca subduction in southern Colombia (Fig.
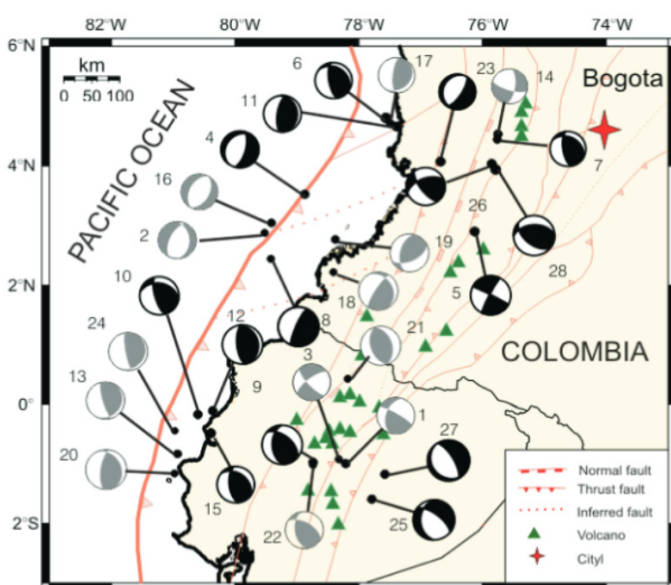

Fig. 2. Locations of major earthquakes and main faults in southern Colombia (Garcia et al., 2007). Earthquake focal mechanisms reflect the general E-W comression, caused by the convergence of the Nazca and South American plates.

2) were processed by several independent groups of scientists (e.g. Garcia et al., 2007; Syracuse et al., 2016). As it was shown by Yoshimoto et al. (2017), earthquakes with epicentres located offshore Colombia can be characterised as complex ruptures with strong interplate coupling in several separate patches along the plate interface (so that the subduction zone is segmented into several rigid "blocks" from south to north). This interpretation fits the general approach used to study the Andean Arc as a set of several slivers rather than a single rigid block (Nocquet et al., 2014). A proposed tear in the slab (Fig. 3) might have originated by the subduction of the Sandra Ridge. Furthermore, extensive seismicity in the Bucaramanga region is interpreted as a point of active ongoing slab break-off, the Caldas tear (Vargas & Mann, 2013). The concept might explain its extraordinary seismic activity (one of the strongest in the world).

The convergence of the Nazca and South American plates and the resulting shortening are accommodated by the subduction of the Nazca Plate in the West and thrusting in the Andean Cordilleras. Seismic data suggests that the angle of subduction steepens drastically between the south west of Colombia with an angle of 17 to 30 degrees to the area south to Bogota with an angle of 45 (Syracuse et al., 2016; Garcia et al., 2007).

Building of the mountain range is accompanied by increasing stresses in the upper crust and their sudden release is recorded as earthquakes. The strongest one in the past decades in Colombia is Armenia event in 1999. This earthquake with magnitude 6.2 killed more than 1000 people and injured another 5000, and caused severe damage to the infrastructure. The hypocenter was located at a depth of ~17 km (Ugalde et al., 2002). I this area, the Romeral Fault System is a major fault system that borders the Western and Central ranges of the Colombian Andes, and separates the accreted sediments and obducted oceanic crust from the continental crust. The damage of the Armenia earthquake was most severe in areas located on sedimentary fillings, while buildings located on top of the bedrock were damaged significantly less (Asfura & Flores, 1999).

References

Asfura, A.P., Flores, P.J. "Quindío, Colombia Earthquake of January 25, 1999: Reconnaissance Report". Technical Report MCEER-99-0017, October 4, 1999.

Garcia, P.P., Vargas, C.A., Monsalve, H.J., 2007, Geometric model of the Nazca plate subduction in southwest Colombia: Earth Sciences Research Journal, v. 11, p. 117-130.

Giunta, G., and S. Orioli, 2011, The Caribbean plate evolution: trying to resolve a very complicated tectonic puzzle: in New Frontiers in Tectonic Research-General Problems, Sedimentary Basins and Island Arcs, edited, InTech.

Gregory-Wodzicki, K.M., 2000, Uplift history of the Central and Northern Andes: A review: Geological Society of America
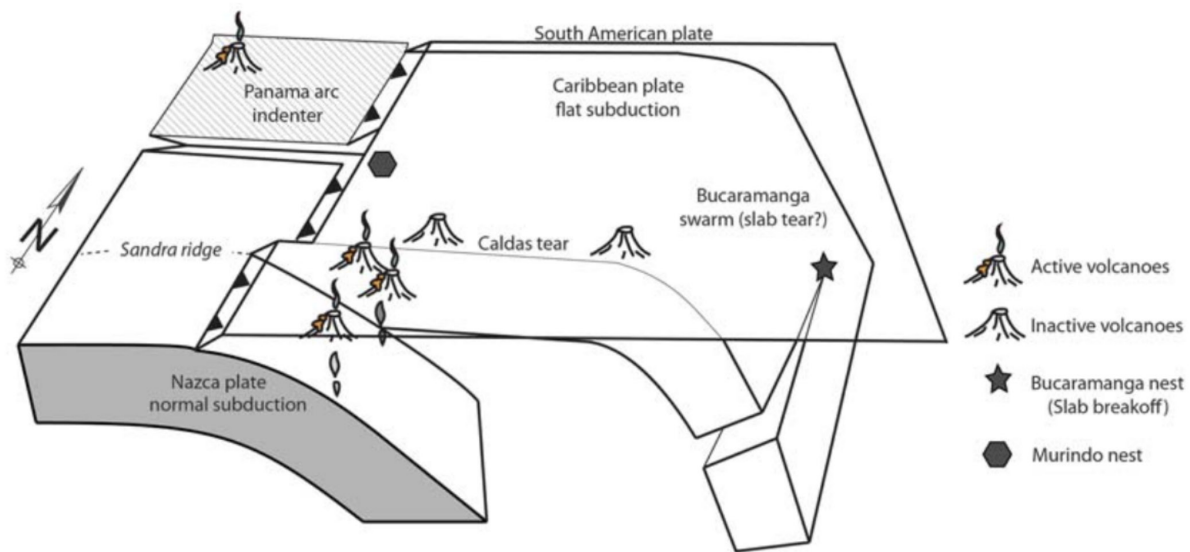
Fig. 3. Slab structure beneath the Andes. Murindo and Bucaramanga nests represent places with high seismic activity (Vargas & Man, 2013).

Bulletin, v. 112, p. 1091-1105.

Nocquet, J.-M., Villegas-Lanza, J.C., Chlieh, M., Mothes, P.A., Rolandone, F., Jarrin, P., Cisneros, D., Alvarado, A., Audin, L., Bondoux, F., Martin, X., Font, Y., Régnier, M., Vallée, M., Tran, T., Beauval, C., Mendoza, J.M.M., Martinez, W., Tavera, H., Yepes, H, 2014, Motion of continental slivers and creeping subduction in the northern Andes: Nature Geoscience, v. 7, 287–291.

Schepers, G., van Hinsbergen, D.J.J., Spakman, W., Kosters, M.E., Boschman, L.M., McQuarrie, N., 2017, South-American plate advance and forced Andean trench retreat as drivers for transient flat subduction episodes: Nature Communications, v. 8, p. 15249.

Syracuse, E.M., Maceira, M., Prieto, G.A., Zhang, H., Ammon, C.J., 2016, Multiple plates subducting beneath Colombia, as illuminated by seismicity and velocity from the joint inversion of seismic and gravity data: Earth and Planetary Science Letters, v. 444, p. 139-149.

Vargas, C.A., Mann, P. , 2013 , Tearing and Breaking Off of Subducted Slabs as the Result of Collision
of the Panama Arc-Indenter with Northwestern South America: Bulletin of the Seismological Society of America, v. 3, p. 2025–2046.

Ugalde, A., Vargas, C.A., Pujades, L.G., Canas, J.A., 2002, Seismic coda attenuation after the Mw = 6.2 Armenia (Colombia) earthquake of 25 January 1999: Journal of Geophysical Research: Solid Earth, v. 107, B6, p. 2107.

Yoshimoto, M., Kumagai, H., Acero, W., Ponce, G., Vásconez, F., Arrais, S., Ruiz, M., Alvarado, A., García, P.P., Dionicio, V., Chamorro, O., Maeda, Y., Nakano, M., 2017, Depth-dependent rupture mode along the Ecuador-Colombia subduction zone: Geophysical Research Letters, v. 44, p. 2203-2210.

Chapter 3
The Metamorphic Basement of Colombia

Nico Küter and Paul Petschnig

1. Introduction

Colombia's metamorphic basement is a framework of three major units, composed of likely more than 34 individual terranes (i.e. lithologically distinct units), witnessing a nearly continuously active geological history lasting from the late Precambrian until today (Suarez, 1990, Spikings et al., 2015). From East to West (i.e. from old to young), Colombia's base is formed by (i) Eastern South America Province (the northwestern cratonic margin of the Guiana Shield), (ii) the Central Andean Province, and (iii) the Western Province (Suarez, 1990; Fig. 1). The provinces themselves are demarked by structural features, namely the SE-NW-trending Borde Llanero Suture separating the Eastern South America Province from the Central Andean Province, and the SSW-NNE trending Romeral-Fault system separating the Central Andean Province from the Western Province. This contribution introduces the three main provinces as the general geological basement frame-

work of Colombia, mainly following Forrero Suarez (1990) and Spikings et al. (2015), with the aim to provide the context for more detailed considerations on the regional geology.

2. Guiana Shield and the Eastern South America Province (ESAP)

The Eastern South America Province (ESAP) of Colombia renders the western margin of the Guiana Cratonic Shield (aka Amazonian Craton), which is the largest and northernmost of the four cratons comprising South America (others are Rio Apa, Sao Francisco which is part of the African Congo craton, and Rio de la Plata). The cratonic core of the ESAP is typically marked by high-grade metamorphic and igneous lithologies of Archean age: the oldest lithologies (granulites, gneisses, amphibolites and metamorphosed banded iron formation "BIF") are reported from the Imataca complex from the Orinoco river in northern
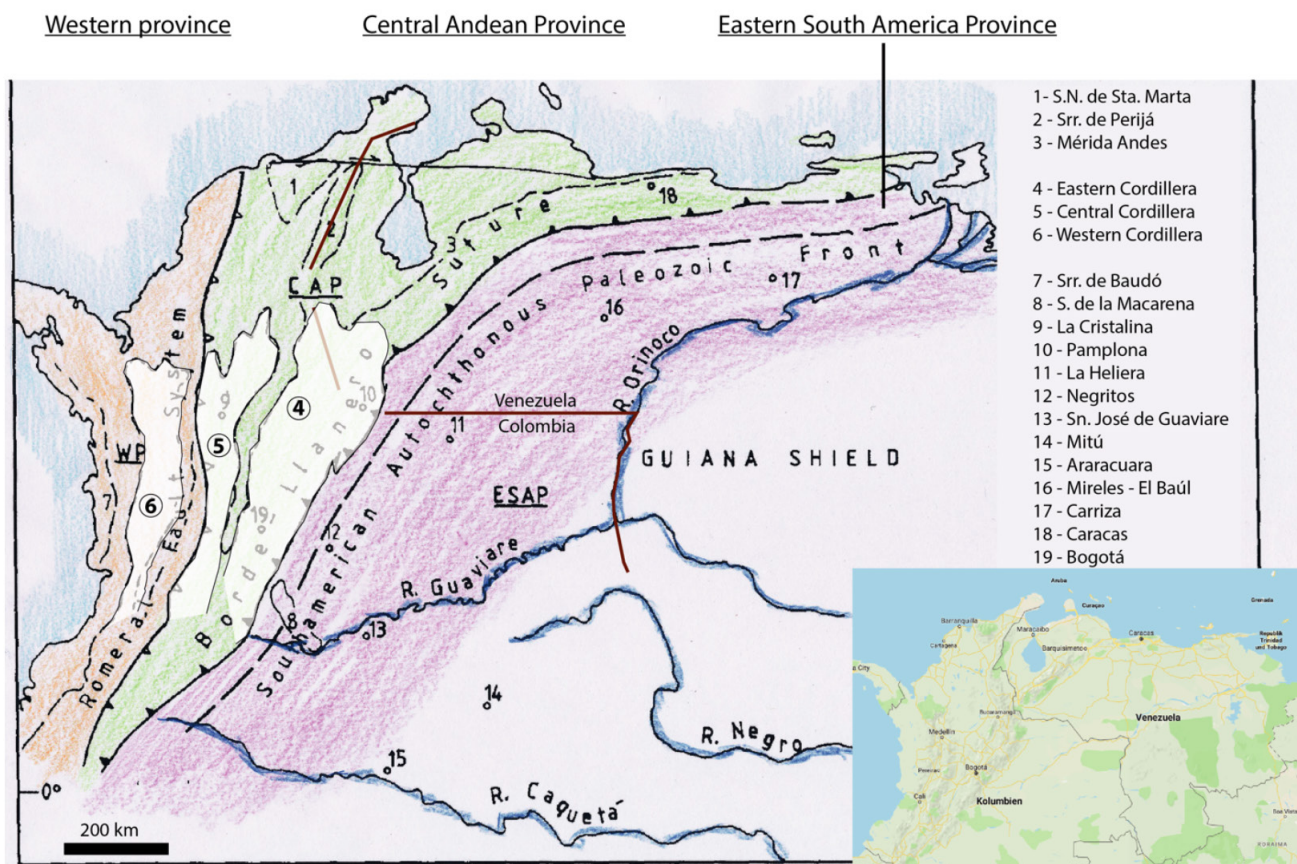

Fig. 1. The three main provinces of Colombia, from East to West (old to young): Eastern South America Province (ESAP, purple; Precambrian cratonic margin of the Guiana Shield); Central Andean Province (CAP, green; allochthoneous metamorphic base of North-American provenance), and Western Province (WP, brown; post-Jurassic framework of accreted oceanic lithosphere). ESAP and CAP are separated by the Borde Llanero Suture, which a high-grade metamorphic and magmatic belt reflects the most-southern core of the 490-390 Ma Caledonian orogeny that amalgamated the North and South American shields. The WP and the CAP are separated by the Romeral Fault System. Figure modified from Suarez (1990).

Venezuela, yielding 3.7 to 3.4 Ga Rb-Sr and U-Pb protolith ages (cf. Kroonenberg, 1982). The most extensive orogenic event comprising the majority of the Guiana Shield took place between 2.1 and 1.8 Ga ago and is summarized as the Trans-Amazonian Orogenic Cycle (Hurley et al., 1967), demarked by metamorphic greenstone and granulite belts and extended granitic and rhyolitic igneous provinces.

Youngest metamorphic/igneous lithologies contributing to the Guiana shield are assigned to the 1.8 to 1.4 Ma Paraguazan Orogenic Event, producing rapakivi granites, extended migmatitic and granitic provinces (Mitú migmatite complex) (cf. Kroonenberg, 1982). Eventually, the cratonic base is unconformably overlain by a succession of typically non-metamorphosed Early Paleozoic sediments (sandstones, siltstones, limestones) covered by Cenozoic sediments (Fig. 2).

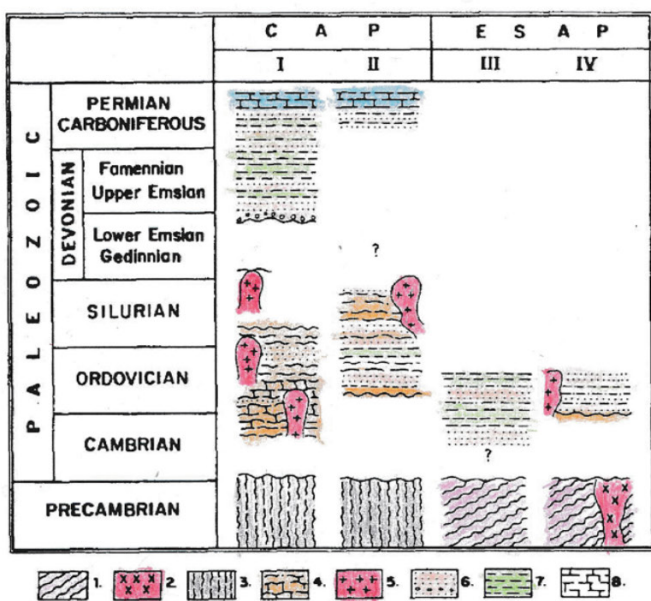## 3. Central Andean Province (CAP)

The Central Andean Province (CAP) is topographically marked by the NNE-SSW trending Eastern Cordillera (Cordillera Oriental) and its northern branch the Sierra de Perija, the N-S trending Central Cordillera, and the strikingly pyramid-shaped Sierra Nevada de Santa Marta located on the Caribbean coast. The northwestern (i.e. Colombian) margin of the Guiana shield frames the Eastern Cordillera, whose base witnessed the collision of the North American Plate with the Guiana Shield in the Early Paleozoic. An igneous belt of gabbros, diorites and quartz-monzonites as well as high-grade metamorphic rocks (gneisses, amphibolites) are dated between 490 to 390 Ma, and hence comprise the most southern known extension of the Caledonian orogeny: the Borde Llanero suture. Interestingly, the collision of the North American Plate left be-

hind pre-Caledonian (i.e. Archean) basement rocks clearly distinct from those known from the Guiana Shield: 1250 to 950 Ma charnockites (dark igneous Kfsp-Opx-Plg-Qtz rocks of metamorphic origin, devoid of OH-bearing minerals) and associated granulite facies rocks of the North American Grenville Province are unambiguous witnesses of the North and South American shield collisions (Kroonenberg, 1982). The unique high-grade lithologies of the Sierra Nevada de Santa Marta (Pyramid) are thought to represent a remaining fragment of the North American plate as well (Kroonenberg, 1982; Fig. 2 & 3).

Today, most of the Eastern Cordillera basement is overlain by the Late Mesozoic back-arc sediments, including a Cretaceous evaporite-limestone-black shale sequence hosting the world's most famous emerald deposits in Mezzo and Chivor (Branquet et al. 1999; Banks et al., 2000).

The N-S trending Central Cordillera (Cordillera Central) is located in the western part of the CAP, separated by the Romeral fault-system from the post-Jurassic Western Province. Its eastern base is composed of roughlyt Early Paleozoic low-grade metamorphous sediments formerly overlying the high-grade metamorphic base exposed in the Eastern Cordillera (Fig. 2). Similar to the lithology and geochronology of Eastern Cordillera metamorphics, the occasionally fossil-bearing low-grade Ordovician to Silurian metasediments (Phyllites, Marbles) yield faunal relationships to the North American and Great Britain fossil records (e.g. brachiopods), yet appear distinctly different from the South American Continent at this time; underlining the allochthoneous origin of the CAP basement (Johnson and Boucout, 1973; Suarez, 1990).

The Central Cordillera presumably outlined in the western active margin of the South-American Pangea continent in

Fig. 2. Generalized comparison of the Precambrian to Paleozoic stratigraphy of the Central Andean Province (CAP, mainly concerning the eastern Cordillera) and Eastern South America Province (ESAP), modified from Suarez (1990). 1) Mitú migmatitic complex; 2) Precambrian magmatism; 3) charnockitic and garnetiferous granulites, ortho- and paragneisses; 4) gneisses, phyllites, marble and slates; 5) Paleozoic magmatism; 6) conglomerates and sandstones; 7) shales; 8) limestones.
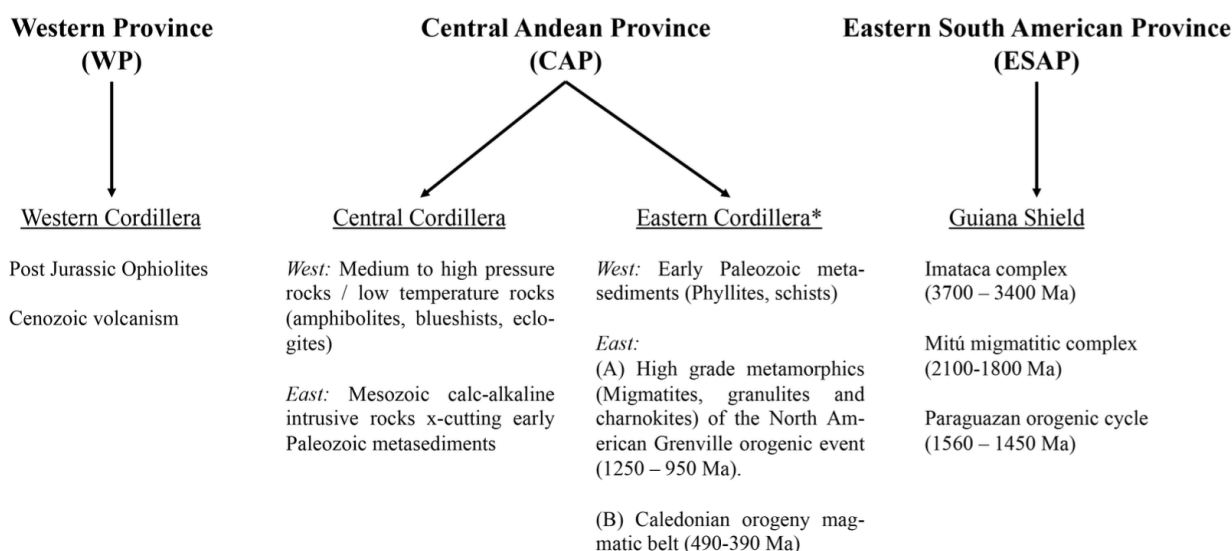
Western Province (WP)	Central Andean Province (CAP)		Eastern South American Province (ESAP)
Western Cordillera	Central Cordillera	Eastern Cordillera*	Guiana Shield
Post Jurassic Ophiolites Cenozoic volcanism	*West:* Medium to high pressure rocks / low temperature rocks (amphibolites, blueshists, eclogites) *East:* Mesozoic calc-alkaline intrusive rocks x-cutting early Paleozoic metasediments	*West:* Early Paleozoic meta-sediments (Phyllites, schists) *East:* (A) High grade metamorphics (Migmatites, granulites and charnokites) of the North American Grenville orogenic event (1250 – 950 Ma). (B) Caledonian orogeny magmatic belt (490-390 Ma)	Imataca complex (3700 – 3400 Ma) Mitú migmatitic complex (2100-1800 Ma) Paraguazan orogenic cycle (1560 – 1450 Ma)

Fig. 3. Overview of the three geological provinces of Colombia. *including the Sierra de Perijá and the Sierra Nevada de Santa Marta.

the late Paleozoic and Mesozoic. Accordingly, an east-directed, paired-metamorphic, belt-like succession of lithologies is found: The western part of the Central Cordillera yields inlayers of medium to high-pressure / low temperature metamorphic rocks (amphibolites, blueshists and eclogites; Bustamante et al., 2012), towards east, numerous intrusions of Arc-related Triassic to Cretaceous calk-alkaline magmas (and associated volcanic rocks) and rift-related Perm-Triassic peraluminous magmas crosscut the predominantly metasedimentary base (Spikings et al , 2015).

4. Western Province (WP)

The western province is the youngest of the three provinces comprising the base of Colombia and host the Western Cordillera (Cordillera Occidental). No pre-Mesozoic high-grade metamorphic inlayers are known and there are no apparent connections to the metamorphic basements of the CAP or ESAP. The WP predominantly hosts oceanic (ophiolitic) fragments such as (ultra-) mafic rocks, serpentinites, deep-sea sediments (red shales, black schists) presumably related to an oceanic hot-spot setting which was active 99 – 87 Ma ago (Kerr et al., 1997; Villagomez et al., 2011). The base of the WP is today crosscut and partly overlain by the active volcanic arc formed during the ongoing subduction of the Nazca plate below Colombia.

References

Banks, D. A., Giuliani, G., Yardley, B. W. D., & Cheilletz, A., 2000, Emerald mineralisation in Colombia: fluid chemistry and the role of brine mixing. Mineralium Deposita, v. 35, no. 8, p. 699-713.

Branquet, Y., Laumonier, B., Cheilletz, A., & Giuliani, G., 1999, Emeralds in the Eastern Cordillera of Colombia: Two tectonic settings for one mineralization. Geology, v. 27, no. 7, p. 597-600.

Bustamante, A., Juliani, C., Essene, E. J., Hall, C. M., & Hyppolito, T., 2012. Geochemical constraints on blueschist-and amphibolite-facies rocks of the Central Cordillera of Colombia: the Andean Barragán region. International Geology Review, v. 54, no. 9, p. 1013-1030.

Hurley, P. M., Rand, J. R., Pinson, W. H., Fairbairn, H. W., de Almeida, F. F. M., Melcher, G. C., ... & Vandoros, P., 1967, Test of Continental Drift by Comparison of Radiometric Ages: A pre-drift reconstruction shows matching geologic age provinces in West Africa and Northern Brazil. Science, v. 157, no. 3788, p. 495-500.

Johnson, J. G., Boucot, A. J., & Hallam, A., 1973. Devonian brachiopods. Atlas of Palaeobiogeography. Elsevier, Amsterdam, p. 89-96.

Kerr, A. C., Marriner, G. F., Tarney, J., Nivia, A., Saunders, A. D., Thirlwall, M. F., & Sinton, C. W., 1997, Cretaceous Basaltic Terranes in western Columbia: elemental, chronological and Sr–Nd isotopic constraints on petrogenesis. Journal of petrology, v. 38, no. 6, p. 677-702.

Kroonenberg, S. B., 1982, A Grenvillian granulite belt in the Colombian Andes and its relation to the Guiana Shield. Geologie en Mijnbouw, v. 61, no. 4, 325-333.

Spikings, R., Cochrane, R., Villagomez, D., Van der Lelij, R., Vallejo, C., Winkler, W., & Beate, B., 2015, The geological history of north-western South America: From Pangaea to the early collision of the Caribbean Large Igneous Province (290–75 Ma). Gondwana Research, v. 27, no. 1, p. 95-139.

Suarez, A. F., 1990, The basement of the Eastern Cordillera, Colombia: An allochthoneous terrane in northwestern South America. Journal of South American Earth Sciences, v. 3, no. 2-3, p. 141-151.

Villagómez, D., Spikings, R., Magna, T., Kammer, A., Winkler, W., & Beltrán, A., 2011, Geochronology, geochemistry and tectonic evolution of the Western and Central cordilleras of Colombia. Lithos, v. 125, no. 3, p. 875-896.

Chapter 4
Tectonics of the Central and Eastern Cordilleras and Sierra Nevada de Santa Marta, Colombia

Nicolas Oestreicher and Riccardo Reitano

1. Introduction

Our journey through Colombia brings us to four main mountain ranges, the three cordilleras and Sierra Nevada de Santa Marta. Here, we attempt to describe and understand the structure and formation of three of them, the Central Cordillera (CC), the Eastern Cordillera (EC) and the Sierra Nevada de Santa Marta (SNSM), from their formation to their current tectonic configuration.

The present-day configuration of the Northern Andean Block (NAB; Cediel et al., 2003) is the result of a complex interaction between three tectonic plates: the South American Plate, the Farallón-Nazca Plate and the Caribbean Plate (Fig. 1). Some authors also consider the presence and the accretion of the Panama Arc (e.g. Gregory-Wodzicki, 2000) as a major tectonic feature in the building of the NAB. This interaction is characterized by a series of orogenic events since the Proterozoic. Different terranes are involved since
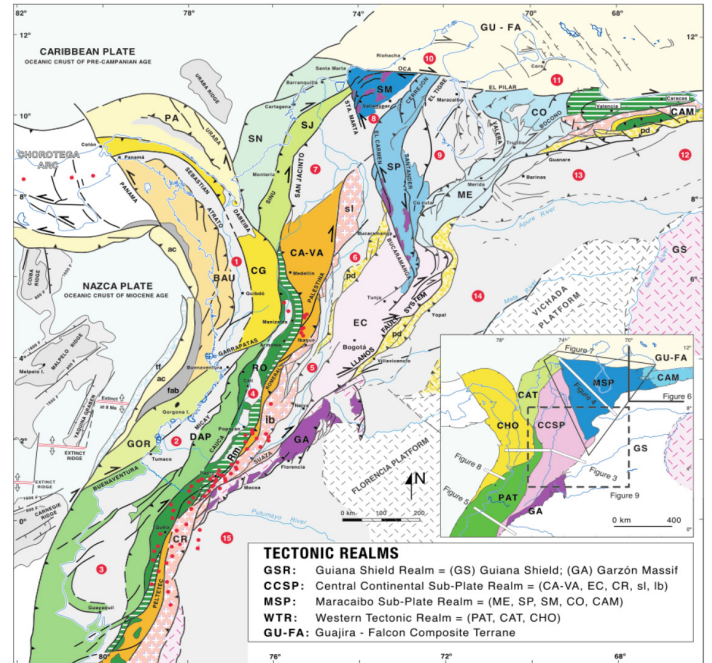

Fig. 2. Lithotectonic and morphostructural map of northwestern South America. GS = Guiana Shield; GA = Garzón massif; SP = Santander massif – Serranı́a de Perijá; ME = Sierra de Mérida; SM = Sierra Nevada de Santa Marta; EC = Eastern Cordillera; CO = Carora basin; CR = Cordillera Real; CA-VA = Cajamarca-Valdivia terrane; sl = San Lucas block; ib = Ibagué block; RO = Romeral terrane; DAP = Dagua-Piñón terrane; GOR = Gorgona terrane; CG = Cañas Gordas terrane; BAU = Baudó terrane; PA = Panamá terrane; SJ = San Jacinto terrane; SN = Sinú terrane; GU-FA = Guajira-Falcon terrane; CAM = Caribbean Mountain terrane; Rm = Romeral mélange; fab = fore arc basin; ac = accretionary prism; tf = trench fill; pd = piedmonte; 1 = Atrato (Chocó) basin; 2 = Tumaco basin; 3 = Manabı́ basin; 4 = Cauca-Patı́a basin; 5 = Upper Magdalena basin; 6 = Middle Magdalena basin; 7 = Lower Magdalena basin; 8 = Cesar-Rancherı́a basin; 9 = Maracaibo basin; 10 = Guajira basin; 11 = Falcon basin; 12 = Guarico basin; 13 = Barinas basin; 14 = Llanos basin; 15 = Putumayo-Napo basin; Additional Symbols: PALESTINA = fault/suture system; red dot = Pliocene-Pleistocene volcano; Bogotá = town or city (from Cediel et al., 2003).

the Paleozoic (Taboada et al., 2000; Cediel et al., 2003; Silva et al., 2013), and today it is possible to recognize four different tectonic realms (in deformation history and provenance) (Fig. 2; Cediel et al., 2003): the Guiana Shield Realm (GSR); the Central Continental Sub-Plate Realm (CCSP), in which Magdalena valley, CC and EC are included; the Maracaibo Sub-Plate Realm (MSP), which the SNSM is part of; and the Western Tectonic Realm (WTR). Throughout much of the Cenozoic, the convergence in the NAB has been dextral-oblique. This information is sustained by onshore kinematic data that show a dominant dextral component between the different terranes.
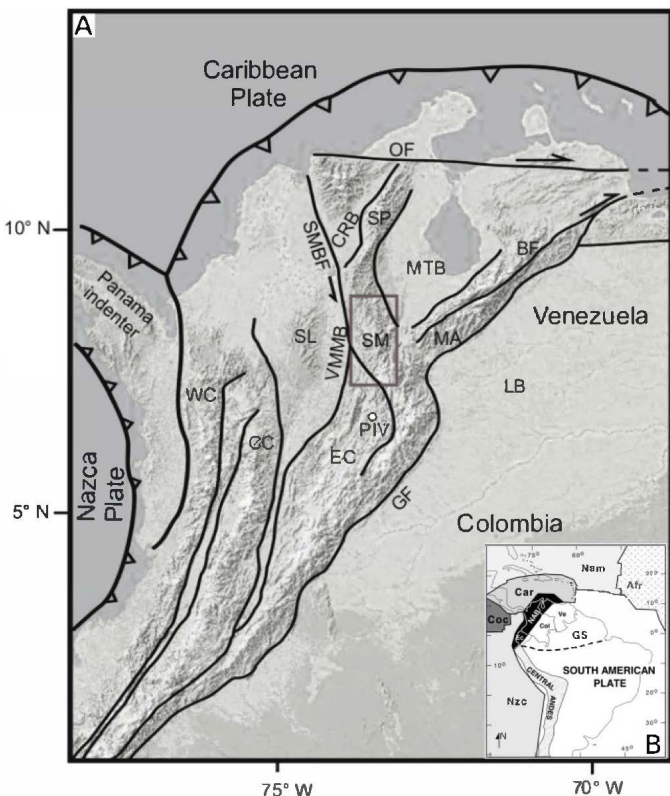

Fig. 1. Overview map of the Northern Andes WC: Western Cordilera, CC: Central Cordillera, EC: Eastern Cordillera; MTB: Maracaibo Triangular Block, SNSM: Sierra Nevada de Santa Marta, MA: Mérida Andes, SM: Santander Massif, SL: Serrania de San Lucas, SP: Sierra de Perija, LB: Llanos Basin, BA: Barinas-Apure Basin, MC: Maracaibo Basin, VMMB: Valley Middle Magdalena Basin, CRB: Cesar-Rancheria Basin, SMBF: Santa Marta–Bucaramanga fault, OF: Oca fault, BF: Bocono fault, GF: Guaicaramo fault, PIV: Paipa-Iza Volcano. Modified from Amaya et al., 2017 and Cediel et al., 2003.

2. Eastern Cordillera

The Colombian EC is a fold-and-thrust belt oriented NNE-SSW, comprised of Precambrian to Paleozoic basement covered by a thick sequence of Mesozoic-Tertiary sedimentary rocks (Alvarez and Roser, 2007). It is an inverted sedimentary basin that records deep crustal rifting in the CCSP (and along the continental margin of South America) during the Late Jurassic to Middle Cretaceous (Cooper et al., 1995, Cediel et al., 2003, Egbue et al., 2014). This is linked to the separation of North and South America and to backarc extension east of the Central Cordillera (Cooper et al., 1995, Mora et al., 2010). The inversion involves two parallel basins (the Tablazo-Magdalena Basin to the west and the Cocuy Basin to the east, separated by the Santander High) and started in the Paleogene. The dual northeast-directed and north-west-directed transpressive stresses exerted by the WTR and MSP, respectively, on the CCSP resulted in the uplift of the EC as a pop-up structure (Cediel et al., 2003). The seismic data (Taboada et al., 2000, Chiarabba et al., 2016) identify a possible slab tear (Caldas Tear; Idárraga-García et al., 2016) at latitude of ~5°N, with a flat subduction north of this tear that increases its steepness to ~50° beneath the EC (Bucaramanga nest in Chiarabba et al., 2016, Fig. 3). Flattening should have started around ~10 Ma, synchronous with the uplift of the EC. Therefore, it is possible to speculate that the surge of com-

pressive deformation at ~10-15 Ma leading to the formation of the EC may be directly related to the onset of the flat subduction episode, due to increased plate coupling. The deformation exploited a pre-existing zone of weakness formed during Late Jurassic to Middle Cretaceous rifting (Chiarabba et al., 2016).

3. Central Cordillera

The Cordillera Central's long tectonic history started as Paleozoic gneisses were intruded by Permian magmatic bodies in a backarc setting, during the formation of the Pangaea (Villagomez et al., 2011). Triassic sediments were deposited on top of them, filling a rift basin that eventually led to their partial melting. During the early Jurassic, the start of the Thetys-Pacific Wilson cycle is marked by subduction and back-arc magmatism (Villagomez et al., 2013). In the Cretaceous, migration of the arc axis to the West (Quebradagrande arc) and synchronous extension of the Central Cordillera is followed by tectonic inversion and uplift during obduction of the Quebradagrande volcanic arc and of the newly formed Caribbean Large Igneous Province (CLIP) (Villagomez and Spikings, 2013, Jaramillo et al., 2017). As in the Eastern Cordillera, influence of the Caldas tear is manifested by the discontinuity in depth of seismic events at the vicinity of 5°N, the location of main mineral deposits, the higher density of volcanoes, and possibly a change in the distribution and properties of hydrocarbon fields and flow paths of the Magdalena and Cauca rivers (Vargas and Mann, 2013, Fig. 4).

4. Sierra Nevada de Santa Marta

The Sierra Nevada de Santa Marta (SNSM) massif is the highest mountain chain in the Caribbean realm and is an isolated tectonic block, formed mainly by assemblage of Precambrian to Late Paleozoic metamorphic rocks, Jurassic-Cretaceous granitoids and metabasites from the Caribbean plate (Piraquive, 2017). The SNSM massif formed in response to the early subduction of the Caribbean Plate during the Paleogene (Ayala et al., 2012, Bayona et al., 2011), and allowed the accretion of allochthonous terranes to NW Gondwana. It is part of the Maracaibo block, and its triangular shape is due to three intracontinental faults: the sinistral Santa Marta-Bucaramanga fault on its western side, the dextral Oca-Ancón fault on its northern side, and the Cesar-Ranchería fault toward the southeast. The SNSM represent a continent-ward dipping monocline, and exposes a complex crustal profile, with highly mobilized high-grade sequences on a undisturbed Meso-proterozoic basement (Piraquive, 2017).

Particularities of the Sierra Nevada de Santa Marta are (Cardona, 2010):
• the high elevation of its summit (>5700 masl.) at only 40 km from the carribean coast. This makes it one of the highest coastal ranges in the world.
• Isolation. Thanks to its particular geomorphology, it is hardly accessible, and less threatened by modern civiliza-
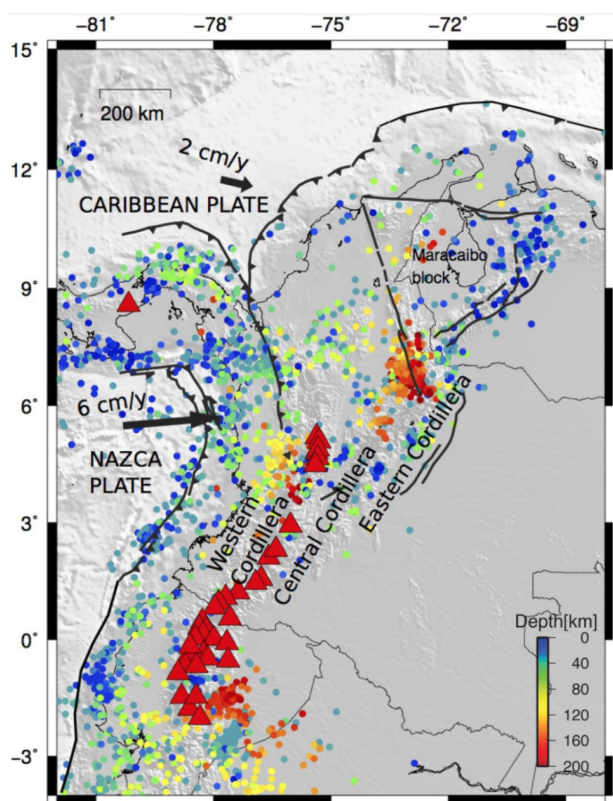

Fig. 3. Seismicity and volcanism of NW South America. Black arrows indicate plate velocity relative to stable South America, red triangles indicate volcanoes. Colored circles indicate earthquakes recorded during 1993–2009. It's possible to observe the depth of earthquakes, the Bucaramanga nest and the stop of the volcanism north of 5°N of latitude (from Chiarabba et al., 2016).
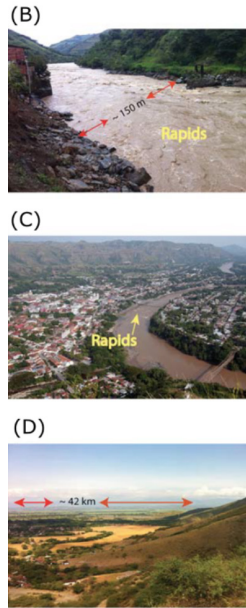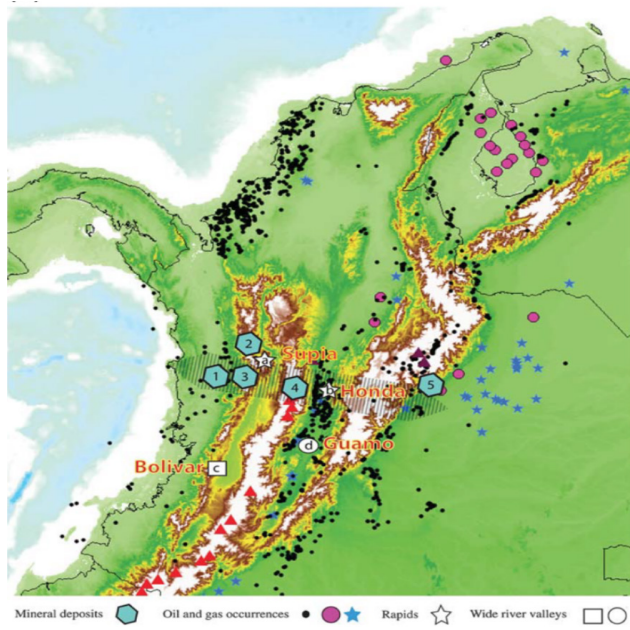
Fig. 4. Surficial evidences of the Caldas tear related to mineral deposits, hydrocarbon occurrences, and geomorphological anomalies. (a) Blue hexagons, map of distribution of high-grade mineral deposits of platinum, gold, and copper: (1) Condoto, (2) Marmato, (3) Quinchia, (4) La Colosa, and (5) Cerro de Cobre. Black dots, oil and gas seepages. Purple circles are giant hydrocarbon fields. Blue stars are other oil and gas fields. White stars, hydraulic anomalies of the Cauca and Magdalena rivers on the Caldas tear (rapids on the Supia and the Honda). White circle and square are places upstream the rivers where there are broad valleys (Bolivar and Guamo). (B), (C), and (D) are geomorphological anomalies that represent surficial evidence of the Caldas tear (Cauca River near Supia town, Magdalena River near Honda town and a broad valley upstream of the Cauca River, near to Guamo town; from Vargas and Mann, 2013).

tion. It is one of the last refuges for pre-colombian cultures and a biodiversity hotspot.

• A strong positive gravimetric anomaly. Together with the high elevation gradient, it shows that the SNSM is out of isostatic balance and that uplift leading to its present shape must be recent.

5. Excursion Stops

Stop 1: Surface Expression of the Caldas Tear.

In the CC, we propose to observe the change of morphologies in valleys crossing our path that are possibly a surface expression of the Caldas tear. We can do this near the cities of Supia and/or Honda (Cauca and Magdalena rivers respectively, Figure 4A and 4B), where it is possible to observe geomorphological anomalies (rapids) possibly related to Caldas tear.

Stop 2: Quaternary Seismic Activity on the Western Margin of SNSM.

In the SNSM, we propose to look for a fault (Structure Satellite A, close to Riofrio city and Frío River in Idárraga-García et al., 2010, Fig. 5) and try to understand its role in the recent deformation of the SNSM. Idárraga-García et al. (2010) identified paleosols of probable Quaternary age deformed by a seismic event, but without dating. The minimum inferred magnitude was Mw 6.4. Seismicity causes significant risks for a couple of large cities in the region and so the estimation of seismic risk is crucial.

References

Alvarez, N.C. and Roser, B.P., 2007, Geochemistry of black shales from the Lower Cretaceous Paja Formation, Eastern Cordillera, Colombia: Source weathering, provenance, and tectonic setting: Journal of South American Earth Sciences, v. 23, no. 4, p. 271–289.

Amaya, S., Zuluaga, C.A. and Bernet, M., 2017, New fission-track age constraints on the exhumation of the central Santander Massif: Implications for the tectonic evolution of
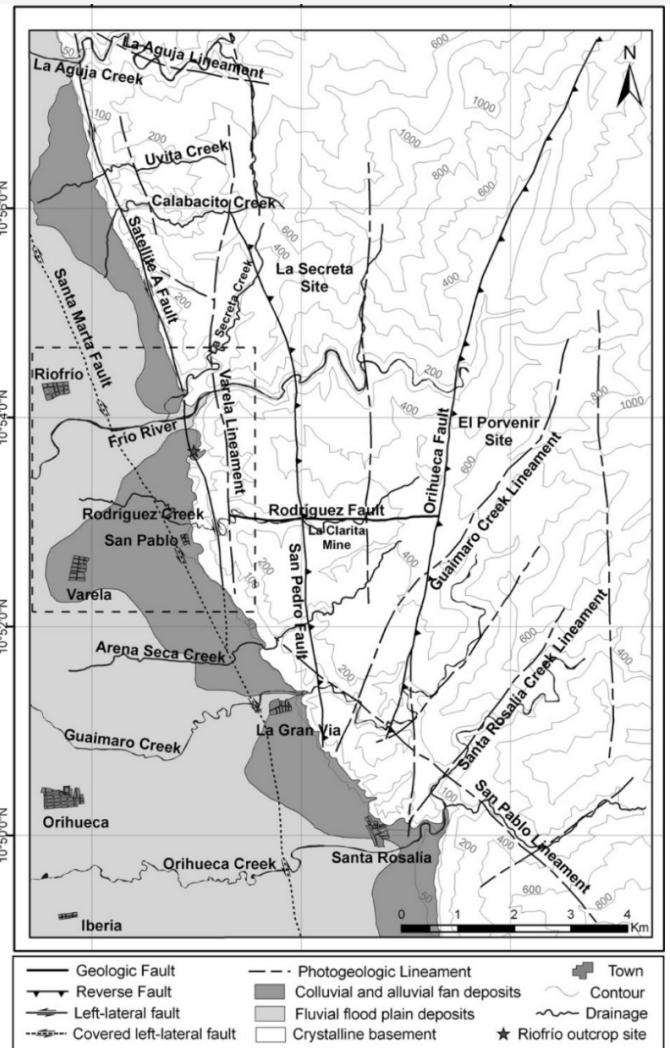
Fig. 5. Fault traces of the SMFS in the La Aguja Creek–Orihueca Creek sector (from Idárraga-García et al., 2010). Our study will be focused on Satellite A Fault, close to Riofrio city and Frio River (dashed square).

the Northern Andes, Colombia: Lithos, v. 282, p. 388–402.

Ayala, R.C., Bayona, G., Cardona, A., Ojeda, C., Montenegro, O.C., Montes, C., Valencia, V. and Jaramillo, C., 2012, The Paleogene synorogenic succession in the northwestern Maracaibo block: tracking intraplate uplifts and changes in sediment delivery systems: Journal of South American Earth Sciences, v. 39, p. 93–111.

Bayona, G., Montes, C., Cardona, A., Jaramillo, C., Ojeda, G., Valencia, V. and Ayala-Calvo, C., 2011, Intraplate subsidence and basin filling adjacent to an oceanic arc–continent collision: a case from the southern Caribbean-South America plate margin: Basin Research, v. 23, no. 4, p. 403–422.

Cardona, A., & Ojeda, G. Y., 2010, Special volume: Geological evolution of the Sierra Nevada de Santa Marta and adjacent basins, Colombian Caribbean region: Journal of South American Earth Sciences, v. 29, p. 761–763.

Cediel, F., Shaw, R.P. and Cáceres, C., 2003, Tectonic assembly of the northern Andean block: American Association of Petroleum Geologists Special Volume.

Chiarabba, C., De Gori, P., Faccenna, C., Speranza, F., Seccia, D., Dionicio, V. and Prieto, G.A., 2016, Subduction system and flat slab beneath the Eastern Cordillera of Colombia: Geochemistry, Geophysics, Geosystems, v. 17, no. 1, p. 16–27.

Cooper, M.A., Addison, F.T., Alvarez, R., Coral, M., Graham, R., Hayward, A.B., Howe, S., Martinez, J., Naar, J., Peñas, R. and Pulham, A.J., 1995, Basin development and tectonic history of the Llanos Basin, Eastern Cordillera, and middle Magdalena Valley, Colombia: American Association of Petroleum Geologists Bulletin, v. 79, no. 10, p. 1421–1442.

Egbue, O., Kellogg, J., Aguirre, H. and Torres, C., 2014, Evolution of the stress and strain fields in the Eastern Cordillera, Colombia: Journal of Structural Geology, v. 58, p. 8–21.

Gregory-Wodzicki, K.M., 2000, Uplift history of the Central and Northern Andes: a review: Geological Society of America Bulletin, v. 112, no. 7, p. 1091–1105.

Idárraga-García, J., & Romero, J., 2010, Neotectonic study of the Santa Marta Fault System, Western foothills of the Sierra Nevada de Santa Marta, Colombia: Journal of South American Earth Sciences, v. 29, no. 4, 849–860.

Jaramillo, J.S., Cardona, A., León, S., Valencia, V. and Vinasco, C., 2017, Geochemistry and geochronology from Cretaceous magmatic and sedimentary rocks at 6° 35' N, western flank of the Central cordillera (Colombian Andes): Magmatic record of arc growth and collision: Journal of South American Earth Sciences, v. 76, p. 460–481.

Mora, A., Horton, B.K., Mesa, A., Rubiano, J., Ketcham, R.A., Parra, M., Blanco, V., Garcia, D. and Stockli, D.F., 2010, Migration of Cenozoic deformation in the Eastern Cordillera of Colombia interpreted from fission track results and structural relationships: Implications for petroleum systems: American Association of Petroleum Geologists Bulletin, v. 94, no. 10, p. 1543–1580.

Piraquive A.B., 2017, Structural Framework, deformation and exhumation of the Santa Marta Schists: accretion and deformational history of a Caribbean Terrane at the north of the Sierra Nevada de Santa Marta [Ph.D. thesis]: Bogotá, Universidad Nacional de Colombia, 394 p.

Silva, A., Mora, A., Caballero, V., Rodriguez, G., Ruiz, C., Moreno, N., Parra, M., Ramirez-Arias, J.C., Ibañez, M. and Quintero, I., 2013, Basin compartmentalization and drainage evolution during rift inversion: Evidence from the Eastern Cordillera of Colombia: Geological Society [London] Special Publications 377, p. 377–418.

Taboada, A., Rivera, L.A., Fuenzalida, A., Cisternas, A., Philip, H., Bijwaard, H., Olaya, J. and Rivera, C., 2000, Geodynamics of the northern Andes: Subductions and intracontinental deformation (Colombia): Tectonics, v. 19, no. 5, p. 787–813.

Vargas, C.A. and Mann, P., 2013, Tearing and breaking off of subducted slabs as the result of collision of the Panama Arc-Indenter with northwestern South America: Bulletin of the Seismological Society of America, v. 103, no. 3, p. 2025–2046.

Villagómez, D., Spikings, R., Magna, T., Kammer, A., Winkler, W., & Beltrán, A., 2011, Geochronology, geochemistry and tectonic evolution of the Western and Central cordilleras of Colombia. Lithos, v. 125, no. 3, p. 875-896.

Villagómez, D., & Spikings, R., 2013, Thermochronology and tectonics of the Central and Western Cordilleras of Colombia: Early Cretaceous–Tertiary evolution of the northern Andes: Lithos, v. 160, p. 228-249.

Chapter 5
Evolution of the Central Cordillera and Volcanic Hazards

Simone Moretti and Tobias Renz

1. Geologic Evolution of the Central Cordillera

The Central Cordillera of Colombia is the highest of three mountain ranges that built the northern part of the Andes mountain belt. There are three peaks above 5000 m (Nevado del Huila 5364 , Nevado del Ruiz 5311 m, Nevado del Tolima 5215 m), all of which are volcanoes belonging to the Northern Volcanic Province. The Central Cordillera is separated from the Western and Eastern Cordillera by the topographic depressions of the Cauca-Patia and Magdalena river valleys, respectively (Fig. 1). The Cauca-Patia valley is located west of the Cauca-Almaguer Fault (CAF), which defines the break-off slope of the Central Cordillera and is the western branch of the Romeral-Fault-System (RFS). The RFS also comprises the Silvia-Pijao Fault (SPF) and San-Jerónimo Fault (SJF) and represents the Jurassic-Early Cretaceous continental margin (Villagómez et al. 2011). To the west, the CAF sutur separates the Paleozoic metamorphic rocks of the Central Cordillera basement from the allochthonous, mafic and ultramafic rocks of the Western Cordillera. To the east, the Central Cordillera is bounded by the Otú-Pericos fault system, which separates it from the Proterozoic metamorphic basement of the Eastern Cordillera (Jaramillo et al. 2017).

The following is a summary of the major geological events that occurred in the Cordillera Centralb:

1) ~600 – 350 Ma: The continental margin of the South American Plate underwent a complete Wilson cycle (Villagómez et al. 2011).

2) South America was the western active continental margin of Pangaea with eastward dipping subduction zone (Permian arc magmatism) (Villagómez and Spikings, 2013).

3) 240 – 216 Ma: In the Middle Permian to Middle Triassic continental rifting led to extension, intrusion of tholeiitic and later ultramafic basalts and partial anatexis of the crust. During the rifting the Central American crustal blocks were detached. The western plate margin was composed of Permo-Triassic meta-granites, gneisses and migmatites that constitute the basement of the Western Cordillera (Spikings et al., 2015; Vinasco et al., 2006).

4) 216 – 209 Ma: South America was the western passive continental margin of Pangaea (Spikings et al. 2015).

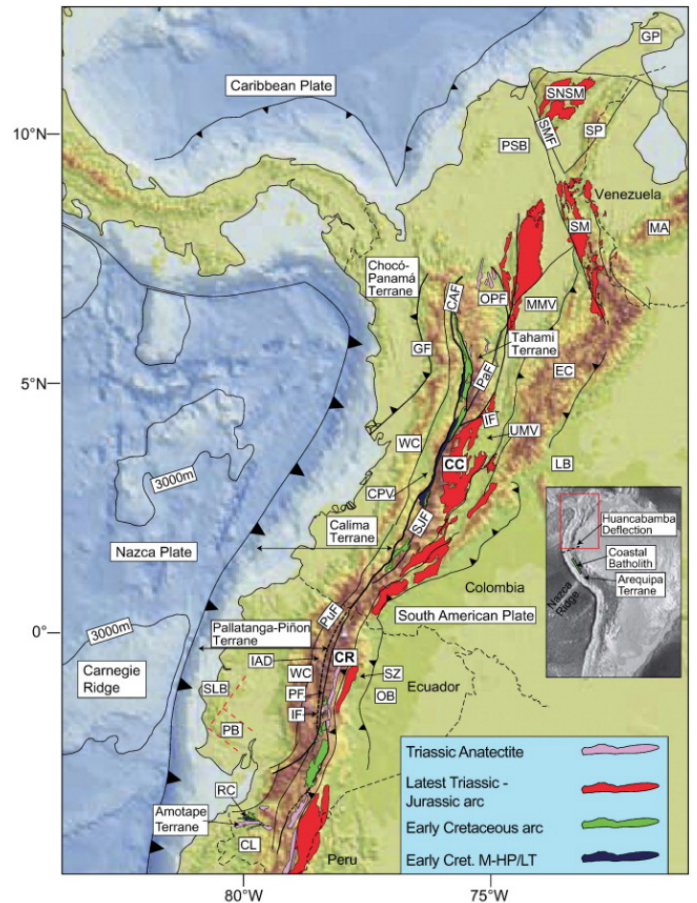5) 209 – 145 Ma: An east-dipping subduction zone was established east of the South American margin during

Fig.1. Digital elevation model for northwestern South America showing the cordilleras, main faults and the exposure of Triassic–Early Cretaceous magmatic rocks in Colombia. Faults: CAF: Cauca-Almaguer Fault, GF: Garrapatas Fault, IF: Ibagué Fault, OPF: Otu-Pericos Fault, PaF: Palestina Fault, PF: Peltetec Fault, PuF: Pujili Fault, SJF: San-Jeronimo Fault, SMF: Santa Marta Fault. Other abbreviations: CC: Cordillera Central, CL: Celica-Lancones Basin, CPV: Cauca-Patía Valley, CR: Cordillera Real, GP: Guajira Peninsula, IAD: Interandean Depression, IF: Ingapirca Fault (western boundary of the Guamote Sequence), LB: Llanos Basin, MA: Merida Andes, MMV: Middle Magdalena Valley Basin, OB: Oriente Basin, PB: Piñon Block, PSB: Plato-San Jorge Basin, RC: Raspas Complex, SLB: San Lorenzo Block, SM: Santander Massif, SP: Sierra de Perija, SZ: Sub-Andean Zone, UMV: Upper Magdalena Valley Basin, WC: Western Cordillera (Spikings et al. 2015).

Late Triassic with a westward migrating continental magmatic arc (Triassic plutons). During the Jurassic, a long-lived calc-alkaline, metalumous arc at the position of the central Cordillera led to the emplacement of batholites (e.g. Ibagué). These Tonalities and granodiorites are typically unfoliated (Spikings et al., 2015).

6) 145 – 130 Ma: Due to slab roll-back, the magmatic arc migrated westwards, which led to extension and thinning

of the continental crust and exhumation of a Proto-Central Cordillera in the back-arc and intrusion of plutons into the Paleozioc metasedimentary rocks and Triassic anatectites (3). These Early Cretaceous diorites and granodiorites are in faulted contact with the Paleozoic rocks to the west and the Jurassic batholithes to the east via the Cosanga Fault (Spikings et al., 2015).

7) 130 – 115 Ma: Formation of an intra-oceanic or epicontinental arc on thinned continental crust (Jaramillo et al., 2017) with a back-arc basin that fringed the western margin of South America. The Quebradagrande Arc Complex is composed of low-grade metamorphosed intrusive and subaqueous extrusive rocks (basalts, andesites and pyroclastics) and pelagic metasediments. Detritus from the Proto-Central Cordillera was deposited to the east (Caballos Fm., Magdalena valley) and west, where it overlies the Quebradagrande Complex as Abejorral Fm. (Villagómez and Spikings 2013, Spikings et al. 2015).

8) 115 – 105 Ma: The closure of the back-arc subsequently led to the accretion of the Quebradagrande Complex, forming the SJF west of the Paleozoic and Triassic sequence. The high and medium pressure, low-temparature rocks of the Arquía Complex (former subduction trench) are juxtaposed against the Quebradagrande Complex along the SPF (Villagómez and Spikings 2013).Further

compression led to uplift of the continental margin and enhanced erosion accompanied by sedimentation to the west and east.

9) 100 – 75: After the collision, the onset of the east-dipping subduction resulted in the development of a Late Cretaceous continental magmatic arc and emplacement of plutons and batholithes (Antioquia, Córdoba). West of the South American plate the plateau flood basalts of Carribean Large Igneous Province (CLIP) erupted and converged towards South America (Villagómez and Spikings, 2013).

10) 90 – 80 Ma: An additional west-dipping subduction zone underneath the CLIP formed, while the east-dipping subduction under South America persisted. The CLIP was subsequently intruded by island arc magmatites (Villagómez and Spikings, 2013, Jaramillo et al., 2017).

11) 80 – 70 Ma: The Collision of the CLIP with South America along CAF led to compression, rapid uplift, and subsequent enhanced erosion and rapid exhumation. The uplift of the Central Cordillera was contemporaneous with the deposition of alluvial sedimentary sequences to the east (Cobre Fm.) and west (Nogales Fm.) (Villagómez and Spikings ,2013).

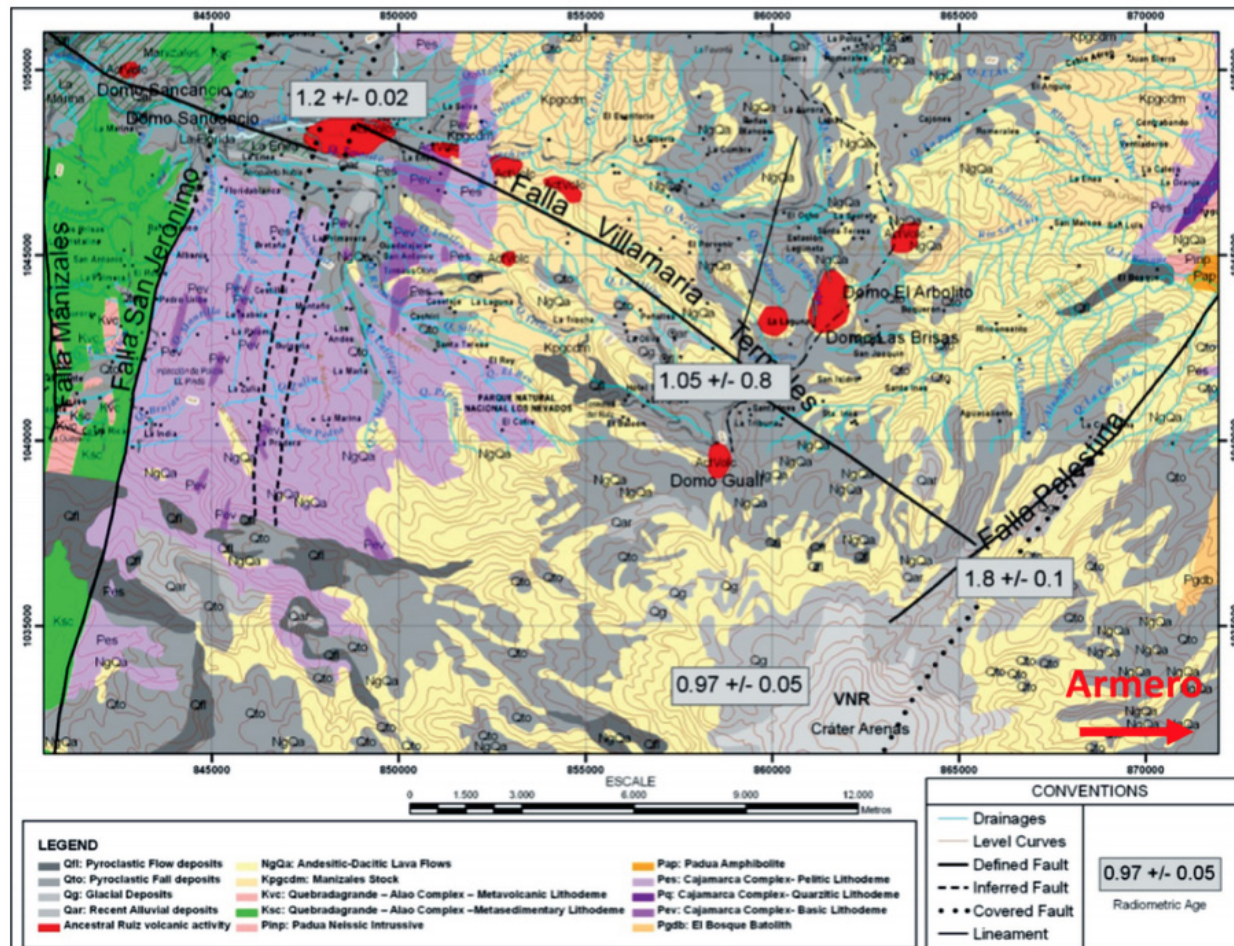12) 70 – 60 Ma: The subduction zone with a continental

Fig. 2. Geological map of the area north of the Nevado del Ruiz

arc persisted after the collision. The uplift of the Central Cordillera was slow and restricted to discrete faulted blocks (Villagómez and Spikings, 2013).

13) 25 – 0 Ma: A change in convergence angle and rates from slow and oblique to a fast E-W convergence initiated a stage of fast uplift in the Andean mountain belt. The magmatic arc was shifted far to the east and moved slowly westward to its present day position underneath the Central Cordillera (McCourt et al., 1984).

2. The Nevado del Ruiz

The Nevado del Ruiz volcano is located approximately 130 km from Bogota and covers an area of 200 km², with a maximum elevation of 5321 m above sea level, representing the largest volcano in the Ruiz-Tolima massif, in the Cordillera Central of the Colombian Andes (Thouret et al. 1990). It is topped with a 10 km² ice-cap above 4800 m (Nevado means "snow-covered" in Spanish), divided into different glacier systems. Due to anthropogenic warming, the ice cover of the volcano has been strongly affected over the last two decades, with estimated losses of 40-50% in ice volume (Huggel et al., 2007). Nevado del Ruiz is an active cone-shaped stratovolcano, overlain by a cluster of 5 lava domes, nested in what is thought to be a collapsed caldera at its summit. The volcano lies at the intersection of two major faults in the area: the Palestina and the Villamaria-Thermales faults (Fig. 2), and it seems clear that these tectonic structures have been playing a major role in channeling the magma produced by the Nazca plate subduction into the Nevado del Ruiz volcano and its surroundings. The volcanic activity of the Nevado del Ruiz is characterized by alternating effusive to explosive phases during the last 2-3 Myr (Thouret et al. 1990). Typical effusive products are volcanic domes and thick lava flows, while explosive products include ash fall and pyroclastic flows deposits. The composition of effusive and explosive products varies between andesitic and dacitic, typical of subduction-related calc-alkaline volcanoes (Borrero et al.

2009).

2. Quaternary History of Nevado del Ruiz Eruptions

The area of Nevado del Ruiz has been volcanically active for millions of years. The first activity that can be closely related to the modern Nevado del Ruiz is a constructive volcanic phase that started at 1.8 Ma with effusion of andesitic lava flows and terminated 1 Ma ago, followed by a first destructive phase that resulted in the formation of a first caldera, part of which can still be observed as a semi-circular depression. A second constructive phase started at 0.8 Ma with the building of a stratovolcano of andesitic lava flows inside this ancient caldera, before being terminated by a second destructive phase at 0.2 Ma, with the formation of a new, second caldera at the summit of this stratovolcano documented by the presence of a pyroclastic deposit. The most recent constructive-destructive cycle started 0.15 Ma, with an initial constructive phase represented by a series of composite domes and short and thick lava flows clustering at the top, nested into what is thought to be the second caldera. The still ongoing destructive phase 0.01 Ma is characterized by multiple ash fall and pyroclastic flows events linked to explosive volcanic activity.

3. Volcanic Hazards and the Armero Tragedy

Despite the explosive activity of Nevado del Ruiz, the relatively small distribution and magnitude of the deposits related to explosive eruptions in the geological record suggest that the eruption per se does not constitute the major threat for local inhabitants. Nevertheless, the presence of large volumes of water (10 km²) in form of ice on the volcano, together with the explosive activity of the volcano, creates the precondition for the formation of catastrophic lahars, cohesive and violent mud- or debris flows created by the interaction of fine volcanic material and water.
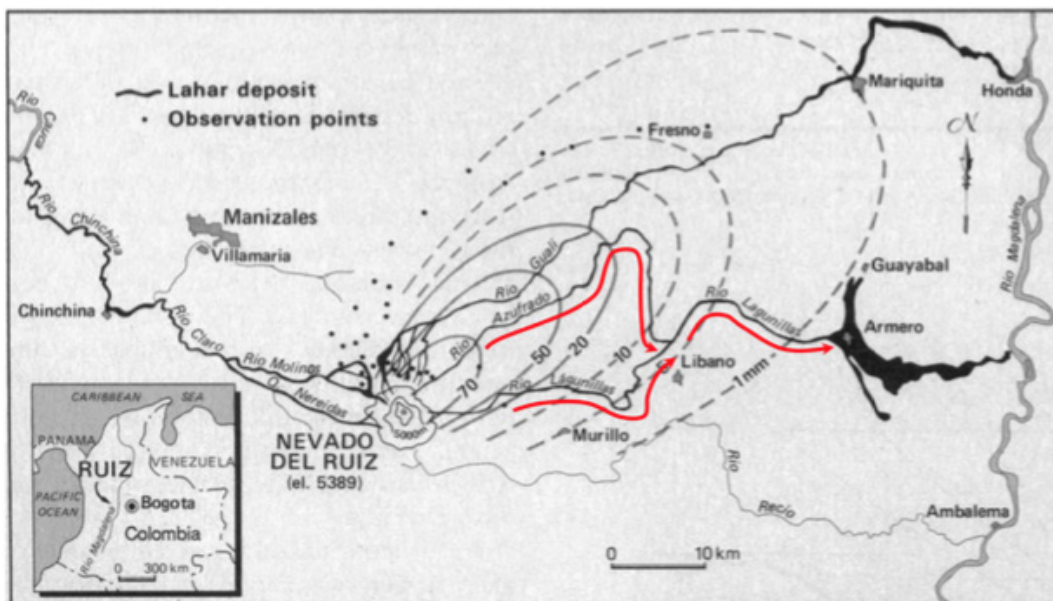

Fig. 3. Distribution of tephra fall (dashed lines) and lahar deposits (black) from the 13 November 1985 eruptions. Red arrows show the flow of the lahars that flooded the town of Armero.

On the evening of November 13th, 1985, a small plinian eruption and its products caused the meltover of around 10% of the volcano's ice caps (Naranjo et al., 1986). This led to the subsequent formation of 3 major lahars, that descended into the major steep valleys surrounding the Nevado del Ruiz. On the eastern flank of the volcano, the lahar that filled the Azufrado valley, joined and merged the ones flowing down the Lagunillas valley (Fig. 3). At 11 p.m. the combined lahar inundated the town of Armero located few km downstream, claiming the life of 25.000 inhabitants, the deadliest lahar in recorded history.

References

Borrero, C., Toro, L. M., Alvarán, M. & Castillo, H., 2009, Geochemistry and tectonic controls of the effusive activity related with the ancestral Nevado del Ruiz volcano, Colombia: Geofísica International, v. 48, p. 149–169.

Huggel, C., Ceballos, J. L., Pulgarĺn, B., Ramírez, J., Thouret, J.-C, 2007, Review and reassessment of hazards owing to volcano-glacier interactions in Colombia: Annals of Glaciology, v. 45, p. 128–136.

Jaramillo, J. S., Cardona, A., Leon, S., Valencia, V., Vinasco, C., 2017, Geochemistry and geochronology from Cretaceous magmatic and sedimentary rocks at 6 degrees 35 ' N, western flank of the Central cordillera (Colombian Andes): Magmatic record of arc growth and collision: Journal of South American Earth Sciences, v. 76, p. 460–481.

McCourt, W. J., Aspden, J. A., Brook, M., 1984, New Geological and Geochronological Data from the Colombian Andes - Continental Growth by Multiple Accretion: Journal of the Geological Society, v. 141, p. 831–845.

Naranjo, J. L., Sigurdsson, H., Carey, S. N. & Fritz, W., 1986, Eruption of the Nevado del Ruiz Volcano, Colombia, On 13 November 1985: Tephra Fall and Lahars: Science, v. 233, p. 961–963.

Spikings R., Cochrane R., Villagomez D., Van der Lelij R., Vallejo C., Winkler W., Beate B., 2015, The geological history of northwestern South America: from Pangaea to the early collision of the Caribbean Large Igneous Province (290–75Ma): Gondwana Research, v. 27, issue 1, p. 95-139.

Villagómez D., Spikings R., Magna T., Kammer A., Winkler W., Beltrán A., 2011, Geochronology, geochemistry and tectonic evolution of the Western and Central cordilleras of Colombia: Lithos, v. 125, issues 3–4, p. 875-896.

Villagómez D., Spikings R., 2013, Thermochronology and tectonics of the Central and Western Cordilleras of Colombia: Early Cretaceous–Tertiary evolution of the Northern Andes: Lithos, v. 160–161, p. 228-249.

Vinasco, C. J., Cordani, U. G., Gonzalez, H., Weber, M., Pelaez, C., 2006, Geochronological, isotopic, and geochemical data from Permo-Triassic granitic gneisses and granitoids of the Colombian Central Andes, Journal of South American Earth Sciences, v. 21, issue 4, p. 355–371.

Thouret, J.-C., Cantagrel, J. M., Salinas, R., Murcia, A, 1990, Quaternary eruptive history of Nevado del Ruiz (Colombia): Journal of Volcanology and Geothermal Research, v. 41, p. 225–251.

Chapter 6
The Nazca subduction and the Western Cordillera

Nadezhda Paneva and Fabio Cafagna

1. Introduction

The Andean Cordillera is one of the most important active orogenic systems and formed by subduction of oceanic crust (the Nazca Plate) underneath continental crust (the South American Plate; Ramos, 2009). The geologic history of the Andes includes several different processes (accretions, collisions, subductions) that contributed to the fragmentation of the Andes in three main sections: Northern, Central, and Southern Andes. The Western Cordillera belongs to the westernmost part of the Northern Volcanic Zone. The Western Cordillera is considered to be part of the Caribbean-Colombian Cretaceous Province (CCCP; Fig. 1), a large oceanic plateau produced by partial melting within the plume head of the Galápagos hot spot (Kerr et al., 1997a). Emplaced on the eastward moving Farallon plate, the oceanic plateau maintained motion in the same direction. The northern part of the oceanic plateau drifted between North and South America, along with the Caribbean plate, whereas the southern segment collided with the NW continental margin of South America. The buoyant oceanic plateau was obducted in Latest Cretaceous-Paleogene, followed by accretion of an island arc in the Miocene (Kerr et al., 1997b). The Farallon plate was completely subducted, followed by the Nazca plate, which is currently subducting with the same eastward direction.
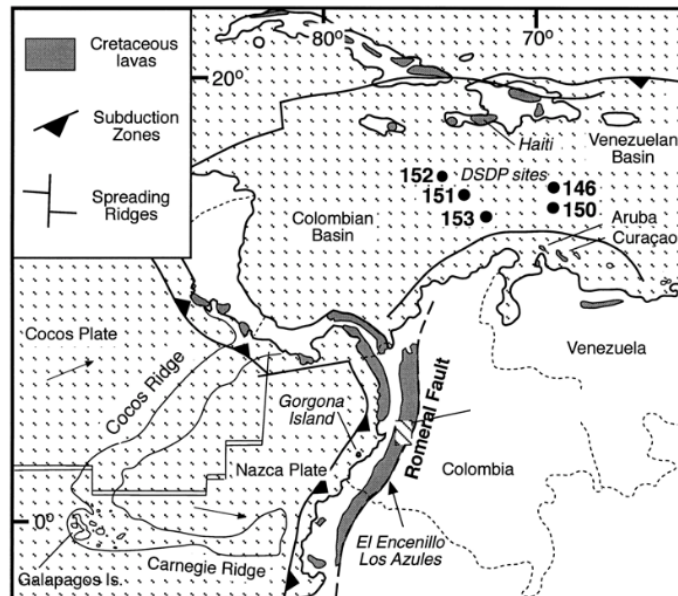
2. Geological History and Structure of the Western Cordillera

The dextral strike-slip Romeral fault marks the eastern boundary between the metamorphic basement with continental affinity to the east (e.g., Central Cordillera) and the terranes with oceanic affinity to the west. The Western Cordillera is divided in three main terranes, from east to west: Amaime, Piñón-Dagua and Chocó. Those three terranes represent genetically distinctive units, which collided sequentially with the NW margin of South America (Ramos, 2009; Fig. 2).
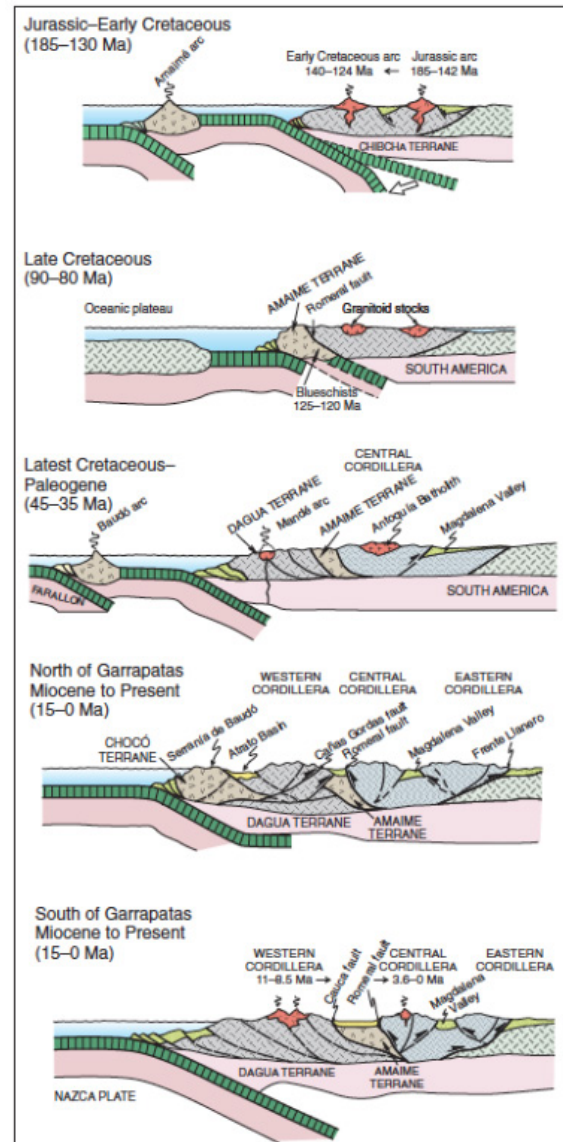

Fig. 1. (a) Map of the main outcrops of the Caribbean-Colobian Cretaceous oceanic plateau from Kerr et al., (1998).

Fig. 2. Schematic tectonic evolution of the Northern Andes at the latitude of Colombia showing the polarity of the subduction and subsequent collisions (from Kerr et al., 1997b).
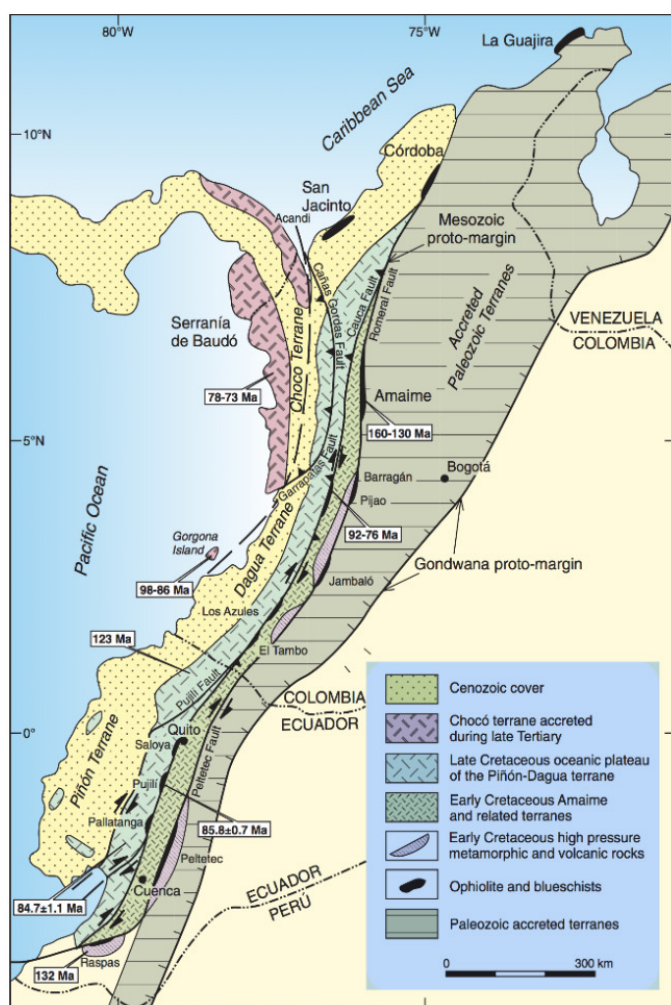
Fig. 3. Different oceanic rocks west of the Romeral-Peltetec fault system in western Colombia and Ecuador: Amaime terrane; Dagua-Piñón oceanic plateau; Chocó terrane (Ramos, 2009). The collision of the Chocó terrane in the middle Miocene thrusted part of the Dagua terrane to the east along the Cañas Gordas fault, north of Garrapatas fault.

The Amaime terrane is bounded by the Romeral Fault to the east and the Cauca-Patia fault to the west (Fig. 3). It is related to accretion of oceanic island arcs (e.g., the Amaime and Arquiá Arcs) during the Late Cretaceous. In addition, the Amaime terrane was partially affected by high pressure metamorphism. The thrusting of the ocean island arc over the active continental margin is marked by blueshist belt (Feininger, 1982) and eclogite lenses outcropping east of Cauca fault, in association with ultramafic tectonites (Aspden and McCourt, 1986). The metamorphic lenses are considered as evidence that this terrane marks the suture between the continental margin (east of the Romeral fault) and the accreted rocks with oceanic affinity (Ramos, 2009). The-Dagua terrane is bounded by the Cauca-Patia fault to the east and extends to the Pacific Ocean (Fig. 3). The Piñón-Dagua terrane is dominantly composed by deformed turbidites, pillow basalts, and smaller tectonically controlled emplacements of mafic and ultramafic rocks. Those mafic-ultramafic igneous bodies (e.g., the Bolivar-Riofrio Complex) were previously considered an ophiolitic sequence (Lebras et al., 1987),

but were later recognized as the accretion of the thick and buoyant oceanic plateau to the continental margin (Lapierre et al., 2000). Petrological, geochronological and paleomagnetic data suggest that a single plateau was accreted (Kerr et al., 1998; Luzieux et al., 2006), rather than multiple plateaus. The part of the Piñón-Dagua terrane south of the Garrapatas Fault has an east vergence, whereas the part located south of the Garrapatas Fault has a western vergence. This is due to the late accretion of the Chocó terrane onto the continental margin. The Chocó terrane is composed partly of rocks with oceanic plateau affinity and partly of rocks belonging to the Baudó oceanic island arc that collided approximately 13 Ma ago with the Northern Andean block and formed the Serranìa de Baudó at the border between Panama and Colombia. The mafic-ultramafic rocks outcropping on the Gorgona Island are also part of the Chocó terrane (Kerr and Tarney, 2005). Gorgona hosts the only known occurrence of Phanerozoic komatiites, but also picritic dykes, picritic breccias, pillow basalts, and olivine gabbros are present (Kerr et al., 1998). Komatiites are a very rare type of ultramafic, high Mg rocks with mantle origin, showing characteristic spinifex texture. They are almost completely restricted to the Archean, when the geothermal gradient was much higher. Proterozoic and Phanerozoic komatiites are extremely seldom.

3. Geological overview of the Bolivar mafic-ultramafic complex

The Bolivar-Riofrio Ultramafic complex (86-90 Ma; Kerr et al., 1997b), is the northernmost of several basic igneous complexes that are located west of the Romeral Fault. The Bolivar complex is approximately 30 km long and 5-10 km wide. It is located at the foothills of the Western Cordillera, east of the Cauca Patia Fault, which marks the contact between the complex and fault slices of pillow basalts and sediments (Fig. 4; Nivia, 1996; Kerr et al., 1998). The complex is a strongly deformed banded sequence of ultramafic and mafic rocks, representing deferent levels of oceanic crust. Based on ophiolite data the oceanic crust is divided from the lower to the upper level in layers: isotropic and layered peridotite, layered and isotropic gabbro, sheeted dike complex, pillow lavas and deep-sea sediments. The Bolivar complex is similar to an ophiolite sequence, composed of layers of serpentinized dunites alternated with lherzolitic bands, olivine websterites and gabbro-norites. These rocks are overlain by cumulative and isotropic gabbros. The southern part shows layered norites, olivine-norites, and gabbronorites, overlain by isotropic gabbro (Kerr et al., 1997a). The gabbro horizons underwent conspicuous amphibolitization, visible as clusters of cummingtonite and hornblende growing in pyroxene and plagioclase or as poikilitic amphiboles enclosing all minerals (Nivia, 1996). The ultramafic complex is migmatized in the lowermost level. The trace element signature in the gabbros and in the amphibolites is com-

27

patible with that of the basalts of the Volcanic Formation, hence suggesting affiliation between the Bolivar complex and the Volcanic Formation: The ultramafic rocks and the gabbros of the complex represent magma cooled either at the bottom (cumulates) or against the wall of a chamber (isotropic gabbro) located at a high crustal level. Conversely, the basalts represent the liquid erupted from the chamber and their geochemical signature is consistent with an oceanic plateau origin (Nivia, 1987; Nivia, 1996).
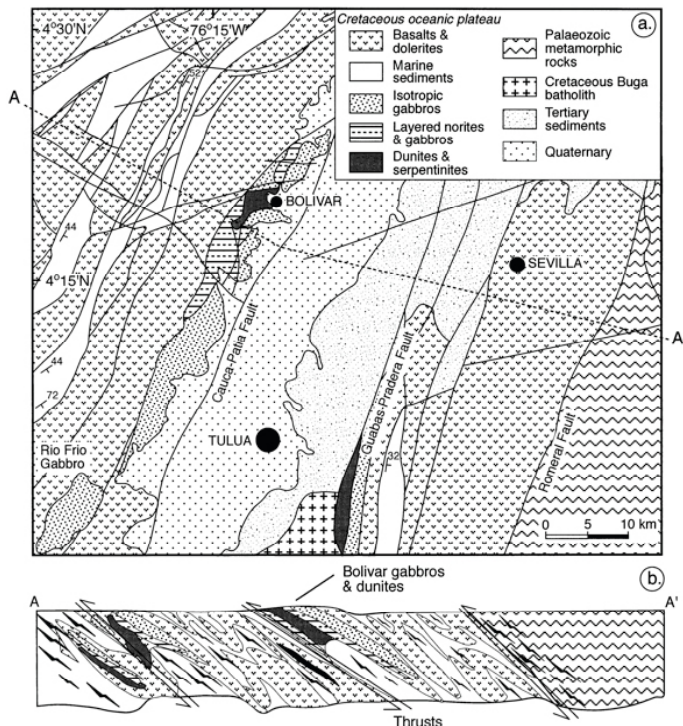

Fig. 4. (a) Map of the geology around the Bolı́var–Rio Frio ultramafic complex, Colombia. (b). Cross-section approximately along A–A' showing the thrust faulted nature of the Cretaceous mafic volcanic, gabbroic and ultramafic rocks and metasediments of the western and central Cordillera (from Kerr et al., 2008).

The ultramafic unit is intruded by pegmatitic dykes. The dykes are composed of hornblende, plagioclase, and quartz. Moreover, they can contain xenoliths of serpentinized dunite, peridotite, and gabbro. The pegmatitic dikes show variation of the infill material– hornblende and plagioclase in the lower and plagioclase, quartz, muscovite and sericite in the upper level. The dykes have an origin different from the formation of the plateau. Most likely, the obduction of the hot and thick oceanic crust over water saturated terrigenous and carbonate units of the continental margin caused positive changes in the local geothermal gradient and induced partial melting of the base of the plateau (Kerr et al., 1997a). The presence of boron-rich dumortierite (Al, Fe^{3+})$7O_3(SiO_4)3(BO)_3$ in the dykes of the Bolivar complex is a supporting evidence for the origin of the pegmatitic dikes. The strong affinity of boron to the marine sediments (100 ppm in marine shales against 3 ppm in ultramafic rocks) suggests that the fluids involved in the partial melting of the plateau were distilled from the marine sediments. In addition, a stock-

work of cryptocrystalline magnesite and late opal veins is hosted by the serpentinite bands in lowermost ultramafic horizon of the complex. The magnesite veins contain approximately 49 wt.% MgO, but also have a fairly high silica component (9.5 wt.%) and minor Ca and Fe. The high MgO content makes the veins of economic importance (e.g., magnesite quarry nearby the town of Bolivar; Nivia, 1996).

References

Aspden, J.A. and McCourt, W.J., 1986, Mesozoic oceanic terrane in the Central Andes of Colombia. Geology, v. 14, 415-418.

Feininger, T., 1982, Glaucophane schist in the Andes at Jambalo, Colombia. Canadian Mineralogist 20, 41-47.

Kerr, A.C., Marriner, G.F., Tarney, J., Nivia, A., Saunders, A.D., Thirlwall, M.F. and Sinton, C.W., 1997a, Cretaceous Basaltic Terranes in Western Colombia: Elemental, Chronological and Sr–Nd Isotopic Constraints on Petrogenesis. Journal of Petrology v. 38, 677-702.

Kerr, A.C., Tarney, J., Marriner, G.F., Nivia, A. and Saunders, A.D., 1997b, The Caribbean-Colombian Cretaceous Igneous Province: The Internal Anatomy of an Oceanic Plateau, in: Mahoney, J.J., Coffin, M.F. (Eds.), Large Igneous Provinces: Continental, Oceanic, and Planetary Flood Volcanism. American Geophysical Union

Kerr, A.C., Tarney, J., Nivia, A., Marriner, G.F. and Saunders, A.D., 1998, The internal structure of oceanic plateaus: inferences from obducted Cretaceous terranes in western Colombia and the Caribbean. Tectonophysics v. 292, 173-188.

Kerr, A.C. and Tarney, J., 2005, Tectonic evolution of the Caribbean and northwestern South America: The case for accretion of two Late Cretaceous oceanic plateaus. Geology, v. 33, 269.

Lapierre, H., Bosch, D., Dupuis, V., Polvé, M., Maury, R.C., Hernandez, J., Monié, P., Yeghicheyan, D., Jaillard, E., Tardy, M., de Lépinay, B.M., Mamberti, M., Desmet, A., Keller, F. and Sénebier, F., 2000, Multiple plume events in the genesis of the peri-Caribbean Cretaceous oceanic plateau province. Journal of Geophysical Research: Solid Earth, v. 105, 8403-8421.

Lebras, M., Mégard, F., Dupuy, C. and Dostal, J., 1987, Geochemistry and tectonic setting of pre-collision Cretaceous and Paleogene volcanic rocks of Ecuador. Geological Society of America Bulletin, v. 99, 569-578.

Luzieux, L.D.A., Heller, F., Spikings, R., Vallejo, C.F. and Winkler, W., 2006, Origin and Cretaceous tectonic history of the coastal Ecuadorian forearc between 1°N and 3°S: Paleomagnetic, radiometric and fossil evidence. Earth and Planetary Science Letters, v. 249, 400-414.

Nivia, A., 1987, Geochemistry and origin of the Amaime and Volcanic Sequences, Southwestern Colombia. University of Leicester, Unpublished, p. 163.

Nivia, A., 1996, The Bolivar mafic-ultramafic complex, SW Colombia: the base of an obducted oceanic plateau. Journal of South American Earth Sciences, v. 9, 59-68.

Ramos, V.A., 2009, Anatomy and global context of the Andes: Main geologic features and the Andean orogenic cycle. Geological Society of America Memoirs, v. 204, 31-65.

Chapter 7
Seismicity in Colombia and the Armenia 1999 Earthquake

Leonardo Echeverria Pazos, Patrick Elison, and Simon Preuss

1. Why and How do Earthquakes Occur?

Earthquakes can generally occur everywhere in the earth's crust, but the largest recorded earthquakes occur along plate boundaries. The overwhelming majority of large earthquakes take place on subduction zones, such as the pacific coast of Colombia. Fig. 1 displays the strain rate modelled from 6739 velocities from time series of (mostly) continuous GPS measurements by Kreemer et al. (2014). The figure shows that the largest strain rates are encountered around the Pacific Ocean. Small earthquakes occur much more frequently than large earthquakes. This is expressed by the Gutenberg-Richter law (Gutenberg & Richter 1954), which states that the magnitude of earthquakes is inversely proportional to the logarithm of the number of events. This means that an earthquake of a certain magnitude is ten times more likely than an earthquake that is one magnitude larger, and one magnitude increase amounts for ten times the ground motion and 33 times the released energy.

The prerequisite for an earthquake to take place is a build-up of stress over a long period of time. This build-up takes place on a so-called locked interface where the stress accumulates. The earthquake itself is then characterized by a very quick release of this stress. The Frequency-Moment relation gives a magnitude scale of an earthquake which depends on Mw and is given by

$$Mw = 2/3 \log_{10}(M0) - 10.7 \quad (1)$$

and depends on the shear modulus μ, the area of the locked interface A, and the average displacement during the rupture slip D (Hank and Kanamori, 1979).

Seismologists record the waves triggered by an earthquake on the earth's surface, which enables them to locate the earthquakes hypocenter, its magnitude and related source mechanism. They distinguish between compressional (p-) and shear (s-) waves. The wavefield they record can be used by structural geologists to understand the structure and mechanisms in the earth's crust, such as fault zone location and orientation. Although it is not possible to predict earthquakes, these insights are crucial for hazard planning and to create risk maps. Early warning systems for earthquakes are based on the different propagation velocities of p- and s-waves that result in different arrival times. The delay from the early p-wave arrival to the late s-wave arrival is usually in the order of a few seconds to minutes only but can be used e.g. to

evacuate buildings. Such systems require, however, very fast recording, evaluation and communication systems, which are typically not available in rural areas such as the Colombian mountains. Further, a distance of a couple of dozens of kilometers to the hypocenter is necessary to ensure a sufficiently large time delay.
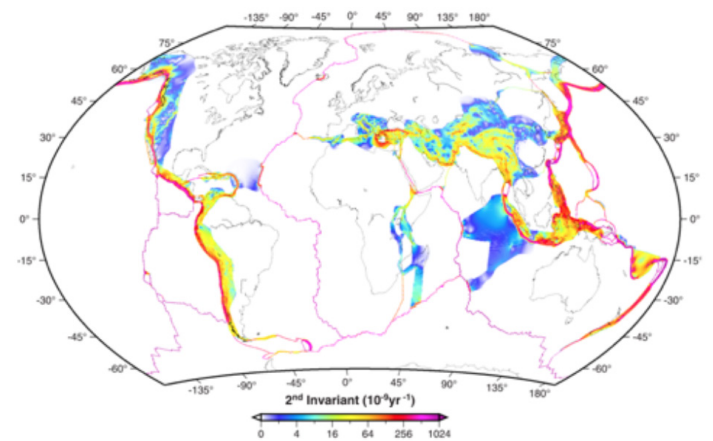

Fig. 1. Contours of the second invariant of the strain rate field to highlight seismically active regions on the earth. White areas were assumed to be rigid plates and no strain rates were calculated there (from Kreemer et al., 2014).

2. Earthquakes and Earthquake Hazards in Colombia

The historical earthquake catalog of Colombia (1900-2015, see Fig. 2) shows that the majority of earthquakes occur along the shallow trench of the Nazca subduction zone. Deeper earthquakes related to the same subduction zone occur further inland, in the area of the Valle del Cauca. However, shallower earthquakes occur on shallow crustal faults in the upper plate; e.g. Armenia 1999. The main seismicity in Colombia takes place on the megathrust of the Nazca plate with major earthquakes in the past century in 1906 (M 8.8), 1947 (magnitude unknown); 1958 (M 7.8) and 1979 (M 7.7). Onshore, one of the main active faults is the 674 km long Bucaramanga-Santa-Marta-Fault, which runs along the Eastern Cordillera up to the Caribbean coast west of Santa Marta. It is a sinistrial transpressional strike-slip fault with a strike of 341± 23 degrees, which separates the Northern Andean block from the Maracaibo block. The most active part of the fault is the so-called Bucaramanga nest in the community of Bucaramanga. In the southern part of the Eastern Cordillera, seismicity is mainly related to the Eastern Frontal Fault System; in the Central Cordillera it is the 697 km long Romeral fault system with charac-
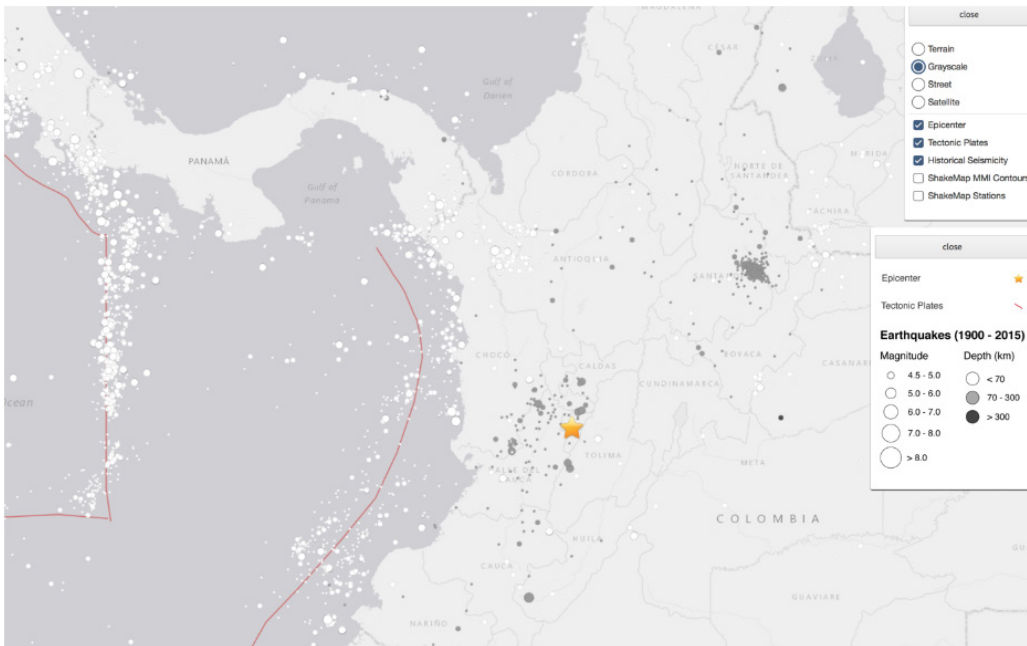
Fig. 2. Historical earthquake catalog in Colombia (USGS 2018). Star shows the epicenter of the Armenia Earthquake (1999).

teristics of both a strike-slip and compressive shear zone. The most severe earthquakes related to the Romeral fault zone are the 1983 Popayan earthquake (5.5) and the 1999 Armenia earthquake. The most severe earthquake in Colombia in terms of casualties happened in 1868 (M 6.3) offshore Ecuador with 70,000 fatalities; the strongest earthquake measured in 1906 with a moment magnitude of 8.8 happened in same region. Colombia is less prone to major earthquakes as the other countries along the Pacific coast of South America, Ecuador, Peru and Chile. This can be explained by the higher convergence rate of the Nazca plate and the South American plate (Fig. 3), since modelling studies show that larger convergence rates lead to higher frequencies of seismic events and larger maximum magnitudes (Fig. 4).

3. Armenia Earthquake

The Armenia earthquake occurred at 1 am on January 25, 1999 with the epicenter located 16 km south of the community of Armenia. Its magnitude was 6.1 at a depth of approximately 17 km (see Fig. 5a). The location is in

the Central Cordillera where the Nazca plate is subducted below the South American Plate. However, the earthquake did not occur on the subduction megathrust but on the Cauca-Romeral fault system (Fig. 5b) that comprises several sinistral strike-slip faults (northern part of the country) and dextral strike-slip faults (south of latitude 5° N), some with an additional normal-faulting component. The moment tensor solution of this particular earthquake reveals a dextral strike-slip focal mechanism with a component of normal deformation (see Fig. 6). The main event was followed by various aftershocks, with the main aftershock having a magnitude of 5.5. Despite the relatively moderate magnitude of the earthquake, its impacts on the local infrastructure and population was devastating: there were 1,900 casualties, more than 4,000 injured and 13,000 structures were destroyed or damaged, leaving entire neighborhoods of Armenia destroyed; 90% of the causalities were reported in the
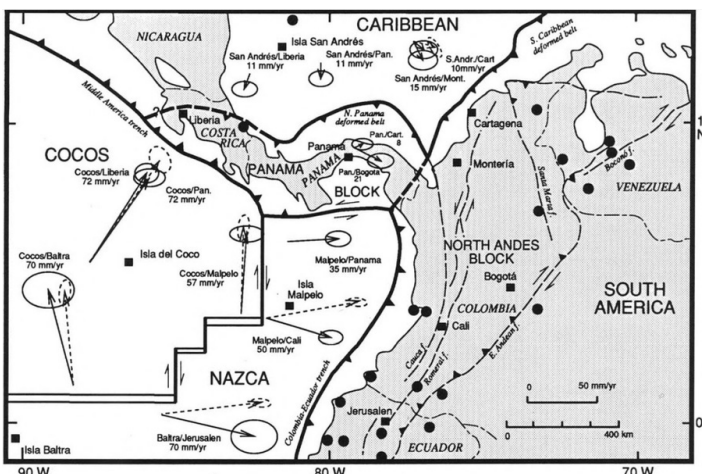

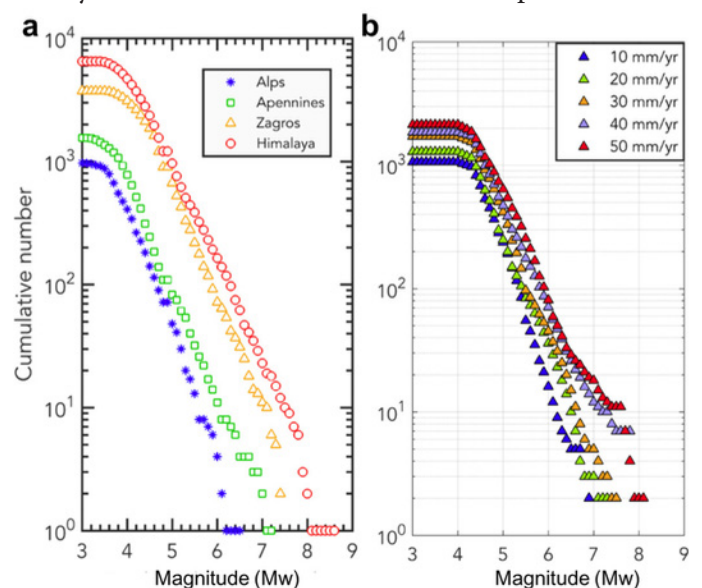**Fig. 3.** GPS measurements of plate motions in Central and Northern South America (Mann, 2007).

Fig. 4. Frequency-Magnitude distributions of (a) modelled and (b) natural mountain belts for different convergent rates (Dal Zilio et al., 2018).
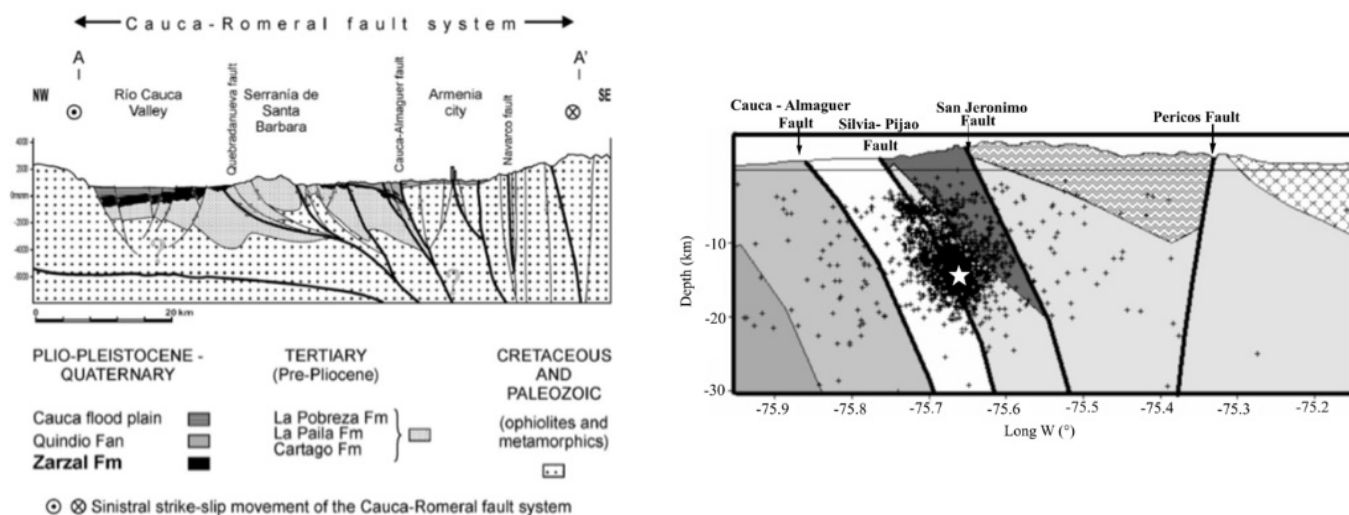
Fig. 5. Location of the Armenia 1999 earthquake (white star) on the Silvia-Pijao fault, which is part of the Romero fault system. Locations of aftershocks are indicated by black crosses on the right subplot. Figure from Vargas et al. (2005).

cities of Armenia and Pereira. The economic damage of the earthquake to this rural region is estimated to be 2.7 billion USD. The region is coined by coffee production, and 80 % of the coffee farms in the region were destroyed (Wikipedia, 2018).

The severe impact of the earthquake can be explained by a number of factors. First, in the agrarian-oriented region typical houses are simple and cheap, and hence do not resist the surface movements of a large earthquakes. Second, the earthquake occurred at night when most people were in their houses. Third, the mountainous area comprises steep and unstable hillslopes. Slope movements led to collapsing houses and landslides, which caused buried houses and blocked roads. In the city of Armenia, this left 85% of the city without electricity and water. Ultimately, the shallow depth of the hypocenter facilitated the surface impact.
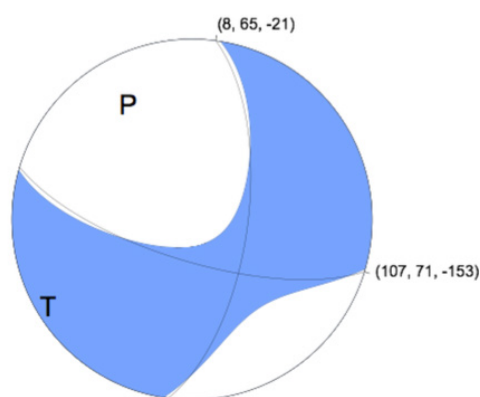
References

Dal Zilio, L., van Dinther, Y, Gerya, T.V., Pranger, C.C., 2018, Seismic behaviour of mountain belts controlled by plate convergence rate, Earth and Planetary Science Letters, v. 482, Pages 81-92.

Gutenberg, B. and Richter, C.F., 1954, Seismicity of the Earth and Associated Phenomena: Princeton, N.J., Princeton University Press.

Hank, T. and Kanamori, H., 1979, A moment magnitude scale, Journal of Geophysical Research, v. 86, B5, p. 2348-2350.

Kreemer, C., Blewitt, G., Klein, E. C., 2014, A geodetic plate motion and Global Strain Rate Model, Geochem. Geophys. Geosyst., v. 15, p. 3849–3889.

Mann, P., 2007, Geologic and Tectonic Development of the Caribbean Plate Boundary in Northern Central America: Geological Society of America.

Petersen, M. D., Harmsen, S., Jaiswal, K. S., Rukstales, K. S., Luco, N., Haller, K. M., Mueller, C. S., Shumway, A. M., 2018, Seismic Hazard, Risk, and Design for South America. Bulletin of the Seismological Society of America.

United States Geological Survey (USGS) online database for earthquakes https://earthquake.usgs.gov/earthquakes/search/, USGS 2018.

Vargas, C.A., Kammer, A., Valdes, M., Rodriguez, C.E., Caneva, A., Sanchez, J.J., Arias, E., Cortes, C.A., Mora, H., 2005, New Geological and Geophysical contributions in the section Ibague - Armenia, Central Cordillera – Colombia: Earth Sciences Research Journal v. 9, no. 2, p. 99-109.

Wikpedia, 2018, 1999 Armenia, Colombia Earthquake. URL: https://en.wikipedia.org/wiki/1999_Armenia,_Colombia_earthquake. Accessed: 17 June 2018.

Fig. 6. Focal mechanism of the Armenia 1999 earthquake from USGS catalog.

Chapter 8
Sedimentology and Coastal Processes of Colombia

José Guitian Bermejo, Richard Ott

1. Introduction

Most of Colombia is covered by sediments (see geologic map). The lowlands of the Amazon and Magdalena River are the largest active sedimentary basins. However, during our field trip we will see sediments mainly where they were uplifted in the Eastern Cordillera, the Upper Magdalena River Valley and the Cauca Valley. Coastal processes along the Colombian Caribbean coast will be explored during the second week of the field trip on our way from Cartagena to the Tayrona National Park.

2. Sediments of the Eastern Cordillera and Magdalena River Valley

The Eastern Cordillera and Upper Magdalena River Valley belong to the same sedimentary basin, whose history can be divided into a rift, postrift and foreland basin part (Horton et al., 2010). The area underwent rifting in the Jurassic and Early Cretaceous (Cooper et al., 1995). Synrift deposits are mainly coarse alluvial fans and volcanoclastics along the active faults and shallow marine carbonates in the deeper basins. Subsequently, a shallow marine shelf basin developed throughout the Cretaceous that was flooded due to the high sea level during this time period that is estimated to have been ~ 200 m higher than modern (Ramkumar, 2016). On this shelf basin, mainly siliciclastic rocks (sandstones, mudstones) were deposited. The sediment was mainly derived from the Guyana Shield area but also from the proto-Central Cordillera (Cooper et al., 1995). The rocks are mainly glauconitic and phosphatic sandstones and foraminifera-bearing siliceous siltstones (Parra et al., 2010; Fig. 1). During the Late Cretaceous, the Andean orogeny started and basin deposition was dominated by coastal, estuarine and fluvial sediments (Parra et al., 2010). Uplift of the Central Cordillera during this time marks the transition from a postrift shelf area to the foreland basin of the Central Cordillera, producing a longterm regression and slowly shifting deformation and deposition towards the east (Horton et al., 2010). The dominant sediment source area changed and siliciclastic sediments of the Paleogene are mainly derived from the Central Cordillera. Restored cross-sections of sedimentary units show large subsidence in the Late Cretaceous and Paleogene in the Eastern Cordillera, due to the filling of the foreland basin and the topographic load of the Central Cordillera. During this time, large alluvial fans were deposited in the modern Magdalena valley area and deltaic deposits in the Eastern Cordillera (Gómez et al., 2005). In the mid-Eocene, uplift of the Eastern Cordillera started, potentially related to indenter tectonics of the Panama block. The propagation of

deformation to the east was episodic and not continuous in space; deformation occurred along crustal inhomogeneities and rift-normal faults were inverted to form the doubly verging fold and thrust belt of today's Eastern Cordillera. Uplift of the Eastern Cordillera has segmented this large foreland basin and formed two new Cenozoic basins: the Magdalena River Basin and the Llanos Basin (Amazon) (Parra et al., 2010). The Magdalena River Basin was subsequently filled mainly by terrestrial, alluvial plain deposits
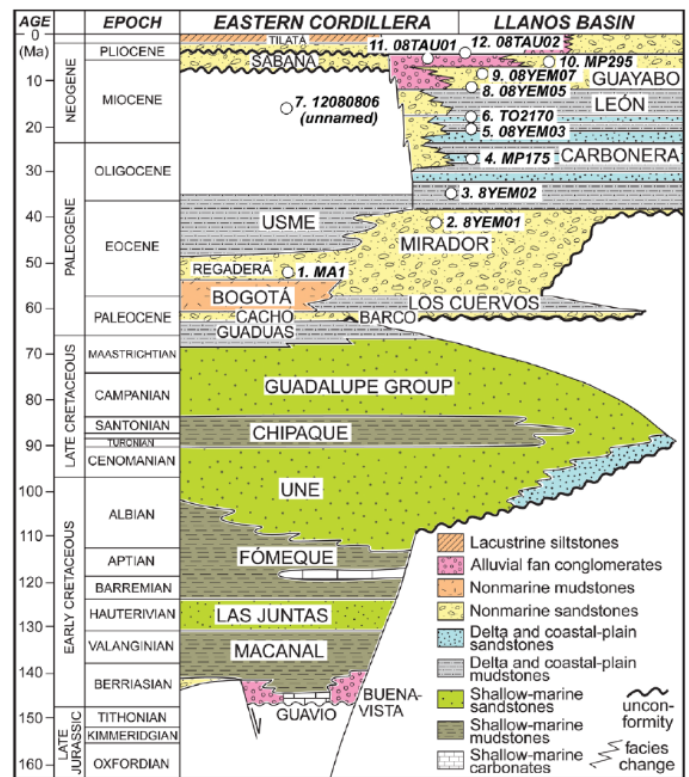

Fig. 1. Stratigraphic framework of sedimentary deposits in the Eastern Cordillera and Llanos Basin from Horton et al., (2010).

shed from the Central and Eastern Cordillera.

3. Sediments of the Cauca – Patía Basin

The basin of Cauca – Patía lies between the Western Cordillera and the Central Cordillera along a geomorphic depression of 450 km. The basin developed by the collision of an oceanic island arc with the continental margin of South America and is divided in two sub-basins: Amagá and Cauca. The pre-Cenozoic basement consists of ophiolite complexes and basal marine sediments, filled with a deformed sedimentary basin fill (Fig. 2) that is locally up to 4 km thick (Alfonso et al., 1994). The sedimentary sequence is characterized by a thick unit of mid-Eocene to mid-Oligocene sandstones and mudstones rocks formed under
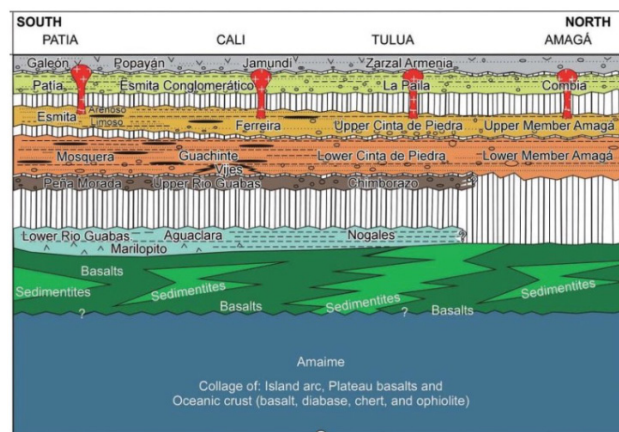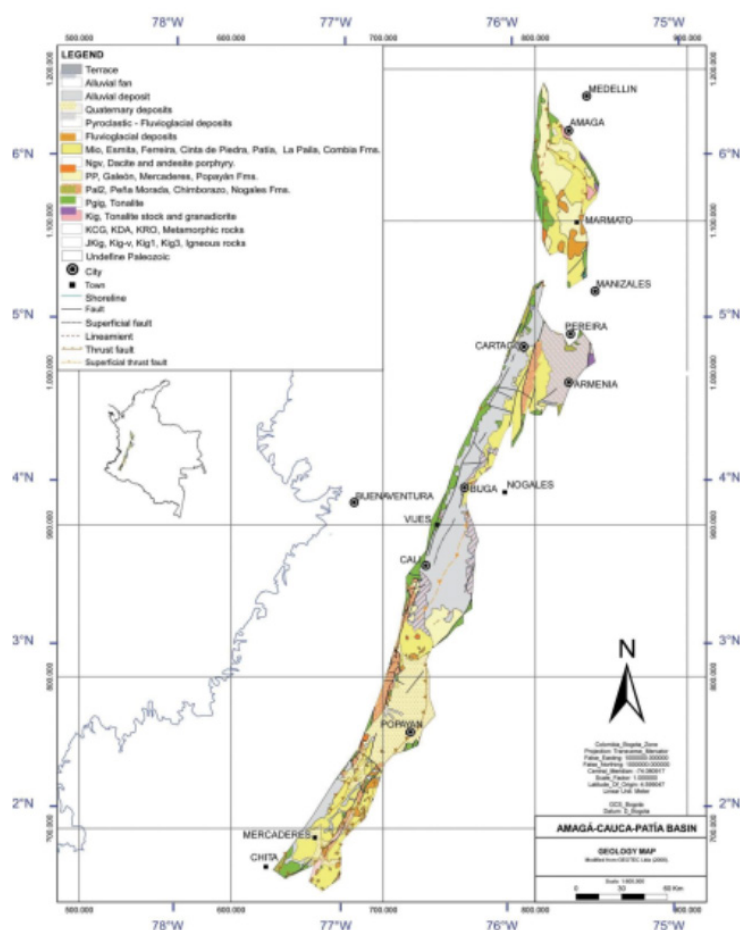
Fig. 2. Cauca-Patía basin geological map and stratigraphic framework (modified after Sierra and Marín-Cerón, 2011 and Lozano and Zamora, 2014).

continental and transitional conditions with decreasing marine influence towards the north. In the late Oligocene to early Miocene period, fluvial conglomerates and sandstones were deposited, while the northern part of the basin was closed and the first volcanic fill documents the onset of volcanism in the Central Cordillera (Alfonso et al., 1994; Lozano and Zamora, 2014). Since, the late Miocene, deformation of the basin stopped and it was filled with alluvial fan deposits and fluvial sediments that alternate with pyroclastic and volcanic ash layers. The unconformity between deformed and undeformed sediments can still be seen by an angular unconformity between pre and post late Miocene – sediments (Alfonso et al., 1994).

4. Coastal Processes

The Colombian Caribbean Coast is about 1600 km long ,with mainly sedimentary sequences in the south and metamorphic units of La Guajira Peninsula in the north. The littoral has interacted with the ocean, leading to a diverse and dynamic geomorphology, characterized by spit-lagoon segments, bars and beaches at the low-relief deltaic plains, or by cliffs and islets where medium-to-high relief mountains define the landscape (Rangel-Buitrago et al., 2013). Erosion is the main process modelling the coastline. For the last 30 years, the Caribbean coastline has experienced erosion along 50% of its length, 18% underwent accretion, while 32% have been stable. The most pronounced retreats are located at three locations: "Km19" (Magdalena River Delta, Magdalena Department) with up to 19m/yr, the

sand bodies migration of 29 m/yr of Puerto Colombia (Atlántico Department), and at the Punta Broqueles (Cordoba Department; Rangel-Buitrago et al., 2015). The main causes of erosion are the long-term factors, such as sea level rise due to global climate change, decadal factors, such as river discharge variations, shore protection, and short-term variations of wave energy related to storms (Rangel-Buitrago et al., 2015).

Relative sea level rise of ~5 mm/yr (Torres et al., 2013), is affecting the low coast and deltaic lowlands and related ecosystems which will become more vulnerable to erosion associated with flood events (Fig. 3). The main source of sand from beaches are local cliffs and rivers, thus changes in sediment supply from rivers unbalance the distribution of sediment. For example, dam structures allow only the fine sediment to reach the coast, which is not stable on the beach, and could affect coral and algae ecosystems (Gardner et al., 2003). Channels within the deltas (e.g. jetty Boca de Ceniza, Barranquilla) stops the distribution of sediments within the landform and redirects them to the ocean. Finally, short term causes are related with extreme events as cold fronts and hurricanes, which produce high energy waves that erode the cliffs, flat the beaches and destroy human constructions.
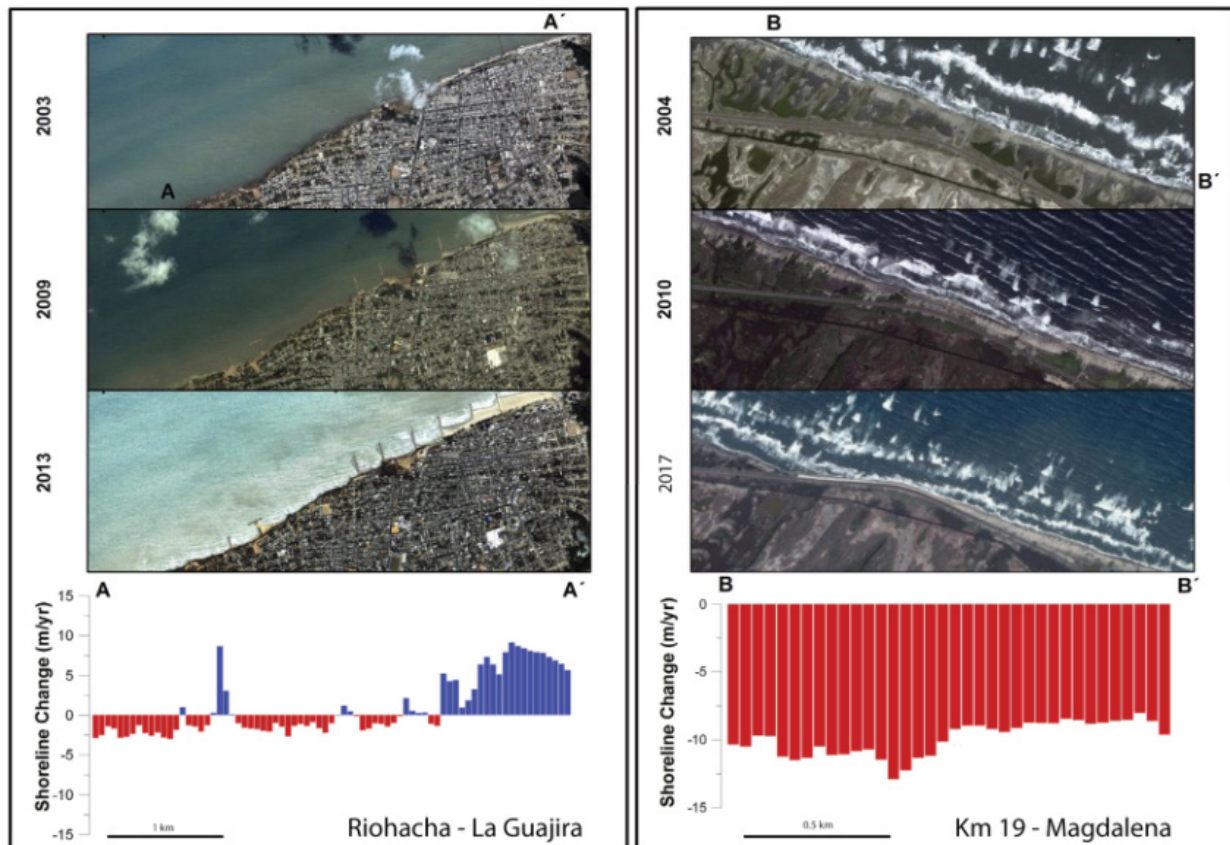
Fig. 3. Shoreline changes at Riohacha, La Guajira and "Km 19", Magdalena (modified after Rangel-Buitrago et al., 2015).

References

Alfonso, C.A., Sacks, P.E., Secor, D.T., Rine, J., and Perez, V., 1994, A tertiary fold and thrust belt in the Valle del Cauca Basin, Colombian Andes: Journal of South American Earth Sciences, v. 7, 3-4, p. 387–402, doi: 10.1016/0895-9811(94)90023-X.

Cooper, M.A., Addison, F.T., Alvarez, R., Coral, M., Graham, R._H., Hayward, A.B., Howe, S., Martinez, J., Naar, J., and Peñas, R., 1995, Basin development and tectonic history of the Llanos Basin, Eastern Cordillera, and middle Magdalena Valley, Colombia: AAPG Bulletin, v. 79, no. 10, p. 1421–1442.

Gardner, T.A., Côté, I.M., Gill, J.A., Grant, A., and Watkinson, A.R., 2003, Long-term region-wide declines in Caribbean corals: Science (New York, N.Y.), v. 301, no. 5635, p. 958–960, doi: 10.1126/science.1086050.

Gómez, E., Jordan, T.E., Allmendinger, R.W., and Cardozo, N., 2005, Development of the Colombian foreland-basin system as a consequence of diachronous exhumation of the northern Andes: Geological Society of America Bulletin, v. 117, no. 9, p. 1272, doi: 10.1130/B25456.1.

Horton, B., Parra, M., Saylor, J., Nie, J., Mora, A., Torres, V., Stockli, D., and Strecker, M., 2010, Resolving uplift of the northern Andes using detrital zircon age signatures: GSA Today, p. 4–10, doi: 10.1130/GSATG76A.1.

Lozano, E., and Zamora, N., 2014, Compilcaión de la Cuenca de Amagá-Cauca-Patía.

Parra, M., Mora, A., Jaramillo, C., Torres, V., Zeilinger, G., and Strecker, M.R., 2010, Tectonic controls on Cenozoic foreland basin development in the north-eastern Andes, Colombia: Basin Research, v. 79, p. 815, doi: 10.1111/j.1365-2117.2009.00459.x.

Ramkumar, M., 2016, Cretaceous sea level rise: Down memory lane and the road ahead: Amsterdam, Elsevier Ltd.

Rangel-Buitrago, N., Correa, I.D., Anfuso, G., Ergin, A., and Williams, A.T., 2013, Assessing and managing scenery of the Caribbean Coast of Colombia: Tourism Management, v. 35, p. 41–58, doi: 10.1016/j.tourman.2012.05.008.

Sierra, G. and M. Marín-Cerón (2011). "Petroleum Geology of Colombia." Geology and Hydrocarbon Potential, Tumaco Basin: Medellín, Colombia, Fondo Editorial Universidad EAFIT 13: 80.

Torres, R. R. and M. N. Tsimplis (2013). "Sea-level trends and interannual variability in the Caribbean Sea." Journal of Geophysical Research: Oceans 118(6): 2934-2947.

Chapter 9
The Influence of Tectonics on Fluvial Reorganization and Sedimentary Deposits in Colombia

Erica Erlanger and Yanyan Wang

1. Introduction

Colombia hosts a number of rivers, some of which flow exclusively within its borders (Fig. 1), and others that flow across the entire continent. Most rivers in Colombia flow transverse to the Andes Mountains, from west to east. Examples include the Japura and Negro Rivers, tributaries of the Amazon River, and the Orinoco River. However, recent uplift of the Northern Andes in Colombia has restricted the Magdalena and Cauca Rivers to flow south to north through the major valleys that separate the Cordilleras of Colombia (Horton et al., 2015). In Colombia, the distribution of these fluvial basins by percent area is as follows: Amazon River tributaries (30.3%), Magdalena-Cauca Rivers (23.8%), Orinoco River (30.4%), other rivers terminating at the Caribbean Sea (9.0%), and other rivers terminating at the Pacific Ocean (6.8%).

Fig. 1. Hillshade GTOPO 30, 1-arc second DEM of Colombia. Major rivers and tributaries are shown in blue and labeled.

2. Drainage Reorganization

Extensive 'source to sink' analysis from detrital zircons, sedimentary records in outcrops, and drilling wells have found evidence for major drainage reorganization of the Magdalena and Cauca Rivers in response to the propagation of deformation from the Western to Eastern Cordilleras since the Jurassic (e.g. Silva et al., 2013; Struth et al., 2015).

The evolution of the Central and Eastern Cordilleras is intimately linked with the development of major drainage networks in the region (Fig. 2; Horton et al., 2015). From the Jurassic to late Cretaceous, the Central and Eastern Cordilleras were part of a shallow marine environment in the back-arc basin, characterized by shallow-marine carbonates inter-bedded with coastal plain mudstones that were derived from the distal Guyana Shield. From Late Cretaceous to Early Paleogene, the dominantly extensional stress regime transitioned to a compressional regime that has persisted to the present day. The Eastern Cordillera emerged primarily through the reactivation of Cretaceous rift structures as thrust faults (Cooper et al., 1995). Growth strata in the eastern flank of the Guaduas Syncline (Fig. 3) place the onset of thrusting in the Eastern Cordillera during the middle Eocene (Gómez et al., 2003). These newly developed thrust faults progressively uplifted the entire area from west to east. In response to the propagation of deformation, a transverse drainage network formed in the high Central Cordillera. Contemporaneous with the formation of the Eastern Cordillera, an axial drainage network developed in the paleo-Magdalena valley. These drainage networks patterns were established in the Oligocene and persist today. Presently, the western foothills of the Eastern Cordillera are dominated by west-verging, thin-skinned thrusts (Honda, Cambao, and La Salina Thrusts) that overthrust the Middle Magdalena River Valley (MMRV) and became active in this region between 15- 5 Ma (Gómez et al., 2003). Since the Oligocene, the north-flowing Magdalena River has migrated west of the emerging fold and thrust belt, incising through the Honda and Cambao thrusts. River terraces cut into the hanging wall of the Honda Fault (San Antonio Formation) record an intense period of activity in the Honda Fault during the Pleistocene (Gómez et al., 2003).

3. Modern Erosion Rates

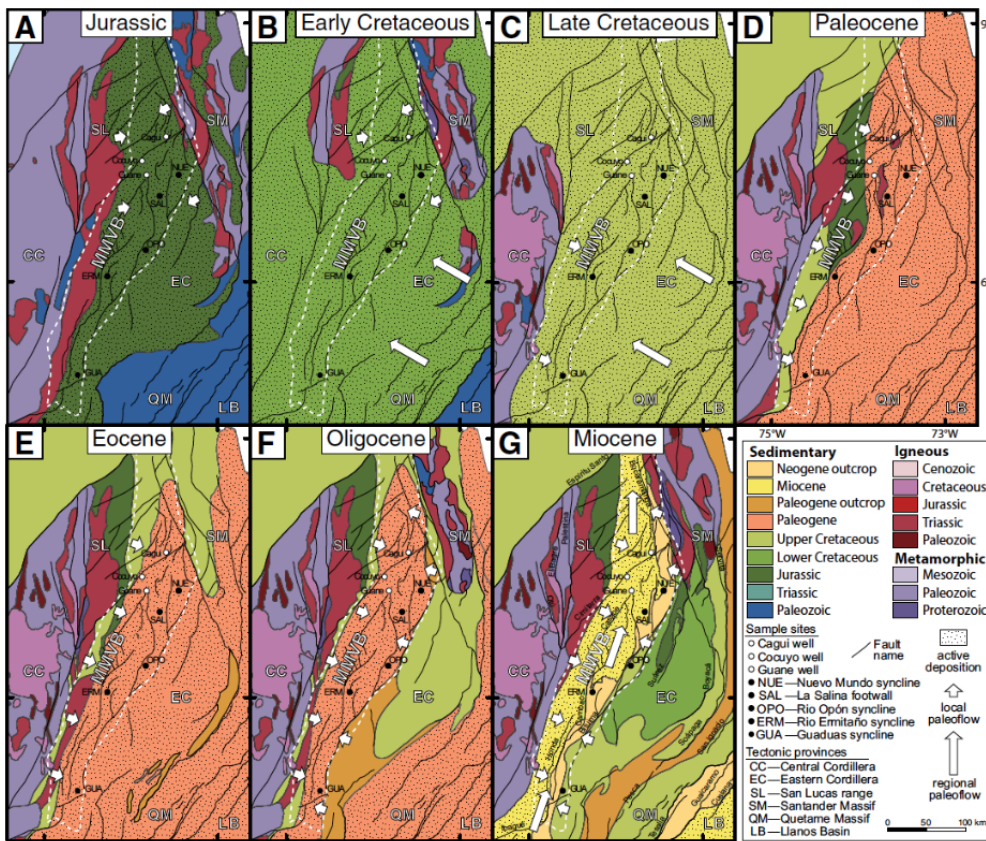The drainage network in the Eastern Cordillera is still

Fig. 2. Jurassic through Miocene non-palinspastically restored map-view paleogeographic reconstructions of the Middle Magdalena Valley Basin (MMVB) and adjacent regions showing major sediment dispersal patterns (arrows), zones of active deposition (stipple pattern), and zones of exhumation (modified from Horton et al., 2015).

ward western flank. Mora et al., (2008) estimate an average exhumation rate of 1-1.6 km/Ma from the cluster of young (<5 Ma) AFT data at the Guayuriba Basin on the eastern flank. With on-going shortening and thickening of the East Cordillera, the axial drainage network in the Sabana de Bogota, the Suarez Basin and the Chicamocha Basin will likely lose drainage area to the channels on the eastern flank and a transverse drainage network will form in the future.

undergoing reorganization through differential erosion between the eastern and western flank of the Eastern Cordillera (Struth et al., 2017; Fig. 4). Cosmogenic nuclide [10]Be derived erosion rates on the eastern flank (.11 mm/yr on average) are much higher than those on the western flank (0.07 mm/yr on average). This discrepancy in erosion rates will drive the drainage divide between the eastern flank and the Sabana de Bogotá to migrate towards the Bogotá side. Long-term exhumation rates from apatite fission track data in the Eastern Cordillera also confirm this spatial variation of erosion rates (Fig. 3). Mora et al., (2008) propose that the Eastern Cordillera forms an efficient orographic barrier, with high rainfall and erosion gradients across the eastern flank of the range and lower rates of deformation and exhumation in the drier lee-

An interesting geomorphologic characteristic in the whole Andes mountain range is that erosion rates derived from terrestrial cosmogenic nuclides data are 0.09 mm/yr-0.19 mm/yr in the Peruvian Andes (Reber et al., 2017); 0.012 mm/yr-0.075 mm/yr in the Northern Chile Andes (Kober et al., 2009); 0.04 mm/yr-0.228 mm/yr (only one sample yield 0.67 mm/yr) in the Colombian Andes (Struth et al., 2017); and 0.04 mm/yr-0.86 mm/yr in the Bolivian Andes (Safran et al., 2005). Reber et al., (2017) propose that millennial-scale erosion rates are controlled by climate rather than tectonics in the Peruvian Andes. However, this interpretation cannot explain the comparable erosion rates at the Eastern Cordillera of the Co-
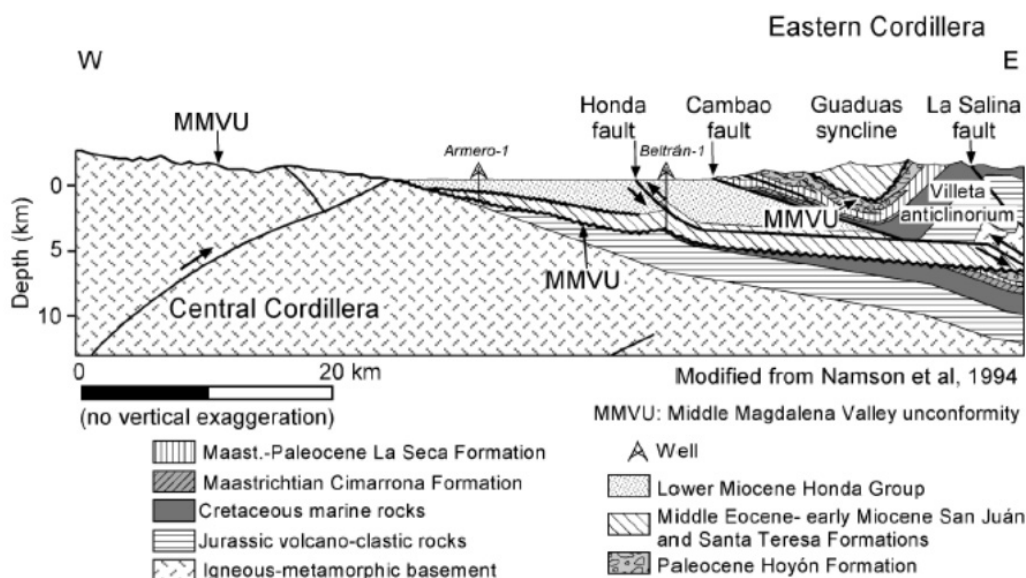

Fig. 3. West-East cross section, showing the structural setting of the Middle Magdalena Valley and surrounding relief.
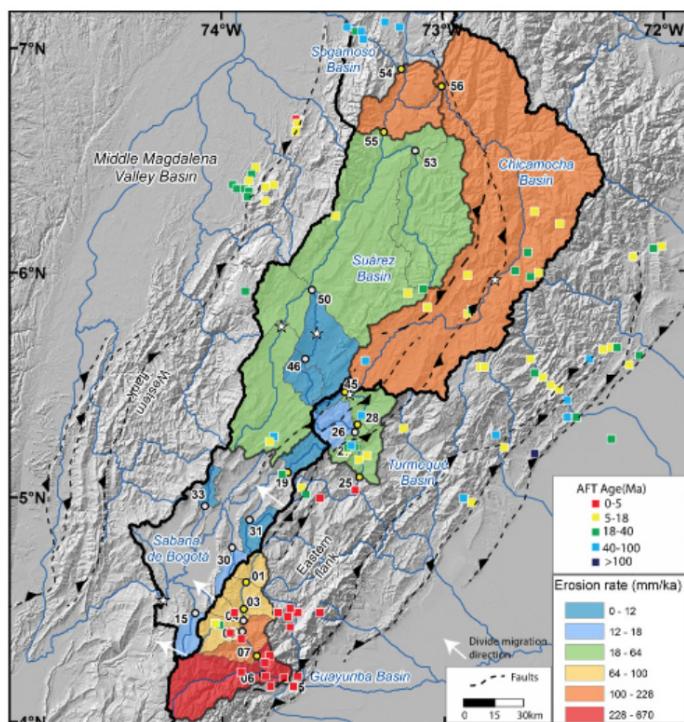
Fig. 4. Erosion rates calculated for selected Eastern Cordillera catchments by terrestrial cosmogenic nuclide 10Be analysis of river sediments. Points and numbers indicate fluvial sample locations. White stars indicate the location of the plateau capture knickpoint in the Suárez, Chicamocha and Bogotá rivers. The main drainage divides are indicated by thick black lines. Thin black dashed lines with filled triangles indicate thrust faults. The thin black dashed line without triangle indications is the Santander strike-slip fault (modified from Struth et al., 2016).

lombian Andes. Precipitation rates at the Peruvian Andes are between 200-400 mm/yr. At the eastern flank of the Eastern Cordillera, precipitation rates are greater than 1000 mm/yr which should result in much higher erosion rates compared with actual measured erosion rates. The interactions between climate, tectonics, and the surface process (especially erosion processes) in the Eastern Cordillera of Colombia remain to be resolved.

4. Alluvial Fans in the Central Cordillera

An alluvial fan, or "Abanico" in Spanish, refers to a cone-shaped deposit typically found in areas of high relief (at the foot of a mountain range or associated with a major fault scarp). In mountainous settings, the alluvial fan forms at the transition from a steep, confined valley to a broader, open lowland (Norini et al., 2016). Typical morphologies of alluvial fans consist of an active fan lobe, inactive fans lobe(s), and an incised stream channel. In the Central Cordillera of Colombia, a number of alluvial fans have been built and influenced by a combination of episodic volcanic debris associated with eruptions, tectonic activity along strike-slip faults, and fluvial deposition.

The Abanico del Quindio (variously known as Quindio Glacis, Quindio Risaralda Fan, Armenia Formation) and Abanico di Ibague are volcaniclastic fans comprised of

unconsolidated sediments from volcanic mudflows (lahars), ashfall deposits, and fluvial deposits. The Ruiz-Tolima volcanic system is the source of these deposits, which has historically produced catastrophic mudflows (Armero Tragedy) formed due to the sudden melting of glaciers from hot volcanic ejecta. The Abanico del Quindio fan presently covers 400 km2 of the Cauca Valley (Fig. 4), which separates the Central Cordillera from the West Cordillera, and has been mapped to include at least 14 individual volcaniclastic fans (Vargas et al., 2008). Ages constraints from palynological evidence of Colombian tree pollen suggest a Plio-Pleistocene age for much of the fan deposits (Neuwerth et al., 2006). Several faults of the Romeral Fault system cross this fan, which most recently produced the 1999 Armenia Earthquale. Prior to the 1999 earthquake, geological and geophysical data from the Abanico del Quindio indicate the youngest earthquake along the Armenia Fault occurred 2560   480 yr B.P (Vargas et al., 2008).

The Abanico di Ibague is located in the Magdalena Valley, which separates the Central Cordillera from the Eastern Cordillera. (Fig. 5). The fan has been heavily dissected by a number of channels, the Rio Cambeima representing the main source of material deposited on the fan. The Ibague Fault crosses the fan, and has been active during the Holocene (Koopmans, B.N., Forero, 1993), producing fault scarps, sag ponds, and pressure ridges (Vergara, 1989). The city of Ibague is located at the apex of the fan, whose location presents both a potential seismic and
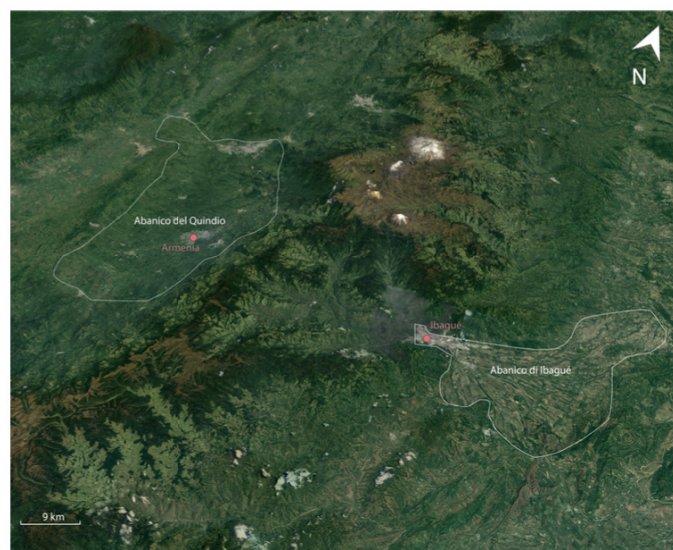

Fig. 5. Google Earth Imagery of the Central Cordillera and surrounding basins, Colombia. White outlines show extents of Abanico del Quindio and Abanico di Ibagué. Locations of Ibagué and Armenia cities are shown as colored circles.

volcanic hazards to its residents (Koopmans, B.N., Forero, 1993). One hazard model predicts a moderate eruption of the Tolima Volcano could produce a 4 - 8 x 106 m3 debris flow that would reach Ibague within 40 minutes (Thouret et al., 1995).

References

Cooper, M. a, Addison, F.T., Alvares, R., Hayward, a B., Howe, S., Pulham, a J., and Taborda, a, 1995, Basin development and tectonic history of the Llanos basin, Colombia: Petroleum basins of South America. AAPG. Memoir no. 62, v. 10, p. 659–666, doi: 10.1306/7834D9F4-1721-11D7-8645000102C1865D.

Fellin, M. G., Chen, C. Y., Willett, S. D., Christl, M., & Chen, Y. G., 2017, Erosion rates across space and timescales from a multi-proxy study of rivers of eastern Taiwan. Global and Planetary Change, v.ol 157, p. 174-193.

Gómez, E., Jordan, T.E., Allmendinger, R.W., Hegarty, K., Kelley, S., and Heizler, M., 2003, Controls on architecture of the Late Cretaceous to Cenozoic southern: GSA Bulletin, v. 115, p. 131–147, doi: 10.1130/0016-7606(2003)115<0131.

Horton, B.K., Anderson, V.J., Caballero, V., Saylor, J.E., Nie, J., Parra, M., and Mora, A., 2015, Application of detrital zircon U-Pb geochronology to surface and subsurface correlations of provenance, paleodrainage, and tectonics of the Middle Magdalena Valley Basin of Colombia: Geosphere, v. 11, p. 1790–1811, doi: 10.1130/GES01251.1.

Kober, F., Ivy-Ochs, S., Zeilinger, G., Schlunegger, F., Kubik, P. W., Baur, H., & Wieler, R., 2009, Complex multiple cosmogenic nuclide concentration and histories in the arid Rio Lluta catchment, northern Chile. Earth Surface Processes and Landforms, v. 34, no. 3, p. 398-412.

Koopmans, B.N., Forero, E.G., 1993, Airborne SAR and Landsat MSS as complementary information source for geological hazard mapping: v. 48, p. 28–37.

Mora, A., Parra, M., Strecker, M. R., Sobel, E. R., Hooghiemstra, H., Torres, V., & Jaramillo, J. V., 2008, Climatic forcing of asymmetric orogenic evolution in the Eastern Cordillera of Colombia. Geological Society of America Bulletin, v. 120, no 7-8, p. 930-949.

Neuwerth, R., Suter, F., Guzman, C.A., and Gorin, G.E., 2006, Soft-sediment deformation in a tectonically active area: The Plio-Pleistocene Zarzal Formation in the Cauca Valley (Western Colombia): Sedimentary Geology, v. 186, p. 67–88, doi: 10.1016/j.sedgeo.2005.10.009.

Norini, G., Zuluaga, M.C., Ortiz, I.J., Aquino, D.T., and Lagmay, A.M.F., 2016, Delineation of alluvial fans from Digital Elevation Models with a GIS algorithm for the geomorphological mapping of the Earth and Mars: Geomorphology, v. 273, p. 134–149, doi: 10.1016/j.geomorph.2016.08.010.

Reber, R., Delunel, R., Schlunegger, F., Litty, C., Madella, A., Akçar, N., & Christl, M., 2017, Environmental controls on 10Be-based catchment-averaged denudation rates along the western margin of the Peruvian Andes. Terra nova.

Safran, E. B., Bierman, P. R., Aalto, R., Dunne, T., Whipple, K. X., & Caffee, M., 2005, Erosion rates driven by channel network incision in the Bolivian Andes. Earth Surface Processes and Landforms, v. 30, no. 8, 1007-1024.

Silva, A., Mora, A., Caballero, V., Rodriguez, G., Ruiz, C., Moreno, N., Parra, M., Ramirez-Arias, J.C., Ibáñez, M., and Quintero, I., 2013, Basin compartmentalization and drainage evolution during rift inversion: evidence from the Eastern Cordillera of Colombia: Geological Society, London, Special Publications, v. 377, p. 369–409, doi: 10.1144/SP377.15.

Struth, L., Babault, J., and Teixell, A., 2015, Drainage reorganization during mountain building in the river system of the Eastern Cordillera of the Colombian Andes: Geomorphology, v. 250, p. 370–383, doi: 10.1016/j.geomorph.2015.09.012.

Thouret, J.C., Cantagrel, J.M., Robin, C., Murcia, A., Salinas, R., and Cepeda, H., 1995, Quaternary eruptive history and hazard-zone model at Nevado del Tolima and Cerro Machin volcanoes, Colombia: Journal of Volcanology and Geothermal Research, v. 66, p. 397–426, doi: 10.1016/0377-0273(94)00073-P.

Vance, D., Bickle, M., Ivy-Ochs, S., & Kubik, P. W., 2003, Erosion and exhumation in the Himalaya from cosmogenic isotope inventories of river sediments. Earth and Planetary Science Letters, v. 206, no. 3-4, p. 273-288.

Vargas, C.A., Nieto, M., Monsalve, H., Montes, L., and Valdes, M., 2008, The Abanico del Quindio alluvial fan, Armenia, Colombia: Active tectonics and earthquake hazard: Journal of South American Earth Sciences, v. 25, p. 64–73, doi: 10.1016/j.jsames.2006.06.001.

Vergara, S.H., 1989, Actividad neotectonica de la Falla de Ibague-Colombia. Memorias V Congreso Colombiano de Geologia, p. 147-168.

Chapter 10
Magdalena River and Mud Volcanoes and their Link to the Global Carbon Cycle

Alexandra Auderset and Hongrui Zhang

1. Introduction to the Global Carbon Cycle

The carbon cycle describes the flow of carbon between reservoirs in the Earth system, such as the atmosphere, the ocean and the land biosphere. The deep ocean is the largest pool of carbon with ~38,100 Gt (1Gt = 1 billion ton) carbon. The land biosphere is a smaller reservoir with ~610 Gt carbon in vegetation and ~1,580 Gt carbon in the soils, but has a larger flux and shorter residual time (Carvalhais et al., 2014). Moreover, the dissolved inorganic carbon from rock weathering delivered by river runoff is an important source of marine carbon reservoir (Singh et al., 2005). Hence, it is not less important to understand its complex set of process interactions, especially facing climatic challenges in the near future regarding anthropogenic CO_2 emissions.

2. Magdalena River

The Magdalena River is the largest river in Colombia, with a length of 1528 km. The basin of Magdalena covers a surface of $257.43*10^3$ km², which is 24% of the country's area and hosts 66% of its population (Restrepo and Kjerfve, 2004). The Magdalena River influences the carbon cycle in different ways. Inorganic or organic carbon dissolves in river runoff and then is transported into the ocean. This process is accelerated by deforestation and the rapid changes of land use in Colombian. In addition, the high nutrient and sediment input into the Caribbean Sea can significantly boost marine primary productivity

(Fig. 1) and affect the costal ecosystem by covering coral reefs with sediment (Fig. 2). The Magdalena River runoff has a tight correlation with hydrologic cycle: the dry and rainy season are caused by seasonal variation of rainfall and the inter-annual river discharge variations are often influenced by the El Niño-Southern Oscillation (ENSO, below and above normal rainfall associated with El Niño and La Niña, respectively; Poveda et al., 2001).

The Magdalena River is among the top ten rivers in terms of sediment load; about 150 Mt yr-1, and it is the largest river discharging directly into the Caribbean Sea (228.1 km³ yr-1; Restrepo et al., 2006). The impacts of heavy sediment loads and freshwater discharges have greatly contributed to the partial disappearance of coral formations and also to a considerable reduction in abundance of seagrass beds in the Cartagena bay and neighboring areas (Restrepo et al., 2006). Sediment load anomalies suggest that there was a high discharge period in the Magdalena River between 1985 and 1995 and another one in the Canal del Dique between 1985 and 1992 (Restrepo et al., 2006). The strong La Niña event in 1990 caused abnormal high precipitation, increased river discharge and sediment loading (Moreno-Madriñán et al., 2015). The higher sediment loading periods coincide with the overall decline of live coral cover around the Rosario Islands, a 145 km2 coral reef complex in the Caribbean Sea that constitutes a marine protected area just offshore Cartagena.
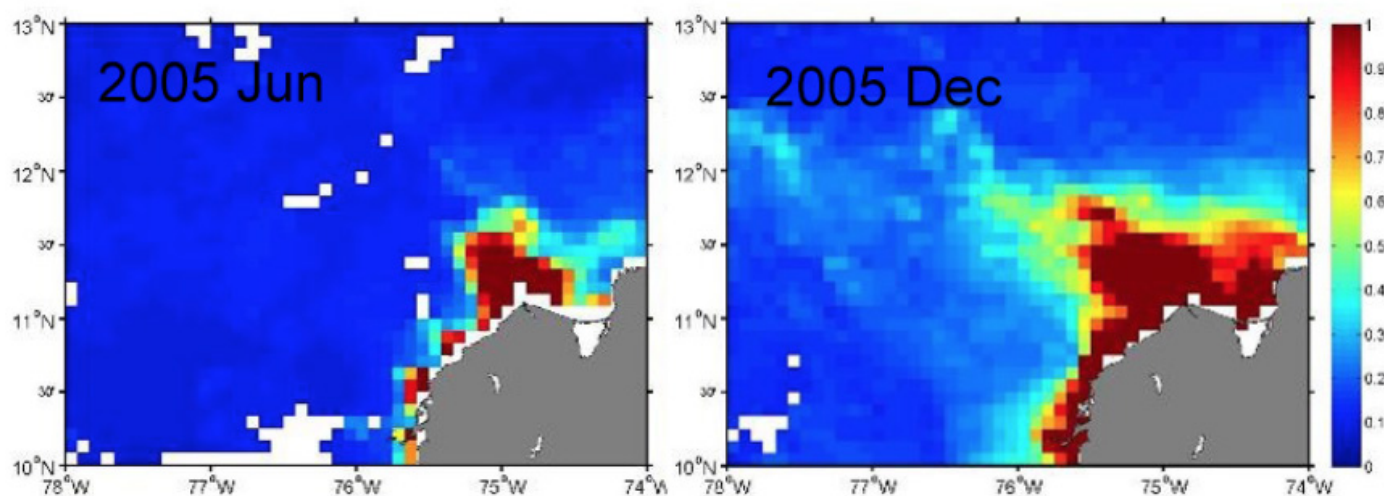
3. Mud Volcanoes

Fig. 1. The chlorophyll a concentration (mg m-3) during the dry season (June) and rainy season (December) in 2005. During the rainy season, larger river discharge brings more nutrient increasing the primary productive in oligotrophic ocean. Data from https://oceancolor.gsfc.nasa.gov.
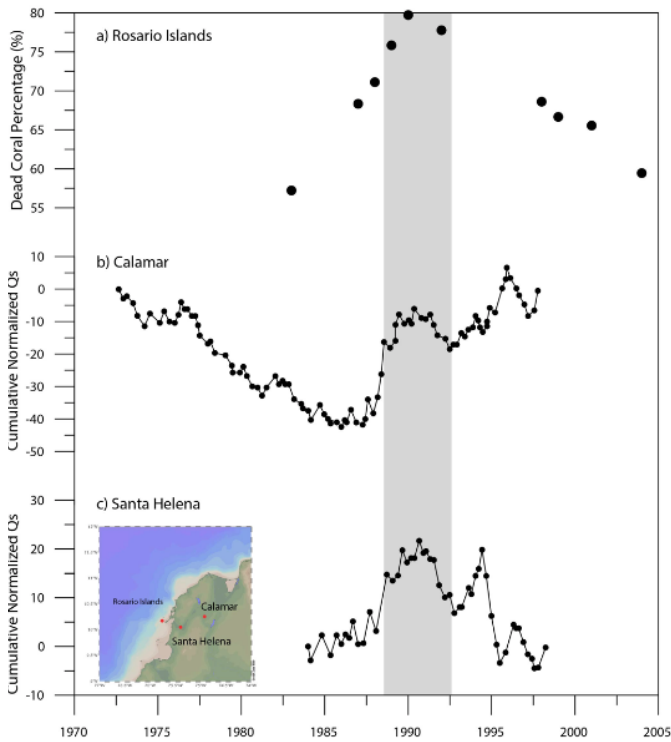
Fig. 2. The dead coral ratio at the Rosario Islands and normalized suspension at Calamar and Santa Helena. The shading area shows the coral reef declining around 1990-1992 in the years of high sediment input (modified from Restrepo et al., 2006).

3.1 Definition and Formation

A mud volcano is a geological structure that is formed as a result of the emission of argillaceous material on the Earth's surface or the sea floor. This argillaceous material contains a sufficient amount of water and gas to make it semi-liquid and to force it up through long narrow openings or fissures in the crust to produce an outflowing mass of mud on the surface. This process can be attributed to fine sediments with high pore water content that get buried quickly in compressional tectonic settings. The extruded material is composed of mud breccia, predominantly composed of quartz feldspatic sandstones, claystones, siltstones, calcareous sandstones, calcite, and locally pyrite blocks. The mud breccia forms characteristically symmetric to elongated morphological features largely varying both in shape (e.g conical shape rising hundreds of meters, funnel shape forming a depression) and size (ranging from very large structures up to 100 km^2 to small landforms of a few tens of square meters; Dimitrov, 2002).

3.2 Mud Volcanoes in Colombia

Several onshore and offshore mud volcanoes are located along the central Colombian Caribbean coastal line and were already described by Humbolt in 1804. The mud diapirism along the active continental margin is generated by the convergence of the Nazca, Caribbean and South American plates. The coastal zone in the northwest of Colombia is characterized by two distinct geological fea-

tures. A stable platform in the North with unfolded continental crust, covered by the lower Magdalena River basin and the geodynamically unstable area in the South, consisting of two main structural zones, the San Jacinto belt and the Sinú belt, both striking NE-SW. This region is also defined by broad and gentle synclines and limited locally by narrow and tight anticlines associated with NW-verging thrust faults. The Sinú belt and its pervasive structural disturbances are related to the formation of the mud volcanoes Arboletes and El Totumo (Fig. 3; Vernette, 1989; Vernette et al., 1992)

During the Neogene and Quaternary, deposition of terrigenous shoreline sediments alternated with delta deposits in NE Colombia favouring the formation of muddy, gas-rich material and porous sand layers, which allow the mud to travel upwards towards Earth's surface. The lowermost unit consists of lithic sandstones, mudstones and conglomerates from the Eocene and Oligocene. The sediments above are lithic sandstones, marls and mudstones deposited in a marine environment during the Miocene; these formations are a source of mud diapirism. Pliocene beds are characterized by calcareous and quartzose arenites, interbedded with mudstones and conglomerates on top. During the Quarternary, alluvial sediments covered the Neogene sediments. There are two sources for the extruded materials in the Totumo area. One is located at depth and is associated with the Miocene turbidites (Ar-
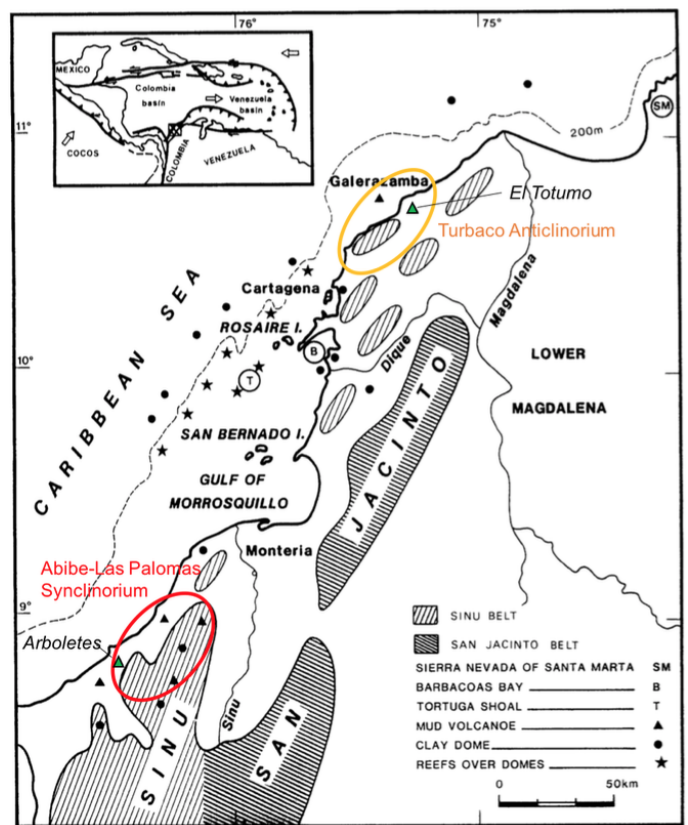

Fig. 3. The tectonic and geomorphological setting of NE Colombia with the location of mud volcanoes. Modified map by Vernette (1989).
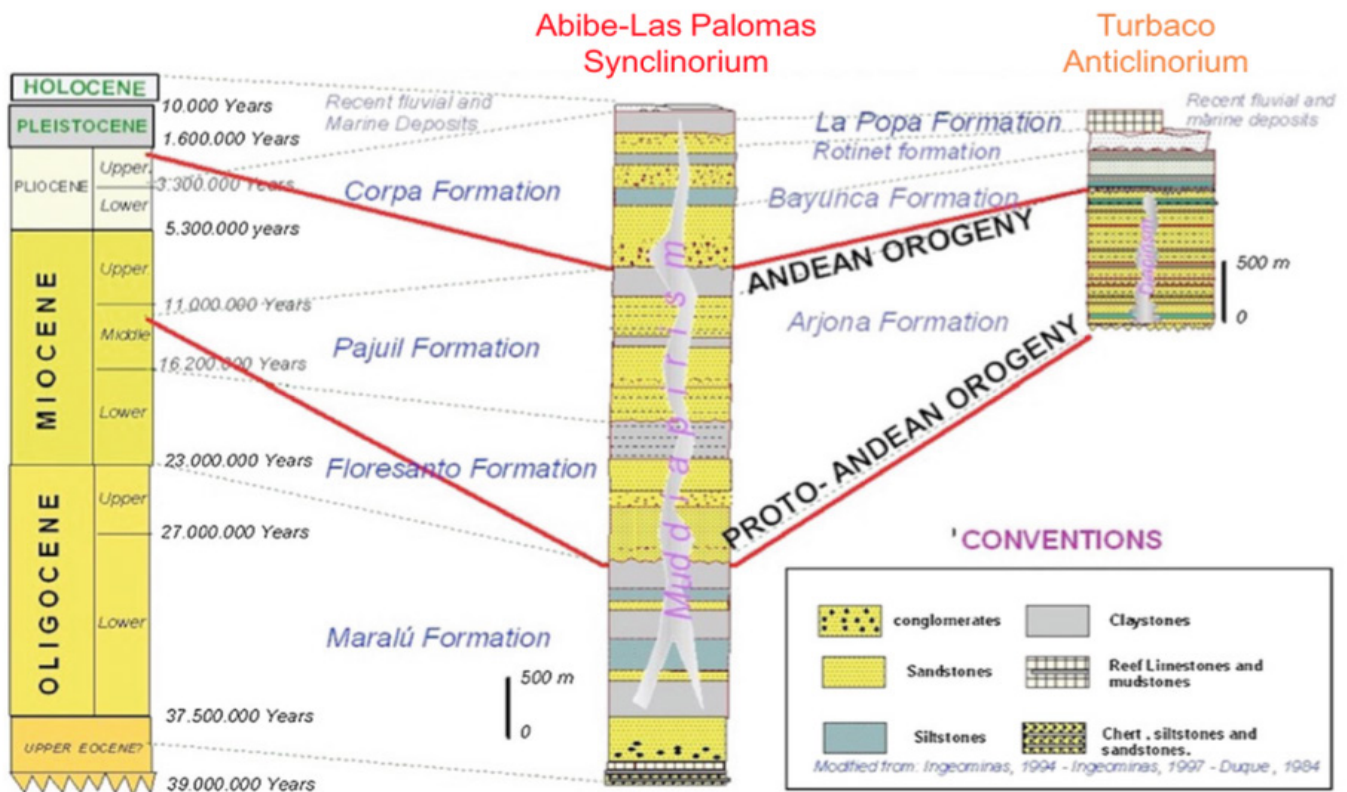
Fig. 4. Generalized stratigraphic columns of the Sinú fold belt for the Abibe-Las Palomas and the Turbaco region (from Carvajal, 2016).

jona Formation), while the second, shallower source, is related to Pleistocene materials of the ancient Magdalena River delta (Fig. 4) (Duque-Caro, 1979).

4. Link to Carbon Cycle

Milkov et al. (2003) describes mud volcanoes as potentially significant but poorly quantified geologic source of fossil hydrocarbon gases and CO_2 to the atmosphere and the ocean. There are about 2000 subaerial and submarine mud volcanos with a flux of 3-4 Tg/year. Methane is a stronger greenhouse gas than carbon dioxide, therefore the estimated flux of CO_2 is 75-100Tg/year (= ~0.1 Gt C/ year). In comparison to the terrestrial reservoir of carbon (2300Gt C) mud volcanoes are only a minor contributor, but one has to consider that this value might be underestimated due to the large unknown number of submarine mud volcanoes.

5. Excursion Stops
29.09.18 – Stop 1 – Magdalena River Delta

The Magdalena River is noted for its high discharge of river sediment and its importance as the sediment source for a large delta complex and downdrift coastal sand bodies. The emplacement of jetties, completed in 1935 to stabilize the river mouth, contributed to major changes in the downstream coastal sand bodies (Martinez et al., 1990).

29.09.18 – Stop 2 – Mud volcano "El Totumo"

"El Totumo" is a mud volcano approximately 50 km northeast of Cartagena. It rises 12 m out of the alluvial shore of the brackish lake with the same name. The base cone is about 25 m in diameter and its slope exceeds 40°. The crater is roughly circular and 1 m in diameter and filled with dark-gray, highly viscous mud. It is a tourist attractions of the region, not only for its landscape expression, but also for therapeutic and medicinal use of the mud (Carvajal et al., 2011).

References

Carvajal, J., Mendivelso, D., Obando, G., Forero, H., Gómez, J., Vásquez, L., Cárdenas, R., Castiblanco, C., Franco, J., and Ruge, G., 2011, Características del "volcanismo de lodo" del Caribe central colombiano: Informe Servicio Geológico Colombiano en proceso de publicación.

Carvalhais, N., Forkel, M., Khomik, M., Bellarby, J., Jung, M., Migliavacca, M., Mu, M., Saatchi, S., Santoro, M., and Thurner, M., 2014, Global covariation of carbon turnover times with climate in terrestrial ecosystems: Nature, v. 514, no. 7521, p. 213.

Dill, H. G., and Kaufhold, S., 2018, The Totumo mud volcano and its near-shore marine sedimentological setting (North Colombia) — From sedimentary volcanism to epithermal mineralization: Sedimentary Geology, v. 366, p. 14-31.

Dimitrov, L. I., 2002, Mud volcanoes—the most important pathway for degassing deeply buried sediments: Earth-Science Reviews, v. 59, no. 1-4, p. 49-76.

Duque-Caro, H., 1979, Major structural elements and evolution of northwestern Colombia: Geological and geophysical investigations of continental margins: AAPG Memoir, v. 29, p. 329-351.

Gansser, A., 1960, Über Schlammvulkane und salzdome, Geologisches Institut der Eidg. Technischen Hochschule und der Universität Zürich.

Higgins, G., 1974, Mud volcanoes, their nature and origin: Verh. Naturfsch. Ges. Basel, v. 84, p. 101-152.

Kopf, A. J., 2002, Significance of mud volcanism: Reviews of Geophysics, v. 40, no. 2.

Martinez, J., Pilkey, O., and Neal, W., 1990, Rapid formation of large coastal sand bodies after emplacement of Magdalena river jetties, Northern Colombia: Environmental Geology and Water Sciences, v. 16, no. 3, p. 187-194.

Milkov, A. V., Sassen, R., Apanasovich, T. V., and Dadashev, F. G., 2003, Global gas flux from mud volcanoes: a significant source of fossil methane in the atmosphere and the ocean: Geophysical Research Letters, v. 30, no. 2.

Moreno-Madriñán, M. J., Rickman, D. L., Ogashawara, I., Irwin, D. E., Ye, J., and Al-Hamdan, M. Z., 2015, Using remote sensing to monitor the influence of river discharge on watershed outlets and adjacent coral Reefs: Magdalena River and Rosario Islands, Colombia: International Journal of Applied Earth Observation and Geoinformation, v. 38, p. 204-215.

Poveda, G., Jaramillo, A., Gil, M. M., Quiceno, N., and Mantilla, R. I., 2001, Seasonally in ENSO-related precipitation, river discharges, soil moisture, and vegetation index in Colombia: Water resources research, v. 37, no. 8, p. 2169-2178.

Restrepo, J., and Kjerfve, B., 2004, The Pacific and Caribbean rivers of Colombia: water discharge, sediment transport and dissolved loads, Environmental geochemistry in tropical and subtropical environments, Springer, p. 169-187.

Restrepo, J., Zapata, P., Diaz, J., Garzonferreira, J., and Garcia, C., 2006, Fluvial fluxes into the Caribbean Sea and their impact on coastal ecosystems: The Magdalena River, Colombia: Global and Planetary Change, v. 50, no. 1-2, p. 33-49.

Singh, S. K., Sarin, M., and France-Lanord, C., 2005, Chemical erosion in the eastern Himalaya: major ion composition of the Brahmaputra and δ13C of dissolved inorganic carbon: Geochimica et Cosmochimica Acta, v. 69, no. 14, p. 3573-3588.

Vernette, G., 1989, Examples of diapiric control on shelf topography and sedimentation patterns on the Colombian Caribbean continental shelf: Journal of South American earth sciences, v. 2, no. 4, p. 391-400.

Vernette, G., Mauffret, A., Bobier, C., Briceno, L., & Gayet, J., 1992, Mud diapirism, fan sedimentation and strike-slip faulting, Caribbean Colombian Margin: Tectonophysics, v. 202, no. 2-4, p. 335-349.

Chapter 11
Climate Change Effects on Colombian Biodiversity

Luz Maria Mejía and Brandi Revels

1. Introduction

Atmospheric concentrations of the potent greenhouse gas, CO_2, increases irradiative forcing on Earth, which in turn increases atmospheric and oceanic temperatures. The warming drives sea ice retreat and sea level rise. As a result, the vertical stratification of the oceans increases, altering currents and perturbing global wind, weather, precipitation and runoff patterns. Increased dissolved CO_2 concentrations in seawater lead to ocean acidification (Ruddiman, 2008). The cascading and pervasive effects of rising anthropogenic CO_2 concentrations are disproportionality extreme by the high and low latitudes (World Bank, 2012). Colombia is South America's northernmost country and its tropical terrestrial location between 4.2 °S and 12.5 °N makes its ecosystems especially vulnerable to climate change, as they are structured around a stable and narrow range of temperatures.

2. Climate Change in Colombia

Colombia has been named a 'megadiverse country' by the United Nations Environment Programme (Mittmeier, 1988), being the most densely biodiverse country per square kilometer in the world (Potes, 2005). Colombia hosts a wide range of climates from arid deserts to frozen glaciers, to wet tropical rainforest, and is the only South American country to have Caribbean and Pacific coasts (Fig. 1). 80% of the Colombian population are reliant on the goods and services provided by the diverse but extremely vulnerable ecosystems of this country (Conservation International, 2017). Therefore, climate change-induced natural disasters are predicted to affect Colombia more than any other Latin American country (UNDP, 2009). Climate change effects in Colombia are already evidenced by the increase of anomalously warm days (Karmalkar et al., 2010), the magnitude of extreme rainfall events (USAID, 2017), and the frequency of tropical cyclones (USAID, 2017).

3. Terrestrial Impacts

In Colombia, precipitation patterns are projected to vary by region, especially affecting the north and the Amazon basin, with decreases of over 40% by 2041 (Fig. 2A). This significant precipitation drop, projected to cause one of the most extreme droughts worldwide (Dai, 2013), added to a temperature increase of 1.5-2 °C (Fig. 2B), are expected to double fire occurrence in the Amazon by 2050 (Silvestrini et al., 2011). The consequence would be the turning of the terrestrially most biodiverse ecosystem on Earth, i.e. tropical rain forests in South America, into

seasonal forests or savannas (Salazar and Nobre, 2010), potentially erasing any possibility of tropical forest reestablishment in the future (Lenton et al., 2008; Malhi et al., 2009; Salazar and Nobre, 2010).

Moreover, increased temperatures coupled with decreased precipitation are expected to culminate in the complete disappearance of snow-covered areas in Colombia by as early as 2030 (USAID, 2017). High-altitude ecosystems located below the glacier line, like Páramos, which are the water source for heavily-dense cities such as Bogotá (~8 million people), would be strongly affected by glacier melt, posing an imminent risk to its endemic faunal and floral species, aggravating land degradation and causing incalculable social and economic losses.

The highest palm tree of the world and Colombia's national tree, Ceroxylon quindiuense, which is endemic to the high mountain environments of the Cocora Valley (2000-300 m), evolved under a narrow temperature and precipitation range with the uplift of the Andes (Sanín et al. 2016). Possibly originating from Antarctic ancestors adapted to cool temperatures in the Eocene-Oligocene, the genus Ceroxylon is especially sensitive to temperature variations, wherewith the predicted extremely fast temperature rise could be catastrophic for the survival of Colombia's emblematic species.
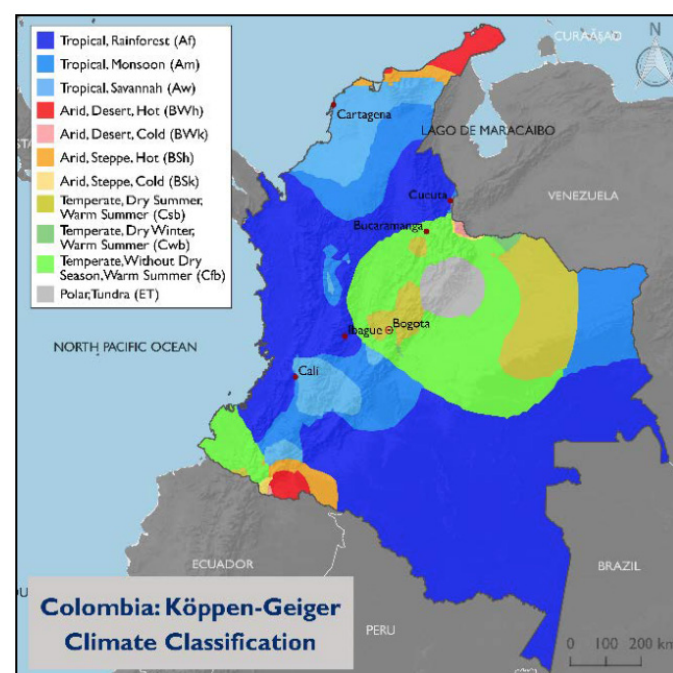

Fig. 1. Climate classification of Colombia. Colombia hosts ecosystems adapted to nearly every climate on Earth, ranging from polar tundra to tropic rainforest (USAID, 2017).
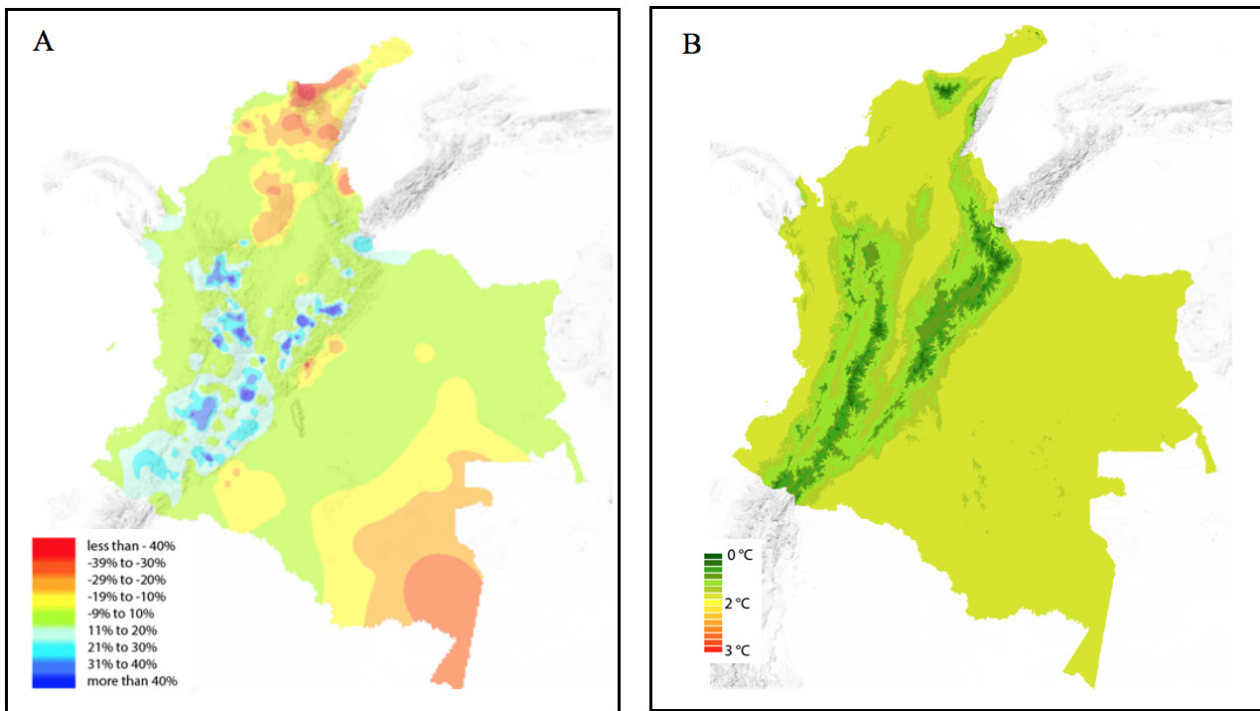
Fig. 2. A. Precipitation pattern projections for Colombia from 2011 to 2041. B. Temperature increase for Colombia predicted between 2041 and 2070. Projections are calculated using reference data from meteorological stations between 1978 and 2005, using OGC WMS 1.1.1 and SLD 1.0 as implementation specifications (IDEAM, 2018).

4. Marine Impacts

4.1 Coral Reefs

One quarter of all marine species are inextricably linked to coral reefs, being considered as one of the most biodiverse, economically relevant and complex ecosystems of our planet (Ransome et al., 2017). Hermatypic (reef-forming) corals, endemic to the shallow tropical coastal waters (e.g. Colombian Caribbean and insular regions) are sensitive to both the oceanic warming and acidification linked to anthropogenic CO_2 production (Hoey et al., 2016; Fig. 3). A reduction in coral cover of 80% in the Caribbean and 50% in the Pacific has been already observed (Jackson 2010). In fact, in a 'business as usual' scenario, a 2011 World Resources Institute report suggests that coral reefs may be completely eradicated by 2050 (Burke et al., 2011), at most postponed to 2100 according to a 2017 UNESCO report (Heron et al., 2017).

Coral reef-forming species rely on a symbiotic relationship with dinoflagellate microscopic algae, zooxanthellae, providing protection in exchange for photosynthetic energy (Hoey et al. 2016). The narrow temperature range for coral survival is mainly caused by the temperature sensitivity of their symbionts, which produce reactive oxygen species that damage the host tissue when their upper thermal limit is surpassed. As a consequence, corals expel the microalgae to seawater, a phenomenon known as coral bleaching, rendering them extremely susceptible to diverse causes of death (Nielsen et al., 2018). Additional detrimental factors related to climate change affecting Colombian coral reefs include 1) more frequent and stronger storms, which mechanically break up reefs, 2) altered ocean currents, which affect larval dispersal, and 3) changes in precipitation patterns and sea level rise, which could increase sedimentation rates and turbidity. The recent discovery of the healthy Varadero coral reef, located at the entrance of the Cartagena Bay in the Colombian Caribbean, an extremely turbid and polluted area (Pizarro et al., 2017), is encouraging, as it shows that some reef-forming species may respond to some of the fast anthropogenically-driven alterations of their environments.

4.2 Mangrove Forests

Colombia hosts mangrove forests both in its Pacific and Caribbean coasts. These ecosystems are important for coastal protection from storms and are key nursery areas for young stages of many marine species. In the Caribbean, the Ciénaga Grande de Santa Marta (CGSM) is considered the lagoon with the highest primary productivity in the world (Rivera-Monroy et al., 2011). It is separated from the Caribbean by a set of small islands formed by the ancient delta of the Magdalena River. Its ecological stability is key for the subsistence of poor local communities relying on its natural resources and services. Moreover, the disproportionate contribution of mangrove forests to carbon sequestration in comparison to other ecosystems (Alongi, 2014), renders its conservation key for climate change mitigation. The ecological stability of the mangrove ecosystem in CGSM is highly dependent on salinity, which is currently controlled by the equilibrium of fresh water input via rivers and seawater input through the Boca de la Barra, located at the easternmost edge of the water body. The three main mangrove species that in-
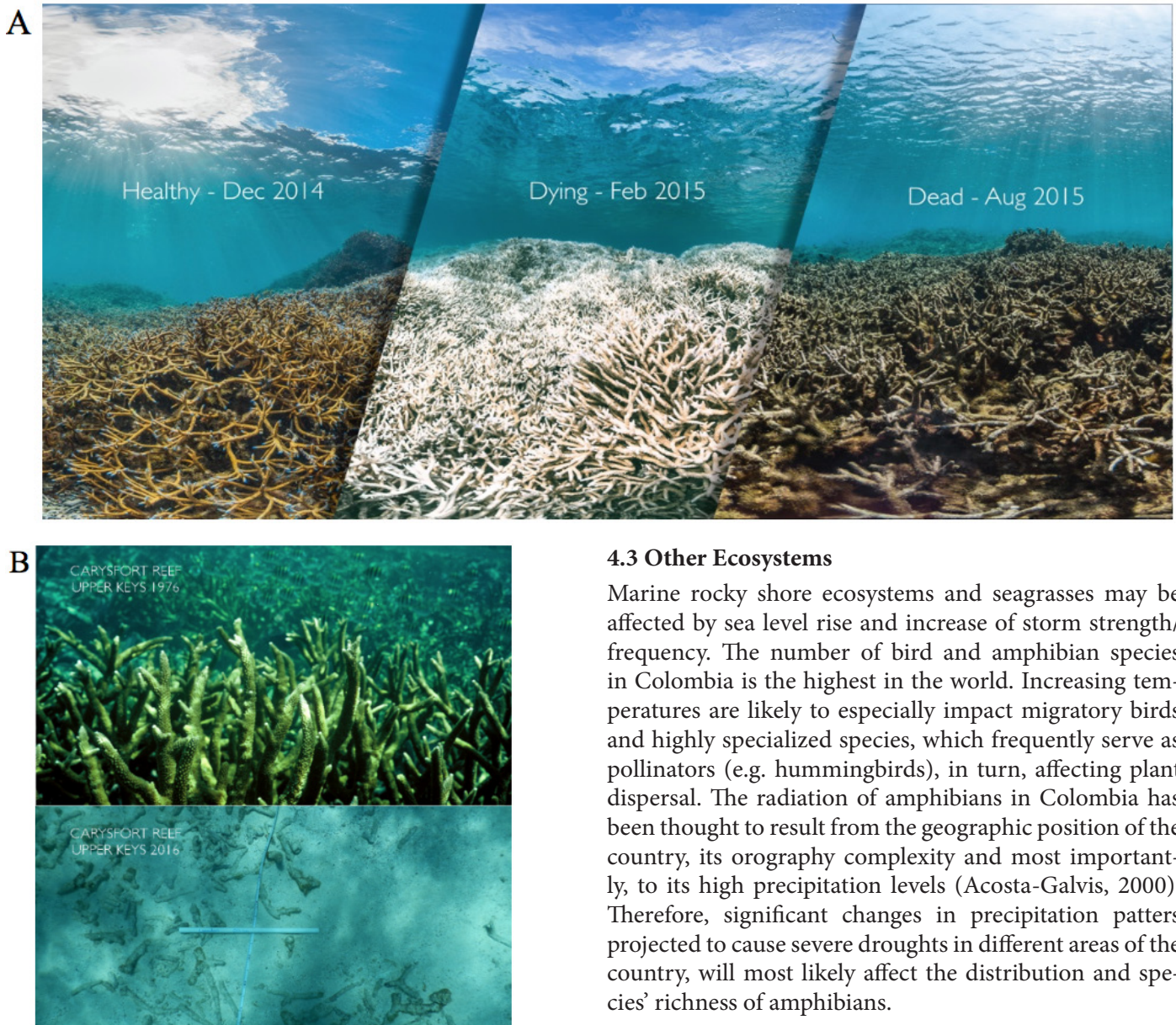
Fig. 3. The effects on coral reefs from increased A) temperature and b) CO$_2$ concentrations. In A) corals surrounding American Somoa between 2014 and 2015 show healthy reefs (left panel), bleached reefs after symbiotic zooxanthellae expel due to temperature increase (middle panel), and dead corals (right panel). In B) healthy corals at the Carysfort reef, Florida in 1976 (upper panel) contrast the dissolved coral skeletons in 2016 (bottom panel), consequence of ocean acidification. Pictures from www.climatecentral.org.

habit this estuary have different tolerance to salinity (i.e. Rhizophora mangle: low salinity; Laguncularia racemosa: intermediate salinity; Avicenia germinans: high salinity) (Parques Nacionales Naturales de Colombia, 2013). Changes in precipitation regimes and sea level rise due to climate change are likely to alter the salinity of the CGSM (USAID, 2017), driving changes in the distribution and composition of mangroves and associated species.

4.3 Other Ecosystems

Marine rocky shore ecosystems and seagrasses may be affected by sea level rise and increase of storm strength/frequency. The number of bird and amphibian species in Colombia is the highest in the world. Increasing temperatures are likely to especially impact migratory birds and highly specialized species, which frequently serve as pollinators (e.g. hummingbirds), in turn, affecting plant dispersal. The radiation of amphibians in Colombia has been thought to result from the geographic position of the country, its orography complexity and most importantly, to its high precipitation levels (Acosta-Galvis, 2000). Therefore, significant changes in precipitation patters projected to cause severe droughts in different areas of the country, will most likely affect the distribution and species' richness of amphibians.

Stability of sea turtle populations and species' survival is highly dependent on sand temperature changes, as warmer temperatures increase the percentage of female hatchlings. Under current sand warming conditions, 92% of the Caribbean Colombian leatherback sea turtle hatchlings are females and complete feminization is projected to occur during the next decade, as production of males requires incubation in 0.4 °C cooler sand nests compared to females (Patino-Martinez et al. 2012). The sea turtle conservation program (ProCTM) of the Universidad Jorge Tadeo Lozano in Santa Marta in the Colombian Caribbean currently carries out monitoring of nesting sites, growing of neonates, liberation and satellite monitoring of released sea turtles.

5. Taking Action to Mitigate Climate Change Effects on Colombia's Biodiversity

Climate change is a phenomenon that shows no political boundaries. All greenhouse gas-emitting countries have

contributed to climate change and it will affect ecosystems worldwide, with a higher impact on the most poor countries located in the tropics (World Bank, 2012). Meeting Paris agreement targets by the government of Colombia and all others, especially those responsible for the highest CO2 emissions, is mandatory to mitigate climate change effects.

Due to the local war that has lasted over decades and to socioeconomic problems, Colombia's government has until very recently ignored climate change as one of the most problematic issues threatening its population and ecosystems. To slow down climate change effects in Colombia's ecosystems, economy and social development, and to establish efficient mitigation strategies, Colombia's new government will need to take full responsibility to promote green energies instead of coal and oil extraction, and increase the protection of key ecosystems providing goods and services to the population. Environmental education needs to be implemented and awareness raised amongst the public, industry and policy makers. It is the citizen's responsibility to encourage and if necessary, press the government to take immediate action, so as to contain biodiversity loss to the lowest possible, recognizing that the well-being of Colombians fully depends on the accomplishment of this task.

References

Acosta-Galvis, A.R., 2000, Ranas, Salamandras y Caecilias (Tetrapoda: Amphibia) de Colombia: Biota Colombiana 1, v. 3, p. 289–319.

Alongi, D.M., 2014, Carbon cycling and storage in mangrove forests: Annual Review of Marine Science, v. 6, p. 195–219, doi: 10.1146/annurev-marine-010213-135020.

Burke, L.M., Reytar, K., Spalding, M., and Perry, A., 2011, Reefs at Rist Revisited: Washington, DC, World Resources Institute. 144 p.

Climate Central, 2018, Pictures of temperature increase and ocean acidification effects on coral reefs: http://www.climatecentral.org (June 2018).

Conservation International, 2017, Adapting to a changing climate in Colombia: https://www.conservation.org/projects/Pages/Adapting-to-a-Changing-Climate-in-Colombia.aspx (June 2018).

Dai, A., 2013, Increasing drought under global warming in observations and models: Nature Climate Change, v. 3, p. 52–58, doi:10.1038/nclimate1633.

Heron, S.F., Eakin, C.M., and Douvere, F., 2017, Impacts of climate change on world heritage coral reefs: a first global scientific assessment, Paris: UNESCO World Heritage Centre.

Hoey, A., Howells, E., Johansen, J., Hobbs, J.P., Messmer, V., McCowan, D., Wilson, S., and Pratchett, M., 2016, Recent advances in understanding the effects of climate change on coral reefs: Diversity, v. 8, no. 12. doi:10.3390/d8020012.

Instituto de hidrología, Meteorología y estudios Ambientales (IDEAM), 2018, Datos para construcción de mapas de proyecciones de precipitación entre 2011-2041 y temperatura entre 2041 y 2070 para Colombia, Servicio de mapas del IDEAM.

Jackson, J.B.C., 2010, The future of the oceans past: Philosophical transactions of the Royal Society of London. Series B, Biological sciences, v. 365, no. 1558, p. 3765–78. doi:10.1098/rstb.2010.0278.

Karmalkar, A., McSweeney, C., New, M., and Lizcano, G., 2010, UNDP Climate Change Country Profiles: Colombia, Oxfornd: School of Geography and the Environment, University of Oxford.

Lenton, T.M., Held, H., Kriegler, E., Hall, J.W., Lucht, W., Rahmstorf, S., and Schellnhuber, H.J., 2008, Tipping elements in the Earth's climate system: Proceedings of the National Academy of Sciences of the United States of America, v. 105, no. 6, p. 1786–1793, doi:10.1073/pnas.0705414105.

Malhi, Y., Aragão, L.E.O.C., Galbraith, D., Huntingford, C., Fisher, R., Zelazowski, P., Sitch, S., McSweeney, C., and Meir, P., 2009, Exploring the likelihood and mechanism of a climate-change-induced dieback of the Amazon rainforest: Proceedings of the National Academy of Sciences of the United States of America, v. 106, no. 49, p. 20610–20615, doi:10.1073/pnas.0804619106.

Mittmeier, R., 1988, Primate diversity and the tropical forest case studies from Brazil and Madagascar and the importance of the megadiversity countries, in Wilson, E.O., and Peter, F.M., eds., Biodiversity: Washington DC, National Academies Press (US).

Nielsen, D.A., Petrou, K., and Gates, R.D., 2018, Coral bleaching from a single cell perspective: The ISME Journal, v. 12, p. 1558–1567, doi:10.1038/s41396-018-0080-6.

Parques Nacionales Naturales de Colombia, 2013, Plan de manejo: santuario de flora y fauna de la Ciénaga Grande de Santa Marta: República de Colombia, 221 p.

Patino-Martinez, J., Marco, A., Quiñones, L., and Hawkes, L., 2012, A potential tool to mitigate the impacts of climate change to the caribbean leatherback sea turtle: Global Change Biology, v. 18, p. 401–411, doi:10.1111/j.1365-2486.2011.02532.x.

Pizarro, V., Rodríguez, S.C., López-Victoria, M., Zapata, F.A., Zea, S., Galindo-Martínez, C.T., Iglesias-Prieto, R., Pollock, J., and Medina, M., 2017, Unraveling the structure and composition of Varadero Reef, an improbable and imperiled coral reef in the Colombian Caribbean: PeerJ, v. 5, e4119, doi:10.7717/peerj.4119.

Potes, L.F., 2005, Megadiversidad, in Potes, L.F., ed., Agencia Universitaria de Periodismo Científico de la Universidad del Valle (AUPEC) y Universidad Nacional de Colombia.

Ransome, E., Geller, J.B., Timmers, M., Leray, M., Mahardini, A., Sembiring, A., Collins, A.G., and Meyer, C.P., 2017, The importance of standardization for biodiversity comparisons: A case study using autonomous reef monitoring structures (ARMS) and metabarcoding to measure cryptic diversity on Mo'orea coral reefs, French Polynesia. PLoS One, v. 12, no. 4, e0175066, doi:10.1371/journal.pone.0175066.

Rivera-Monroy, V.H., Twilley, R.R., Mancera-Pineda, J.E.,

Madden, C.J., Alcantara-Eguren, A., Moser, E.B., Jonsson, B.F., Castañeda-Moya, E., Casas-Monroy, O., Reyes-Forero, P., and Restrepo, J., 2011, Salinity and chlorophyll a as performance measures to rehabilitate a mangrove-dominated deltaic coastal region: the Ciénaga Grande de Santa Marta-Pajarales lagoon complex, Colombia: Estuaries and Coasts, v. 34, no. 1, p. 1-19, doi:10.2307/41059021.

Ruddiman, W.F, 2008, Earth's climate: past and future: New York, W. H. Freeman and Company, 388 p.

Salazar, L.F., and Nobre, C.A., 2010, Climate change and thresholds of biome shifts in Amazonia: Geophysical Research Letters, v. 37, L17706, doi:10.1029/2010GL043538.

Sanín, M.J., Kissling, W.D., Bacon, C.D., Borchsenius, F., Galeano, G., Svenning, J.-C., Olivera, J., Ramírez, R., Trénel, P., and Pintaud, J.C., 2016, The Neogene rise of the tropical Andes facilitated diversification of wax palms (Ceroxylon : Arecaceae) through geographical colonization and climatic niche separation: Botanical Journal of the Linnean Society, v. 182, p. 303–317, doi:10.1111/boj.12419.

Silvestrini, R.A., Soares-Filho, B.S., Nepstad, D., Coe, M., Rodrigues, and H., Assunção, R., 2011, Simulating fire regimes in the Amazon in response to climate change and deforestation: Ecological applications, v. 21, p. 1573–1590.

United Nations Development Programme (UNDP), 2009, Diálogos nacionales sobre cambio climático, Bogotá: UNDP Climate Community.

United States Agency for International Develpment (USAID), 2017, Climate risk in Colombia: country risk profile, USAID.

World Bank, 2012, Turn down the heat: why a 4°C warmer world must be avoided, Washington DC: World Bank, 84 p.

Chapter 12
The Interaction of Humans with Colombia's Geology

Sascha Winterberg, Max Mandl, and Friedrich Hawemann

1. Humboldt and his Holistic View on Humans and Nature

Alexander von Humboldt, the leading scientist and philosopher of his time, visited Colombia in 1801. He visited local mines, made magnetic measurements, studied volcanoes and the climate, and also collected local plants. In addition, he considered himself a humanist and was outspoken and sceptical about the colonial system in South America. He favoured the concept of independent colonies, an idea he shared with Simon Bolivar. It is therefore not surprising that many connections between human activity and nature were first identified by Humboldt. In this chapter, the authors want to discuss Humboldt's fascination for the interaction between the living and the life-giving environment and discuss Colombia's history form an interdisciplinary perspective.

2. History of Colombia

2.1 Pre-Colombia History

Prior to the arrival to the Spanish colonists, Colombia was inhabited by indigenous people with a rich history. Jewellery made of gold and pottery hint at a civilisation and thriving, functioning culture. Nevertheless, no single kingdom or unifying power was ever dominant in Colombia. Muisca (Eastern Cordillera), Tairona (Sierra Nevada de Santa Marta), Sinu, Quimbaya (Central Cordillera) and San Agustin are some of the groups that formed long-lived civilisations.

2.2 Spanish Colonisation

Alonso de Ojeda and Amerigo Vespucci were the first Spanish explorers, reaching Colombia in 1499. This is peculiar as Colombia is named after Christopher Columbus, who never set foot in this particular region of South America. Two decades after the arrival of the first Spanish party, Santa Marta (1525) and Cartagena (1533) were the first colonial cities founded in Colombia. The colony became the viceroyalty New Granada in the middle of the 16th century. At the same time, the city of Cartagena established itself as a major hub for the slave trade and a rich market for colonial commodities. In 1741, Cartagena was attacked by 186 English battleships hoping to establish control of this rich region. However, despite their fire-power, the English failed and could not conquer the city.

2.3 Independence until Today

As other South American colonies in the 19th century, the local population demanded partial or complete independence from their European ruling nations. However, subsequent rebel operations against the Spanish rule were unsuccessful. Only in 1811, after the French Revolution weakened Spain, did the first attempts to achieve independence show successes. With the help of Venezuelan-born Simon Bolivar, Colombia gained independence in 1819. At that time, the territory of Colombia was significantly larger than today and included Panama, Ecuador, Venezuela, and parts of Guyana. The independence made Colombia the first constitutional country in South America. Until today, the Colombian liberal and conservative parties, which were first founded in 1848 and 1849, exist and hold important political powers.

Other than the parties themselves, the political situation was anything but stable from the very beginning of the young nation. The secession of Panama in 1903 was successful, even if it was mostly because of the support from the USA, which was interested in a nation willing to support its ambition to build a canal between the Atlantic and the Pacific Ocean. After 1948, a decade-long civil war between Liberals and Conservatives weakened Colombia. The internal conflict was a strain to democratic forces and ultimately lead the military to assume power. Lead by the military, government forces fought against left guerrilla groups and right wing paramilitaries as early as in the 1960s. It was not until 1990, however, that the conflict escalated. To complicate matters even more, the USA was al-
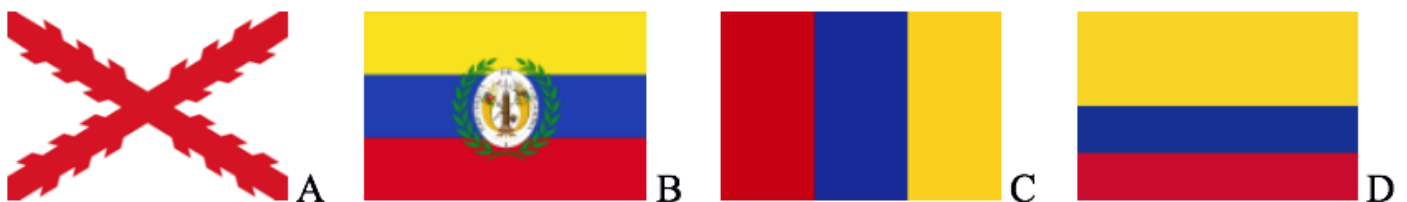

Fig. 1. Historic and present flags of Colombia: A Flag of New Granada (1538 – 1717), B Flag of Gran Colombia (1821 – 1830), C Flag of the Republic of New Granada (1834 – 1861), D Flag of the Republic of Colombia (1861 – today).

ways strongly involved in the Colombian conflicts because of their fear that communism would spread throughout South America.

Only in 2002, Colombia started to work towards peace and unification and initiated a long term negotiation- and mediation-process between the entrenched FARC (Revolutionary Armed Forces of Colombia), the Colombian government, and the civil population. The peace process is a great example for using mediation as a political tool to unify fa ormer adversary.

For its successful outcome, President Santos was awarded the Nobel Peace Prize in 2016. Even though a referendum about the peace deal was rejected in 2017, the country remained stable and on a path towards stability and peace.
The ultimate and lasting success of the peace process also strongly depends on the recent elections (May 27th, 2018) and the second and final round on 17th of June to secure an absolute majority of the electorate. Iván Duque Márquez, the right-wing candidate and opponent of the current peace deal won the 2nd round of elections and is now the official president-elect, starting his term on the 7th of August 2018. His criticism of the peace-deal focuses on the lenience and forgiveness, arguing that some former FARC-leaders would enter Colombia's federal government without having to testify or admit to their potential violent past. His unsuccessful incumbent adversary was not a center-candidate either, coming from a leftist party. The former rebel at M-19, a former FARC-like group, was the first leftist candidate who has come this close to becoming president. Analysts say that despite the outcome, the peace between the FARC and the government is likely to last because of a generally low support of the FARC among the population and the aging demographic makeup of the rebels.

Interestingly, the disassembling of the FARC has left a power-vacuum in many of the regions the FARC used to control. Given the FARC's main source of income – the growth of coca and drug-trade – the disputed areas are prime land for these purposes. This prospect draws gang-like groups to try to control the area and the financial opportunities that lies in the drug trade. No one has clear predictions of how this new development will shape Colombia, its people, the security situation, or the international drug trade in the coming years. However, coca production seems to be on the rise and reach a decade high, indicating that Colombia's path into a brighter future may not be out of the weeds yet.

References

Wulf, Andrea (2015), The Invention of Nature: Alexander von Humboldt's New World, Knopf Doubleday Publishing Groupv. 182, p. 303–317, doi:10.1111/boj.12419.

https://en.wikipedia.org/wiki/History_of_Colombia (2018)

https://de.wikipedia.org/wiki/Kolumbien (2018)

http://atlantablackstar.com/2015/07/04/cartagena-colombia-spanish-americas-biggest-slave-port/ (2018)